Click Here for Full Article

Exhumation with a twist: Paleomagnetic constraints on the evolution of the Menderes metamorphic core complex, western Turkey

Douwe J. J. van Hinsbergen,[1,2] Mark J. Dekkers,[1] Erdin Bozkurt,[3] and Marijn Koopman[1]

Received 13 August 2009; revised 29 December 2009; accepted 12 January 2010; published 10 June 2010.

[1] Much remains to be understood about the links between regional vertical axis rotations, continental extension, and shortening. In western Turkey, Miocene vertical axis rotations have been reported that occur simultaneously with the extensional exhumation of the Menderes metamorphic core complex, which has been related to back-arc extension in the eastern part of the Aegean back arc. In this paper we explore the spatial and temporal relationships between vertical axis rotations in southwestern Turkey and extensional unroofing of the Menderes Massif. To this end, we provide a large set of new paleomagnetic data from western Turkey, and integrate these with the regional structural evolution to test the causes and consequences of oroclinal bending in the Aegean region. The Lycian Nappes and Bey Dağları are shown to rotate ~20° between 16 and 5 Ma, defining the eastern limb of the Aegean orocline. This occurred contemporaneously with the exhumation of the central Menderes Massif (along extensional detachments) and after the latest Oligocene to early Miocene exhumation of the northern and southern Menderes massifs. Exhumation of the latter two was not associated with vertical axis rotations. The lower Miocene volcanics in the region from Lesbos to Uşak, to the north of the central Menderes Massif underwent a small clockwise rotation, insignificant with respect to Eurasia. This shows that exhumation of the central Menderes Massif was associated with a vertical axis rotation difference between the northern and southern Menderes massifs of ~25°–30°. This result is in excellent agreement with the angle defined by the trends of Büyük Menderes and Alaşehir detachments, as well as the angle defined by the regionally curving stretching lineation pattern across the central Menderes Massif. These structures define a pivot point (rotation pole) for the west Anatolian rotations. The rotation of the southern domain, including the southern Menderes Massif, the Lycian Nappes, and Bey Dağları, must have led to N–S contraction east of this pole. The eastern limit of the rotating domain is formed by the transpressional couple of the Aksu thrust and Kırkkavak Fault in the center of the Isparta angle. Previously reported clockwise rotations in the volcanic fields near Afyon may be the result of distributed N–S shortening east of the pivot point. The precise accommodation of this shortening history remains open for investigation. Late Oligocene to early Miocene extension in the eastern part of the Aegean back arc was NE–SW oriented and likely bounded by a discrete transform. This transform may be associated with an early evolution of the eastern Aegean subduction transform edge propagator fault. Oroclinal bending in the west Anatolian region is likely related to a reconnection of the eastern part of the Aegean orocline with the African northward moving plate in tandem with roll back in the Aegean back arc, comparable to a recently postulated scenario for western Greece. **Citation:** van Hinsbergen, D. J. J., M. J. Dekkers, E. Bozkurt, and M. Koopman (2010), Exhumation with a twist: Paleomagnetic constraints on the evolution of the Menderes metamorphic core complex, western Turkey, *Tectonics*, *29*, TC3009, doi:10.1029/2009TC002596.

1. Introduction

[2] Cenozoic extension and exhumation have led to exposure of previously subducted and metamorphosed portions of the Aegean and west Anatolian mountain belts, which have inspired geological reconstructions of the orogen's root over the past decades [e.g., *Schuiling*, 1962; *Andriessen et al.*, 1979; *Bonneau and Kienast*, 1982; *van der Maar and Jansen*, 1983; *Lister et al.*, 1984; *Schermer*, 1990; *Jolivet et al.*, 1994a, 2004; *Lips et al.*, 1998; *Gautier et al.*, 1999; *Bozkurt*, 2001b; *Mposkos and Kostopoulos*, 2001; *Brun and Sokoutis*, 2007; *Jolivet and Brun*, 2010]. The database from both the metamorphic and nonmetamorphic domains of the Aegean and west Anatolian orogen is among the richest in the world, making the region instrumental to geologically calibrate geodynamic processes, linking, e.g., back-arc extension and exhumation to slab roll-back [*Berckhemer*, 1977; *Le Pichon and Angelier*, 1979; *Meulenkamp et al.*, 1988; *Jolivet and Faccenna*, 2000; *Jolivet*, 2001], nappe stacking to subduction [*Faccenna et al.*, 2003; *van Hinsbergen et al.*, 2005a, 2005c; *Jolivet and Brun*, 2010], exhumation of (ultra-) high-pressure ((U)HP) metamorphic rocks to subduction channel

[1]Paleomagnetic Laboratory Fort Hoofddijk, Faculty of Geosciences, Utrecht University, Utrecht, Netherlands.
[2]Now at Physics of Geological Processes, University of Oslo, Oslo, Norway.
[3]Department of Geological Engineering, Middle East Technical University, Ankara, Turkey.

Copyright 2010 by the American Geophysical Union.
0278-7407/10/2009TC002596

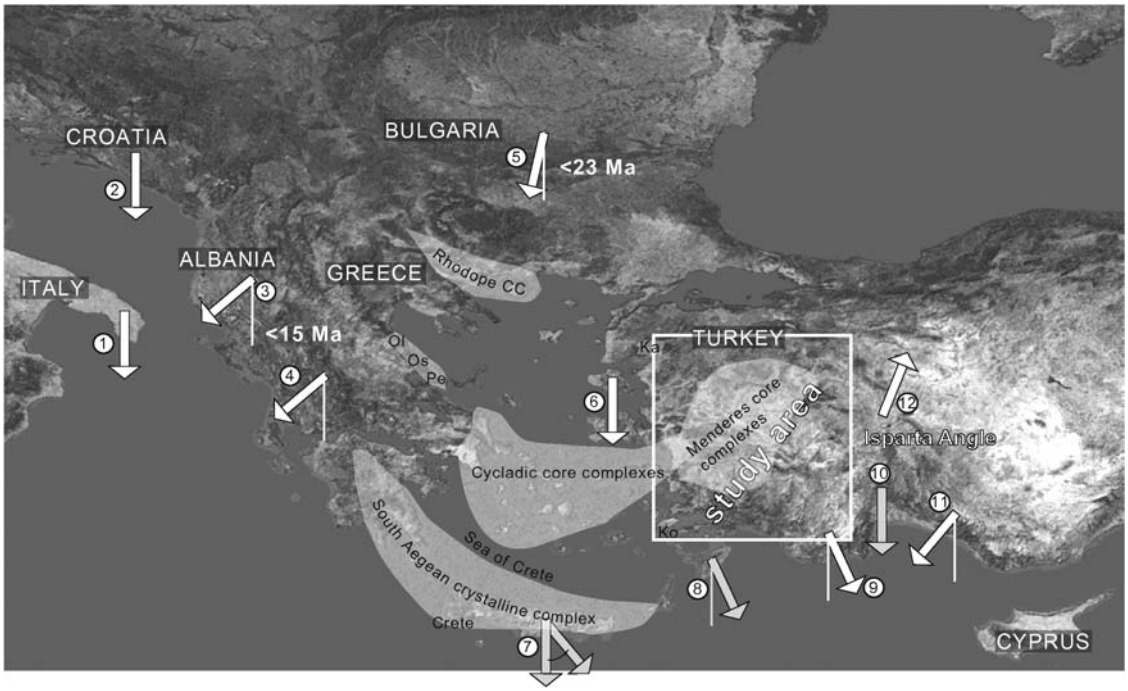

Figure 1. Topography image of the eastern Mediterranean region (blue marble data set) (see R. Stöckli et al., The blue marble next generation—A true color Earth dataset including seasonal dynamics from MODIS, 2005, available at http://earthobservatory.nasa.gov/Features/BlueMarble/) with the main loci of late Oligocene and younger extension in the Aegean back arc (white shadows; Ka, Kazdağ; Ko, Kos; Ol, Olympos; Os, Mount Ossa; Pe, Pelion). Arrows represent a selection of the most important reported paleomagnetic declinations with respect to south, giving the outline of the Aegean orocline, which runs from northern Albania to the Isparta Angle. White arrows represent directions measured in lower Miocene and older rocks, and gray arrows represent late Miocene and younger directions: 1, Apulian platform, no or little rotation since Eocene [*Tozzi et al.*, 1988; *Scheepers*, 1992; *Speranza and Kissel*, 1993]; 2, Dinarids, no rotation since the Cretaceous [*Kissel et al.*, 1995]; 3, Albania, ~50° of rotation since the early Miocene [*Speranza et al.*, 1992, 1995; *Mauritsch et al.*, 1995, 1996]; 4, western Greece and Peloponnesus, ~50° clockwise rotation since the early Miocene [*Horner and Freeman*, 1982, 1983; *Kissel et al.*, 1984, 1985; *Kissel and Laj*, 1988; *Márton et al.*, 1990; *Morris*, 1995; *van Hinsbergen et al.*, 2005b]; 5, Moesian platform and Rhodope, no significant post-Eocene rotation with respect to the Eurasian APWP [*van Hinsbergen et al.*, 2008a]; 6, Lesbos, no significant rotation of Miocene volcanics [*Kissel et al.*, 1989; *Beck et al.*, 2001]; 7, Crete, local, variable, strike-slip-related post-Messinian counterclockwise rotations [*Duermeijer et al.*, 1998]; 8, Rhodos, Pleistocene counterclockwise rotation, without rotation between early Miocene and Pleistocene [*Laj et al.*, 1982; *van Hinsbergen et al.*, 2007]; 9, Bey Dağları, ~20° counterclockwise rotations [*Kissel and Poisson*, 1987; *Morris and Robertson*, 1993; *van Hinsbergen et al.*, 2010]; 10, Isparta Angle, no Pliocene or younger rotations in its center [*Kissel and Poisson*, 1986]; 11, clockwise rotations between the Eocene and Miocene of the eastern limb of the Isparta Angle, delimiting the eastern edge of the Aegean orocline [*Kissel et al.*, 1993]; 12, post-early Miocene clockwise rotation of the volcanic fields of Afyon [*Gürsoy et al.*, 2003].

[*Thomson et al.*, 1999; *Jolivet et al.*, 2003; *Ring et al.*, 2007, 2010] or back-arc evolution [*Avigad et al.*, 1997; *Ring and Layer*, 2003], and dating and calibrating tectonic and volcanic responses to slab edge tectonics [*Govers and Wortel*, 2005; *van Hinsbergen et al.*, 2007; *Zachariasse et al.*, 2008; *Dilek and Altunkaynak*, 2009].

[3] However, the extension and exhumation history deformed and complicated the original nappe configuration of the mountain range, and reconstructing its preextensional configuration is subject to lively discussion. A particular problem in attempts to reconstruct this is that the amount of extension is laterally discontinuous across the back arc (Figure 1). The amount of roll-back-related extension has been estimated based on the amount of extension in post-Eocene metamorphic core complexes of particularly the Rhodope, Cyclades, and southern Aegean in Greece, and amounts 300 to 400 [*Gautier et al.*, 1999; *Jolivet*, 2001], or even 500 km [*Jolivet and Brun*, 2010] in the central part of the Aegean arc. Such numbers are in line with the amount of southward migration of the volcanic arc, ascribed to the southward retreat of the dehydrating subducting slab that feeds the arc [*Pe-Piper and Piper*, 2002; *Dilek and*

Altunkaynak, 2009]. However, *Ring et al.* [1999a, 2003a] and *Pe-Piper and Piper* [2002] already noted that the amount of N–S extension in west Anatolia is significantly less. Comparably, post-Eocene extension in western Greece is restricted to half graben tectonics [*van Hinsbergen et al.*, 2005c, 2006] and is insignificant compared to the strain in the central back arc.

[4] Lateral variation of back-arc extension requires some sort of tectonic accommodation: either lateral extension variations are accommodated by discrete transform faults or fault zones (such as postulated by, e.g., *Ring et al.* [1999a] between the Aegean and Cycladic regions) or gradually, by rotation differences around a vertical axis between two sides of the extending terrain [*Kissel and Laj*, 1988].

[5] Establishing the mode of accommodation of the laterally changing amounts of Aegean back-arc extension may have implications for the geodynamic causes for back-arc extension, such the shape and dimensions of the subducting slab. But more importantly, vertical axis rotations may deform older structural patterns that are used to reconstruct the preextensional anatomy of the orogen, such as stretching lineations or fold axes [*Morris and Anderson*, 1996; *Avigad et al.*, 1998; *Walcott and White*, 1998]. For example, prior to the paleomagnetic recognition that the west Aegean region underwent 50° clockwise rotation [*Horner and Freeman*, 1983; *Kissel et al.*, 1985; *Kissel and Laj*, 1988; *van Hinsbergen et al.*, 2005b], those studying the west Aegean nappe stack [*Aubouin*, 1957; *Institute for Geology and Subsurface Research and Institut Français du Pétrole*, 1966; *B.P. Co. Ltd.*, 1971; *Jenkins*, 1972] inferred a NE–SW thrusting history, whereas this was N–S throughout most of the orogenic history.

[6] The amount of Aegean back-arc extension decreases from a central line over the Rhodope and Crete (Figure 1) to both west and east. Vertical axis block rotations in the west Aegean region (50° since ~15 Ma [*van Hinsbergen et al.*, 2005b]) are well established, but have been shown to postdate most of the back-arc extension history [*van Hinsbergen et al.*, 2008a], illustrating that the block rotation history of the Aegean is perhaps partly accommodated by, but not directly caused (if at all) by, back-arc extension. Moreover, most of the rotating region lies to the northwest of the Cycladic and south Aegean crystalline complexes where much of the Aegean extension was accommodated [*Gautier et al.*, 1993; *Fassoulas et al.*, 1994; *Gautier and Brun*, 1994; *Jolivet et al.*, 1994b, 1996; *Ring et al.*, 2003b; *Jolivet and Brun*, 2010]. Although relations between rotation and exhumation in the Rhodope core complex have been postulated [*Brun and Sokoutis*, 2007; *van Hinsbergen et al.*, 2008a], the region that could have experienced major extension-related rotations in the west lies offshore central or southwestern Greece (Figure 1).

[7] Western Anatolia, however, exposes the eastern part of the Aegean back arc, and both the exhumed crystalline core of the orogen and the nonmetamorphosed fore arc are well exposed, and contain Neogene synextensional deposits (Figure 2). Aegean back-arc extension was accommodated here in the 200 × 200 km large Menderes Massif, recognized by many workers to exhibit Miocene extensional detachments along which metamorphosed rocks were exhumed [*Bozkurt and Park*, 1994, 1997b; *Hetzel et al.*, 1995b; *Bozkurt*, 2001b, 2007; *Gessner et al.*, 2001b; *Gökten et al.*, 2001; *Isik and Tekeli*, 2001; *Lips et al.*, 2001; *Okay*, 2001; *Isik et al.*, 2003], as well as smaller Oligo-Miocene metamorphic windows such Kazdağ [*Okay and Satir*, 2000; *Bonev et al.*, 2009; *Cavazza et al.*, 2009] or the islands of Kos [*van Hinsbergen and Boekhout*, 2009], Samos [*Ring et al.*, 1999b], and Ikaria [*Kumerics et al.*, 2005] in eastern Greece (Figure 2).

[8] These metamorphic domains are surrounded and overlain by volcanic and sedimentary rocks [*Aldanmaz et al.*, 2000; *Beck et al.*, 2001; *Gürsoy et al.*, 2003; *Emre and Sözbilir*, 2007; *Ersoy and Helvaci*, 2007; *Karacik et al.*, 2007; *Çiftçi and Bozkurt*, 2009b; *Dilek and Altunkaynak*, 2009], which are particularly suitable for paleomagnetic analysis. Recently, *van Hinsbergen et al.* [2010] recalibrated the timing and dimension of vertical axis rotations in the Bey Dağları region to the southeast of the Menderes Massif, studied earlier by *Kissel and Poisson* [1986, 1987] and *Morris and Robertson* [1993], and showed that this region experienced no rotation between the late Cretaceous and middle Miocene, followed by ~20° counterclockwise rotation between 16 and 5 Ma. The northern accommodation of this rotation phase and the dimensions of the region that underwent this rotation are presently unknown.

[9] In this paper we provide the results of an extensive paleomagnetic survey to calibrate the patterns of vertical axis block rotations in the Lycian Nappes and across the Menderes Massif in western Anatolia, and determine their timing. We will test rotation differences that can be predicted on the basis of the first-order structural history of the Menderes Massif to reconstruct the tectonic accommodation history of the eastward decreasing Aegean back-arc extension. Thus, we will reconstruct the four-dimensional evolution of the exhumation of the Menderes metamorphic core complex in western Anatolia. We will discuss these results within the context of the geodynamic processes that drive Aegean back-arc extension and that determine its dimensions.

2. Geological Setting

2.1. Regional Orogenic Structural Evolution

[10] Western Turkey exposes a stack of thrusted metamorphosed and nonmetamorphosed units that amalgamated upon closure of the Neotethyan ocean since the Mesozoic. The Neotethyan suture is represented by the Izmir-Ankara ophiolite and ophiolitic mélange belt that separated units of Eurasian affinitiy in the north ("Sakarya continent") from a Gondwana-derived continental fragment ("Anatolide-Tauride block") to the south [*Sengör and Yilmaz*, 1981; *Robertson and Dixon*, 1984; *Sengör et al.*, 1984] (Figure 2). The Anatolide-Tauride block is presently still separated from Africa by the oceanic crust of the eastern Mediterranean region [*Erduran et al.*, 2008]. During its collision with the overriding Eurasian plate, thrust slices derived from the Anatolide-Tauride block were accreted and metamorphosed between the Cretaceous to the Eocene [*Collins and Robertson*, 1997, 1998, 1999; *Okay et al.*, 2001]. During Oligo-Miocene Aegean back-arc extension, metamorphosed parts of the thrust stack were exhumed and are presently exposed in the tectonic window of the Menderes Massif [e.g., *Hetzel et al.*,

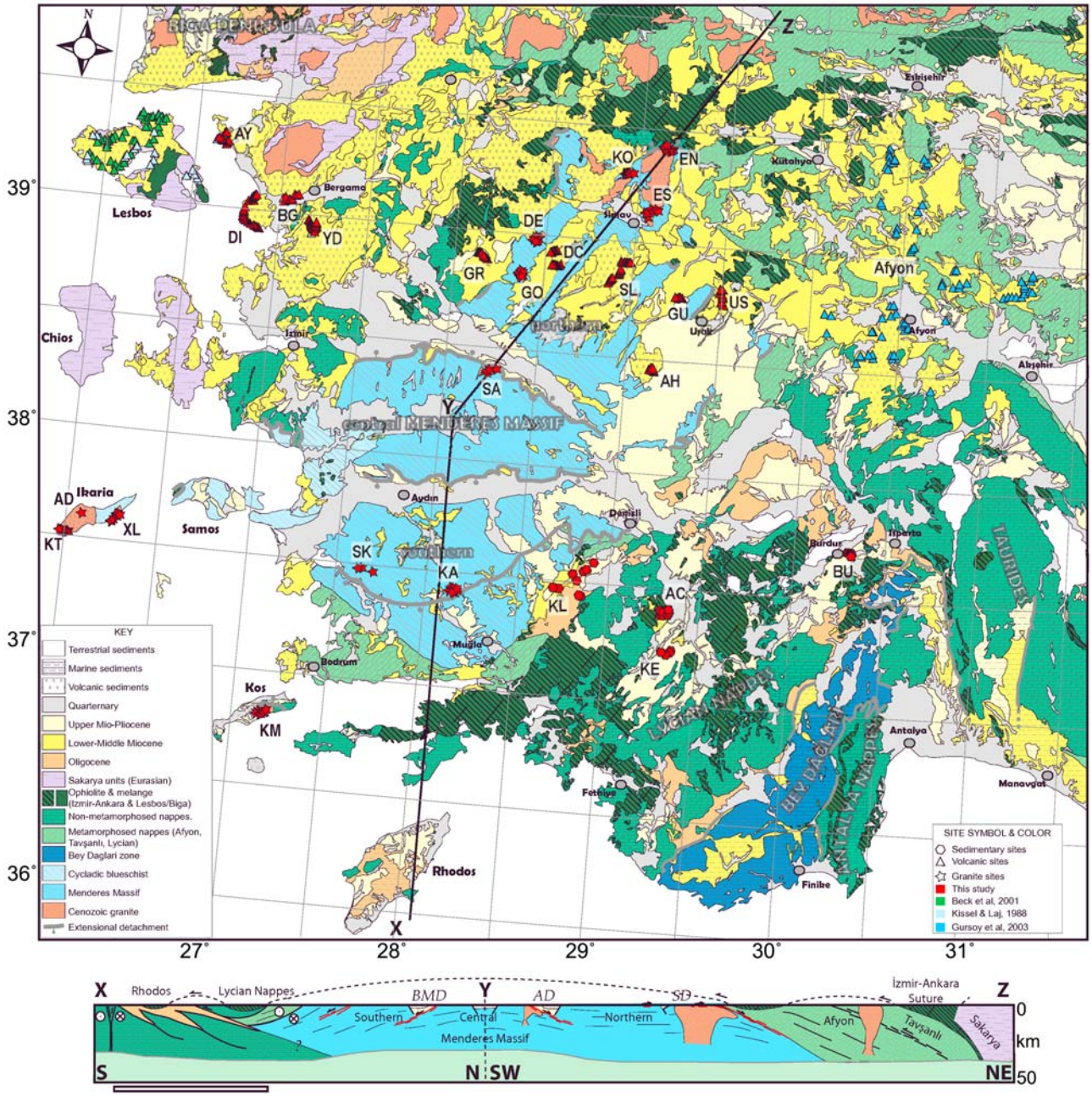

Figure 2. Geological map of and simplified cross section across southwestern Turkey, with sample locations, modified after *Mineral Research and Exploration Institute of Turkey* (*MTA*) [2002]. For sample location acronyms, see Tables 1, 2, and S1 (in the auxiliary material). Abbreviations in the cross section are BMD, Büyük Menderes Detachment; AD, Alaşehir Detachment; SD, Simav Detachment.

1995b; *Bozkurt and Oberhänsli*, 2001; *Gessner et al.*, 2001b] (Figure 2). Part of the pre-Oligocene thrust slices is now exposed in the Lycian Nappes, a megaklippe that overlies the Menderes Massif to the south, which is correlatable to the units overlying the Menderes Massif to the north [*Collins and Robertson*, 1998, 2003; *Candan et al.*, 2005] including the Afyon zone [*Candan et al.*, 2005] and the Bornova flysch north of Izmir and east of Lesbos [*Okay and Altiner*, 2007].

[11] A continuous subduction-accretion history from the Cretaceous to the Eocene can be inferred from the ages of thrusting and metamorphism: ophiolitic fragments of the Izmir-Ankara zone from the highest nappe that underthrusted below the Sakarya continental block. Both north and south of the Menderes Massif, these ophiolites have metamorphic soles with ages around 90 Ma [*Önen and Hall*, 2000; *Çelik and Delaloyle*, 2003; *Önen*, 2003; *Çelik et al.*, 2006], which dates the onset of underthrusting below these fragments.

During the late Cretaceous to Eocene, the northern former passive margin of the Anatolide-Tauride block was deformed into a thrust stack, which was partly metamorphosed. The tectonostratigraphy includes from top to bottom includes the high-pressure–low-temperature (HP-LT) metamorphic Tavşanlı zone [*Okay*, 1981, 1984, 1986; *Davis and Whitney*, 2006, 2008; *Whitney and Davis*, 2006; *Çetinkaplan et al.*, 2008] with cooling ages of ~80 Ma [*Okay and Kelley*, 1994; *Sherlock et al.*, 1999], underlain by greenschists and blueschists of Paleocene metamorphic age of the Afyon zone [*Okay*, 1984; *Okay et al.*, 1996; *Candan et al.*, 2005]. Both HP zones exhumed already in the Paleocene to Eocene, and were at, or close to the surface throughout most of the metamorphic history of the Menderes Massif [*Özcan et al.*, 1988; *Göncüoglu et al.*, 1992; *Harris et al.*, 1994]. South of the Menderes Massif, the northern and lowermost part of the Lycian Nappes also experienced late Cretaceous to Paleocene HP metamorphism, possibly equivalent to the Afyon zone [*Oberhänsli et al.*, 2001; *Rimmelé et al.*, 2003a, 2005, 2006; *Candan et al.*, 2005], whereas the southern part of the Lycian Nappes experienced no metamorphism [*Dumont et al.*, 1972; *Bernoulli et al.*, 1974; *Gutnic et al.*, 1979; *Collins and Robertson*, 1997, 1998]. In the west, the Menderes Massif is overlain by the Dilek nappe, an Eocene HP-LT metamorphic unit, overprinted by Barrovian regional greenschist metamorphism, which is correlated to the Cycladic Blueschist of the central Aegean region [*Candan et al.*, 1997; *Oberhänsli et al.*, 1998; *Ring et al.*, 1999b; *Okay*, 2001].

2.2. Structure and Metamorphism of the Menderes Massif

[12] The deepest structural unit is the Menderes Massif [*Paréjas*, 1940], which consists of an imbricated stack of high-grade orthogneisses [*Hetzel et al.*, 1995b; *Gessner et al.*, 2001c; *Okay*, 2001; *Bozkurt*, 2007] representing metamorphosed Pan-African granites [*Satir and Friedrichsen*, 1986; *Hetzel and Reischmann*, 1996; *Hetzel et al.*, 1998; *Loos and Reischmann*, 1999; *Gessner et al.*, 2004; *Koralay et al.*, 2004; *Catlos and Cemen*, 2005] as well as fossil-bearing marbles and schists that represent a Paleozoic to Eocene sedimentary cover sequence [*Caglayan et al.*, 1980; *Konak et al.*, 1987; *Özer*, 1998; *Özer et al.*, 2001; *Özer and Sözbilir*, 2003]. The Menderes Massif is intensely sheared during high-temperature and medium-pressure (Barrovian) metamorphism (the so-called Main Menderes Metamorphism, or MMM [*Akkök*, 1983; *Ashworth and Evirgen*, 1984; *Sengör et al.*, 1984; *Satir and Friedrichsen*, 1986; *Bozkurt and Park*, 1999; *Whitney and Bozkurt*, 2002; *Sengün et al.*, 2006]. This MMM postdates a phase of HP metamorphism and eclogite formation in mafic pockets in the Pan-African orthogneisses [*Oberhänsli et al.*, 1997; *Candan et al.*, 2001] and also postdates HP metamorphism [*Régnier et al.*, 2007] under blueschist facies conditions [*Candan et al.*, 1997; *Oberhänsli et al.*, 1998; *Rimmelé et al.*, 2003b; *Whitney et al.*, 2008] in the Paleozoic to Eocene sedimentary cover. The age of the eclogites and the age of the MMM are matter of fierce debate, with the majority of researchers now preferring a Pan-African age of HP metamorphism in the Pan-African basement and a Paleogene age for HP metamorphism in the cover sequence [*Satir and Friedrichsen*, 1986; *Lips et al.*, 1998; *Bozkurt and Satir*, 2000; *Candan et al.*, 2001; *Bozkurt*, 2004, 2007]. The age of the MMM is debated as well, but an Eocene age seems most likely because Barrovian MMM-related metamorphism affected metasediments with Cretaceous Rudist fossils in the central Menderes Massif [*Okay*, 2001; *Özer and Sözbilir*, 2003]. For the purpose of this paper, however, it is most important to note that the deformation associated with MMM is widespread and leads to a regionally very consistent structural grain defined by north to northeast trending stretching lineations with a persistent top-to-the-north and in the south locally top-to-the-south sense of shear [*Sengör and Yilmaz*, 1981; *Akkök*, 1983; *Sengör et al.*, 1984; *Verge*, 1993; *Hetzel et al.*, 1998; *Bozkurt and Park*, 1999; *Ring et al.*, 1999a; *Bozkurt*, 2000; *Lips et al.*, 2001; *Whitney and Bozkurt*, 2002] (Figure 3). The MMM is postdated by greenschist facies metamorphism associated with a series of extensional detachments that exhumed the Menderes Massif since the late Oligocene [*Seyitoglu et al.*, 1992; *Verge*, 1993; *Bozkurt and Park*, 1994, 1997a, 1997b; *Hetzel et al.*, 1995a, 1995b, 1998; *Bozkurt and Satir*, 2000; *Bozkurt*, 2001b; *Bozkurt and Oberhänsli*, 2001; *Gessner et al.*, 2001a, 2001b; *Gökten et al.*, 2001; *Isik and Tekeli*, 2001; *Lips et al.*, 2001; *Isik et al.*, 2003, 2004; *Bozkurt and Mittwede*, 2005]. This occurred in two stages: geochronologic evidence suggests that the northern and southern Menderes massifs (NMM and SMM) exhumed between ~25 and ~15 Ma, followed by the exhumation of the central Menderes Massif (CMM) since ~15 Ma [*Gessner et al.*, 2001b; *Ring et al.*, 2003a]. The NMM is bounded in the north by the ductile-to-brittle top-to-the-northeast Simav detachment, separating the Menderes Massif from the blueschist facies Afyon zone, and nonmetamorphosed ophiolitic mélange of the Izmir-Ankara suture [*Isik and Tekeli*, 2001; *Isik et al.*, 2004; *Ring and Collins*, 2005]. The NMM is bounded in the east and west by discrete lineaments (which may be transform faults (Figure 2) [*Özkaymak and Sözbilir*, 2008; *Uzel and Sözbilir*, 2008]) from the Afyon zone and the nonmetamorphosed Bornova flysch (believed to belong to the tectonostratigraphy of the Lycian Nappes [*Okay and Siyako*, 1993; *Okay and Altiner*, 2007]), respectively.

[13] The southern Menderes Massif exhibits a ductile top-to-the-south shear zone, which is believed to have played a role in the post-Eocene exhumation history and may have been antithetic (during the early stages of exhumation) to the Simav detachment. However, it did not develop into a full-blown ductile-to-brittle extensional detachment [*Bozkurt and Park*, 1994, 1997a; *Hetzel and Reischmann*, 1996; *Hetzel et al.*, 1998; *Bozkurt*, 2007] and the early exhumation history seems to have been accommodated by dominantly top-to-the-north sense of shear [*Bozkurt and Park*, 1999; *Lips et al.*, 2001; *Bozkurt*, 2004, 2007; *Seyitoglu et al.*, 2004], comparable to the Cycladic region of the central part of the Aegean back arc [*Gautier et al.*, 1993; *Jolivet et al.*, 2004; *Tirel et al.*, 2009; *Jolivet and Brun*, 2010]. The southern Menderes Shear Zone separates a domain of dominantly Pan-African gneisses from the Paleozoic to Eocene schists and marble cover. The cover sequence is separated by a semiductile shear zone from

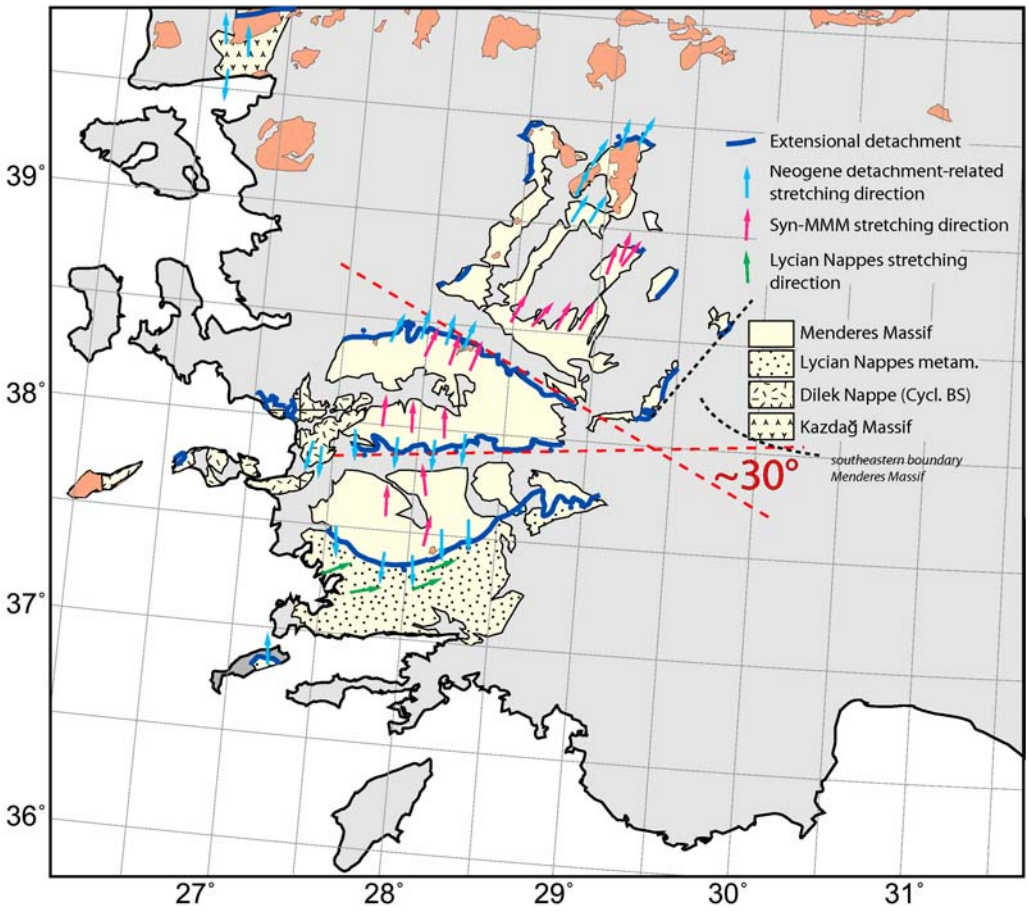

Figure 3. Schematic map of the eastern Aegean and west Anatolian region outlining the main metamorphic terrains with dominant stretching lineations. Note that the stretching lineations (both associated with regional Barrovian metamorphism, as well as with late stage extensional exhumation of the Menderes Massif) define a distinct curved pattern with an angle across the central Menderes Massif of ~30°. A comparable angle is defined by the two main bounding extensional detachments of the CMM. Stretching lineations compiled from *Hetzel et al.* [1995b], *Bozkurt and Satir* [2000], *Isik and Tekeli* [2001], *Lips et al.* [2001], *Okay* [2001], *Isik et al.* [2003, 2004], *Rimmelé et al.* [2003b], *Ring et al.* [2003a], *Cavazza et al.* [2009], and *van Hinsbergen and Boekhout* [2009].

the HP metamorphic rocks of the Lycian Nappes, which is interpreted as a thrust [*Bozkurt and Park*, 1999], a shear zone that was active during exhumation of the Lycian Nappes, with a top-to-the-east sense of shear [*Rimmelé et al.*, 2003a], or a likely Miocene N–S extensional evolution, with passive rotation of N–S stretching directions into the modern E–W directions [*Régnier et al.*, 2003; *Ring et al.*, 2003a].

[14] The CMM is a bivergent metamorphic dome that was exhumed along two extensional detachments: the northern one has a top-to-the-north sense of shear and has many names in literature, including Alaşehir detachment [*Isik et al.*, 2003], Gediz detachment [*Lips et al.*, 2001], Çanköy detachment [*Koçyiğit et al.*, 1999] or Kuzey detachment [*Ring et al.*, 1999a]). The southern detachment has a top-to-the-south sense of shear and is referred to as the Büyük Menderes detachment [*Bozkurt*, 2000, 2001b; *Lips et al.*, 2001] or Güney detachment [*Ring et al.*, 1999a]. Exhumation of the CMM dome seems essentially parallel, although *Lips et al.* [2001] reported only semibrittle fabrics and no overprint of the $^{40}Ar/^{39}Ar$ system in the footwall of the Büyük Menderes detachment, suggesting a slight dominance of the Alaşehir detachment. The middle Miocene age of onset of exhumation for the CMM suggested by crystallization and cooling ages and fission track dating [*Hetzel et al.*, 1995b; *Gessner et al.*, 2001b; *Lips et al.*, 2001; *Ring et al.*, 2003a; *Catlos and Cemen*, 2005; *Glodny and Hetzel*, 2007; *Catlos et al.*, 2010] is in line with the age of the supradetachment basins of the Alaşehir and Büyük Menderes grabens of ~16–15 Ma [*Sen and Seyitoğlu*, 2009]. The central axis of the CMM is formed by the Kücük Menderes Graben, which contains relics of middle Miocene (14.6–13.9 Ma) volcanics [*Bozkurt et al.*, 2008], indicating that this axis was already at or close to the surface at the onset of activity of the two flanking detachments. The amount of middle Miocene and younger exten-

sion accommodated by the CMM is thus more or less equal to the modern dimensions of the CMM.

[15] Finally, the northern Menderes Massif is overlain by a series of NE–SW trending, early Miocene basins [*Yilmaz et al.*, 2000; *Bozkurt*, 2001a, 2003; *Purvis and Robertson*, 2005]. From east to west, these include the Uşak, Güre, Selendi, Demirci, and Gördes basins, which hereafter will be referred to as the NMM basins. They are filled with terrestrial sediments and contain both felsic and mafic volcanic deposits [*Aldanmaz et al.*, 2000; *Ersoy et al.*, 2008; *Dilek and Altunkaynak*, 2009].

2.3. Rotations and Regional Structural Grain

[16] The Lycian Nappes, south of the Menderes Massif, consist of a stack of thrust slices derived from the northern passive margin of the Anatolide-Tauride block, and transported southward since the late Cretaceous [*Sengör and Yilmaz*, 1981; *Okay*, 1989; *Collins and Robertson*, 1998, 1999, 2003]. The final emplacement of the Lycian Nappes over the Bey Dağları region in southwestern Turkey (Figure 2) occurred in the early Miocene. This episode of south or southeastward thrusting is marked by the formation of an Aquitanian to Burdigalian foreland basin [*Poisson*, 1977; *Gutnic et al.*, 1979; *Hayward and Robertson*, 1982; *Hayward*, 1984a, 1984b; *Karabiyikoğlu et al.*, 2005]. Southward emplacement of the Lycian Nappes ceased at the end of the Burdigalian [*Poisson*, 1977; *Flecker et al.*, 1995].

[17] Recently, *van Hinsbergen et al.* [2010] redated the rotation history of Bey Dağları previously constrained by *Kissel and Poisson* [1987] and *Morris and Robertson* [1993] and showed that this region underwent no rotation between the late Cretaceous and middle Miocene (i.e., throughout the subduction and accretion history, as well as throughout the exhumation of the NMM and SMM and the southward thrusting of the Lycian Nappes), followed by ~20° counterclockwise rotation since the middle Miocene (between ~16 and 5 Ma, i.e., time equivalent with the exhumation of the of the CMM). In this paper we test whether the rotation of southwestern Turkey, identified in the Bey Dağları region, was associated with the exhumation of the central Menderes Massif.

[18] The central Menderes Massif is laterally discontinuous, disappearing eastward. The two bounding extensional detachments clearly converge eastward, at an angle of ~30° (Figure 3). This angle is also found in the regional pattern of stretching lineations: The regional structural grain related to MMM is remarkably (anti)parallel to the stretching lineations associated with the extensional shear zones and detachments along which the Menderes Massif(s) were exhumed (Figure 3). Moreover, both show a very consistent curved pattern, trending N–S in the SMM [*Bozkurt and Satir*, 2000; *Rimmelé et al.*, 2003b; *Bozkurt*, 2007] and NE–SW in the NMM [*Isik and Tekeli*, 2001; *Ring et al.*, 2003a; *Isik et al.*, 2004], curving over the CMM [*Hetzel et al.*, 1995b; *Bozkurt*, 2001b; *Lips et al.*, 2001; *Okay*, 2001; *Isik et al.*, 2003; *Ring et al.*, 2003a]. The stretching lineations span a circle segment with a center near the intersection point of the Alaşehir and Büyük Menderes detachments. To the west, extension becomes partitioned over several time-overlapping and time-consecutive extensional shear zones in, e.g., the Kazdağ massif [*Okay and Satir*, 2000; *Cavazza et al.*, 2009], Samos [*Ring et al.*, 1999b; *Kumerics et al.*, 2005], Ikaria [*Kumerics et al.*, 2005] and Kos [*van Hinsbergen and Boekhout*, 2009] (Figures 2 and 3).

3. Sampling

[19] To establish whether the southwest Anatolian rotations are correlated to the evolution of the central Menderes Massif, we focused our sampling strategy at the Oligo-Miocene basins of the Lycian Nappes (to test whether there are major rotation differences in the region between Bey Dağları and the Menderes Massif) and on the lower Miocene volcanic fields north of the CMM, filling the data gap between the Aegean island of Lesbos (where a large paleomagnetic data set was provided by *Kissel et al.* [1989] and *Beck et al.* [2001]) and the Afyon region to the east of the Menderes (where data were published by *Gürsoy et al.* [2003]). We refrained from sampling of Oligo-Miocene volcanic fields further to the north, where strands of the right-lateral North Anatolian Fault Zone are likely to lead to local rotations, disturbing the regional rotation pattern that is pursued in this paper. Finally, we collected samples from synkinematic granites in the Menderes Massif.

[20] We collected a total of 1827 independently oriented samples from 240 sites. All sampling locations, as well as the locations of previously published sites, are shown in Figure 2. We collected 974 samples from 140 lavas, ignimbrites and shallow intrusive rhyolitic plugs in lower to lower middle Miocene volcanic rocks (age range largely between ~21–15 Ma, see Table 1) in basins covering the NMM, as well as the region between the NMM and the west coast of Turkey overlying the Bornova flysch zone (Table 1).

[21] In western Turkey, we sampled 14 mafic lavas near Ayvalık (~20–21 Ma [*Aldanmaz et al.*, 2000]) and in the Bergama graben, a total of 14 lava sites were collected from a series of volcanic plugs and the southern flanks of the mount Kozak magmatic complex [see *Altunkaynak and Yilmaz*, 1998; *Boztuğ et al.*, 2009], with ages of ~15–18 Ma [*Borsi et al.*, 1972; *Aldanmaz et al.*, 2000]. Twenty-five lavas were sampled in the volcanic center of Dikili, which was described in detail by *Karacik et al.* [2007], with ages of 15–18 Ma [*Borsi et al.*, 1972; *Benda et al.*, 1974; *Aldanmaz et al.*, 2000]. Finally, 17 lavas were sampled in the Yuntdağ volcanic region (Figure 2). No radiometric ages were published from the Yuntdağ range, but *Akay and Erdogan* [2004] correlated its stratigraphy to the lower Miocene volcanics of Dikili and Bergama.

[22] We collected 10 sites from lavas north of Uşak (17–21 Ma [*Bingöl*, 1977]), 6 sites north of Güre (~16 Ma [*Seyitoglu et al.*, 1997]) and 7 sites near Ahmetlar, south of Güre (~13 Ma [*Ercan et al.*, 1996]). To the west, 20 sites were collected from felsic ignimbrites in the Selendi graben (15–20 Ma [*Ercan et al.*, 1996; *Seyitoglu et al.*, 1997; *Purvis et al.*, 2005; *Ersoy et al.*, 2008]). In the basin of Demirci, 17 lava sites were sampled in two flanks of a large caldera. No radiometric ages were reported from this volcano, but an early Miocene age of the Demirci basin stratigraphy was reported by *Kaya et al.* [2007]. Finally, 10 sites were sampled from two intrusive

Table 1. Paleomagnetic Results and Ages for the New and Published Lava Sites in Northwestern Turkey[a]

Locality and Lava Site	Lat	Lon	Type	Na	Nc	D	I	k	α95	Age (Ma)	A95	$A95_{min}$
Uşak				69						16.9–20.8 (1)		
US 1	38.7915	29.5543	gc	7	7	73.2	44.6	99.2	6.8			
US 2	38.7904	29.5534	gc	7	7	2.3	40.9	135.2	5.2			
US 3	38.7857	29.5487	gc	7	7	193.3	−41.9	72.1	7.2			
US 4[b]	38.7847	29.5493	gc/L	7	7	19.8	11.4	14.3	16.5			
US 5[b]	38.7831	29.5496	gc/L	7	7	347.4	32.7	16.2	15.5			
US 6[b]	38.7818	29.5580	gc/L	7	7	326.3	−15.4	11.4	18.7			
US 7[b]	38.7800	29.5527	gc/L	6	6	271.8	44.7	11.5	20.7			
US 8	38.7780	29.5543		7	5	314.0	61.0	173.8	5.8			
US 9	38.7620	29.5555	gc	7	6	342.8	57.8	134.7	5.8			
US 10	38.7744	29.5432	gc/L	7	6	159.6	72.1	67.6	7.4			
Güre				42						15.9 (2)		
GU 1	38.7796	29.2699	gc	7	6	195.4	−46.8	53.6	9.2			
GU 2[b]	38.7798	29.2691		7	7	98.1	−70.6	4.7	31.3			
GU 3[b]	38.7798	29.2691		7	4	213.1	−65.1	39.3	14.8			
GU 4	38.7798	29.2691		7	3	195.5	−46.6	519.9	5.4			
GU 5	38.7801	29.2683	gc	7	6	273.7	75.7	137.9	5.2			
GU 6	38.7801	29.2683		7	7	192.6	−47.8	161.9	4.8			
Ahmetlar				48						13.1 (3)		
AH 1[c]	38.44377	29.1547		7	7	166.9	18.1	177.1	4.5			
AH 2[c]	38.4468	29.1535		6	6	168.0	14.7	82.4	7.4		1.7	9.0
AH 3[c]	38.4483	29.1523		7	6	167.5	17.3	74.2	7.8			
AH1,2,3				21	19	167.0	15.8	105.0	3.3			
AH 4[b]	38.4548	29.1544	gc	7	7	193.2	−61.0	10.3	19.8			
AH 5[b]	38.4545	29.1545	gc	7	7	184.0	−68.2	9.3	20.9			
AH 6	38.4544	29.1550		7	7	151.9	8.9	77.2	6.9			
AH 7[b]	38.4550	29.1541		7	7	284.3	0.6	1.4	95.6			
Selendi				140						14.9–20.2 (2–5)		
SL 1	38.8246	28.8697		7	7	198.5	−59.5	375.0	3.1			
SL 2	38.8617	28.9249	gc	7	7	213.6	−42.1	267.7	3.7			
SL 3	38.8750	28.9289		7	5	203.6	−58.5	1121.9	2.3			
SL 4	38.8751	28.9290		7	7	202.1	−62.5	846.4	2.1			
SL 5	38.8731	28.9287		7	7	198.1	−59.7	252.9	3.8			
SL 6	38.8658	28.9281	gc	7	4	176.8	−56.2	108.2	8.9			
SL 7	38.9110	28.9369		7	7	356.5	50.8	204.8	4.2			
SL 8	38.9107	28.9416		7	3	184.9	−53.0	106.8	12.0			
SL 9	38.9093	28.9598		7	7	6.1	58.4	283.5	3.6			
SL 10	38.9093	28.9598	gc	7	7	166.9	−60.0	86.0	6.5			
SL 11	38.9093	28.9598		7	7	353.9	54.6	91.3	6.4			
SL 12	38.9131	28.9674	gc	7	7	7.8	56.7	27.0	11.8			
SL 13	38.9130	28.9676	gc	7	7	7.3	56.7	92.2	6.3			
SL 14	38.9130	28.9678	gc	7	6	358.2	56.7	144.1	5.6			
SL 15[b]	38.9130	28.9681	gc	7	7	2.9	56.2	41.5	9.5			
SL 16	38.9129	28.9686	gc	7	7	354.2	51.8	110.2	5.8			
SL 17	38.9127	28.9690	gc	7	7	352.2	54.5	251.5	4.2			
SL 18[b]	38.9129	28.9683	gc	7	7	311.6	44.2	21.2	13.4			
SL 19	38.8458	28.8845		7	7	210.0	−18.9	172.4	4.6			
SL 20	38.8412	28.8795		7		174.0	−37.2	125.3	6.0			
Demirci				117						early Miocene (6)		
DC1[c]	38.8812	28.5778		7	7	32.0	39.0	627.5	2.4			
DC2[c]	38.8807	28.5770		7	7	26.8	39.2	176.5	4.6			
DC3[c]	38.8802	28.5763		7	6	31.1	38.7	186.2	4.9		2.8	7.6
DC4[c]	38.8799	28.5759		7	7	33.1	41.9	363.2	3.2			
DC5[c]	38.88004	28.5755		7	7	34.0	43.4	328.7	3.3			
DC1–DC5				35	33	31.9	40.5	272.3	1.5			
DC6	38.88546	28.57002		7	7	14	29.6	676.9	2.3			
DC7[c]	38.88546	28.57		7	6	2.2	30.1	362.1	3.5			
DC8[c]	38.88546	28.57		7	7	5.4	30.8	284.7	3.6		3.6	8.2
DC9[c]	38.88546	28.57		7	7	1.8	31.8	440.5	2.9			
DC10[c]	38.88546	28.57		6	6	357.5	29.2	337.8	3.7			
DC7–DC10	38.88546	28.57002		27	26	1.9	30.6	277.3	1.7			
DC11	38.9405	28.5463		7	6	48.7	49.9	417.0	3.3			
DC12	38.9405	28.5460		7	7	53.5	46.4	70.2	7.3			
DC13	38.9403	28.5453		6	6	71.9	61.4	385.3	3.4			
DC14	38.9399	28.5439	gc	7	7	60.6	64.2	281.0	3.6			

Table 1. (continued)

Locality and Lava Site	Lat	Lon	Type	Na	Nc	D	I	k	α95	Age (Ma)	A95	$A95_{min}$
DC15	38.9400	28.5437		7	7	353.8	26.5	179.6	4.5			
DC16[b]	38.94009	28.54253		7	7	75.7	44.8	8.9	21.4			
DC17	38.93959	28.54189		7	7	42.8	60.8	1309.5	1.7			
Gördes				69						17.6–20.9 (4)		
GR 1[c]	38.8875	28.1719		7	7	167.4	−64.9	818.2	2.1			
GR 2[c]	38.8879	28.1719		7	7	161.2	−62.6	232.6	4.0			
GR 3[c]	38.8888	28.1718		7	7	153.2	−66.3	2547.1	1.2		5.8	8.2
GR 4[c]	38.8892	28.1715		7	7	167.9	−66.3	380.7	3.1			
GR1–GR	38.8875	28.1719		28	28	162.5	−65.1	139.1	2.4			
GR 5	38.8901	28.1705		7	7	164.0	−81.2	421.5	2.9			
GR 6[b]	38.8907	28.1705		7	0	-	-	-	-			
GR 7[c]	38.9027	28.1427		6	6	251.2	−57.7	261.7	4.1			
GR 8[c]	38.9032	28.1424		7	7	248.3	−61.8	145.1	5.0		5.9	8.2
GR 9[c]	38.9032	28.1427		7	7	261.0	−60.9	325.4	3.4			
GR 10[c]	38.9040	28.1430		7	7	247.3	−58.6	187.4	4.4			
GR7–GR10	38.9027	28.1427		27	27	248.7	−60.1	173.3	2.1			
Ayvalık				97						19.7–20.9 (7)		
AY 1	38.2929	26.6678		7	5	181.0	−58.7	182.7	5.7			
AY 2	39.2876	26.6720		7	5	206.8	−48.8	425.9	3.7			
AY 3	39.2882	26.6730		6	5	205.3	−42.3	3068.4	1.4			
AY 4	39.2895	26.6729	gc	7	7	34.3	48.6	21198.7	0.5			
AY 5	39.2904	26.6726	gc	7	6	6.5	58.6	1785.8	1.6			
AY 6	39.2741	26.6694	L	7	3	200.7	−34.1	196.1	8.8			
AY 7	39.3017	26.6259	gc	7	7	194.8	−45.0	212.4	4.2			
AY 8	39.3162	26.6566	gc	7	6	340.3	41.3	75.4	7.8			
AY 9	39.3027	26.6339	gc	7	7	175.7	−39.7	58.3	8.0			
AY 10	39.2924	26.6330	gc	7	7	227.4	−47.6	231.1	4.0			
AY 11	39.2913	26.6375		7	6	184.9	−40.4	441.7	3.2			
AY 12	39.2843	26.6430		7	7	158.1	−51.1	640.7	2.6			
AY 13	39.2844	26.6432		7	7	159.0	−41.1	96.1	6.2			
AY 14[b]	39.2874	26.6425		7	7	184.2	−44.0	15.9	11.6			
Dikili				175						15.2–18.2 (7–9)		
DI 1	38.9306	26.8941		7	7	207.5	−24.1	423.3	2.9			
DI 2	38.9297	26.8924		7	6	203.9	−32.5	339.5	3.6			
DI 3	38.9283	26.8894	gc	7	6	191.6	−63.4	92.5	6.3			
DI 4	38.9263	26.8903	gc	7	6	181.8	−56.4	1323.0	1.8			
DI 5[d]	38.9284	26.8788	gc	7	7	32.9	−33.2	167.8	4.7			
DI 6	38.9301	26.8751	gc	7	7	325.2	20.8	765.1	2.2			
DI 7	38.9315	26.8678	gc	7	7	352.9	73.8	498.2	2.7			
DI 8[b]	38.9350	26.8606	gc	7	7	211.1	18.1	46.3	9.0			
DI 9[d]	38.9374	26.8566	gc	7	7	298.3	−21.0	185.8	4.4			
DI 10	38.9463	26.8336	gc	7	7	7.1	36.9	254.4	2.5			
DI 11	38.9564	26.8152	gc	7	7	208.9	5.6	620.3	2.4			
DI 12	38.9573	26.8088	gc	7	7	211.9	−25.7	1194.9	1.7			
DI 13	38.9686	26.8024	gc	7	7	226.7	−35.0	52.1	8.4			
DI 14	38.9698	26.8017	gc	7	7	240.0	−27.1	1142.1	1.8			
DI 15[d]	38.9783	26.8026	gc	7	7	299.0	−24.3	72.0	7.2			
DI 16	38.9801	26.8021		7	7	237.1	−25.6	720.0	2.3			
DI 17	38.9823	26.8010		7	7	209.3	−28.3	93.0	6.3			
DI 18[d]	38.9842	26.7994	gc	7	7	143.8	−47.9	55.7	8.2			
DI 19	38.9855	26.7986	gc	7	7	209.0	−35.0	276.4	3.6			
DI 20	38.9848	26.7995	gc	7	7	211.7	−38.6	137.2	5.2			
DI 21[d]	39.0328	26.8572	gc	7	7	278.5	−11.9	178.6	4.5			
DI 22	39.0346	26.8362	gc	7	7	9.4	15.7	625.9	2.4			
DI 23	39.0447	26.8427	gc	7	7	326.9	21.4	72.9	7.1			
DI 24	39.0481	26.8451	gc	7	6	8.2	15.2	1677.6	1.6			
DI 25	39.0545	26.8506	gc	7	7	241.7	−4.9	549.7	2.6			
Bergama				98						15.2–18.5 (7, 8)		
BG 1	39.0528	27.0623	gc	7	7	346.6	54.3	161.9	4.8			
BG 2	39.0537	27.0619	gc	7	7	329.2	51.6	112.5	5.7			
BG 3	39.0571	27.0694	gc	7	7	16.6	15.4	1687.6	1.5			
BG 4	39.0603	27.0703	gc	7	7	327.6	63.9	268.5	3.7			
BG 5	39.0757	27.0923		7	7	353.8	60.4	425.1	2.9			
BG 6[b]	38.0830	27.1121		7	7	133.2	73.2	47.1	8.9			
BG 7	39.0783	27.1021		7	7	332.6	67.4	359.3	3.2			

Table 1. (continued)

Locality and Lava Site	Lat	Lon	Type	Na	Nc	D	I	k	α95	Age (Ma)	A95	$A95_{min}$
BG 8	39.0759	27.0878		7	7	28.6	52.7	217.8	4.1			
BG 9	39.0791	27.0794		7	7	3.7	35.8	1684.8	1.5			
BG 10[d]	39.0648	27.0232	gc	7	7	133.1	−67.0	172.8	4.6			
BG 11	39.0642	27.0157	gc	7	6	297.3	−79.9	37925.5	0.3			
BG 12	39.0647	27.0128	gc	7	7	81.7	67.8	993.4	1.9			
BG 13	39.0480	27.0205		7	7	18.0	63.4	435.5	2.9			
BG 14	39.0529	27.0265		7	7	17.0	32.6	1238.0	1.7			
Yuntdağ				119						early Miocene (10)		
YD 1[d]	38.9700	27.1776	gc	7	7	289.9	−13.4	86.8	6.5			
YD 2	38.9686	27.1780	gc	7	6	198.1	−8.7	96.7	6.2			
YD 3[d]	38.9643	27.1768	gc	7	6	118.6	−16.8	64.8	8.4			
YD 4[b]	38.9577	27.1824	gc	7	7	191.0	−17.3	36.1	10.2			
YD 5	38.9573	27.1828	gc	7	7	179.7	11.8	809.1	2.1			
YD 6[d]	38.9538	27.1822	gc	7	7	91.5	−23.0	65.1	7.5			
YD 7[b,d]	38.9502	27.1845	gc	7	6	112.7	−82.1	44.9	10.1			
YD 8	38.9417	27.1930	gc	7	7	234.5	−65.8	1499.3	1.6			
YD 9[d]	38.9368	27.2040	gc	7	7	294.5	−14.2	79.9	6.8			
YD 10	38.9353	27.2075	gc	7	7	34.8	−38.7	1425.0	1.6			
YD 11[d]	38.9391	27.2082	gc	7	7	264.3	−55.4	323.1	3.4			
YD 12	38.9420	27.2081		7	6	203.4	−29.5	367.5	3.5			
YD 13	38.9499	27.2042	gc	7	6	247.0	−38.5	8657.8	0.7			
YD 14[d]	38.9542	27.2031	gc	7	7	104.6	−44.1	79.1	6.8			
YD 15	38.9575	27.2041	gc	7	7	238.5	−37.1	1643.0	1.5			
YD 16[d]	38.9600	27.2042	gc	7	7	358.8	−28.3	212.3	4.3			
YD 17[d]	38.9663	27.2067	gc	7	7	151.9	−1.0	494.7	2.7			
Lesbos [*Kissel and Laj*, 1988]										20–16 (11, 12)		
LE 249	unknown	unknown			10	8.0	37.0	280.0	2.6			
LE 252	unknown	unknown			8	0.2	49.0	153.0	4.0			
LE 253	unknown	unknown			9	13.6	59.5	196.0	4.0			
LE 255	unknown	unknown			11	11.3	53.3	704.0	1.6			
LE 256	unknown	unknown			11	340.5	55.0	229.0	2.8			
LE 257	unknown	unknown			10	350.0	69.0	262.0	3.0			
LE 263	unknown	unknown			9	177.8	−49.0	1333.0	1.3			
LE 269	unknown	unknown			8	146.0	−63.6	177.0	3.7			
LE 271[b]	unknown	unknown			11	214.0	−20.0	15.0	10.0			
LE 272	unknown	unknown			10	191.7	−44.7	181.0	3.3			
LE 273	unknown	unknown			10	31.4	58.5	257.0	2.7			
LE 274	unknown	unknown			10	358.6	44.3	134.0	3.8			
LE 275	unknown	unknown			9	17.3	64.0	233.0	3.0			
LE 277	unknown	unknown			9	349.5	45.5	170.0	3.5			
LE 278	unknown	unknown			9	10.0	44.5	72.0	5.0			
LE 279	unknown	unknown			7	199.5	−20.0	144.0	4.4			
LE 280[b]	unknown	unknown			7	191.0	−41.0	46.0	7.8			
Lesbos [*Beck et al.*, 2001]												
Lesbos 01	39.3790	26.2130			8	261.1	−63.5	304.3	3.1			
Lesbos 02	39.3750	26.3000			8	27.3	67.8	184.2	4.1			
Lesbos 03	39.3610	26.2490			8	197.5	−19.3	318.2	3.1			
Lesbos 04	39.3620	26.2630			7	208.2	−15.9	400.0	3.0			
Lesbos 05	39.3510	26.3060			9	192.1	−41.7	320.0	2.9			
Lesbos 06	39.3510	26.3060			7	169.8	−31.1	166.7	4.7			
Lesbos 07	39.3640	26.3430			11	203.1	−54.1	500.0	2.2			
Lesbos 08	39.3650	26.3210			8	342.1	64.8	148.9	4.5			
Lesbos 09	39.3740	26.3170			8	99.0	−60.6	333.3	3.0			
Lesbos 10a	39.2500	26.1810			6	180.1	−69.0	1250.0	1.9			
Lesbos 10b	39.2500	26.1810			6	195.9	−55.5	74.6	7.8			
Lesbos 11[b]	39.2510	26.1720			9	215.1	−55.4	38.8	8.4			
Lesbos 12	39.3630	26.2720			5	194.3	−40.3	500.0	3.4			
Lesbos 13	39.3650	26.3000			9	247.8	−49.4	101.3	4.3			
Lesbos 14[b]	39.2570	26.1090			10	11.4	17.3	33.1	8.5			
Lesbos 15	39.2620	26.0650			10	19.0	49.2	333.3	2.6			
Lesbos 16	39.2460	26.0510			10	355.5	8.2	160.7	3.8			
Lesbos 17	39.2370	26.0310			6	326.9	48.8	625.0	2.7			
Lesbos 18	39.2370	26.0310			11	305.9	76.8	500.0	2.3			
Lesbos 19	39.2350	26.0340			5	325.9	41.8	148.1	6.3			
Lesbos 20	39.2390	26.2620			8	181.7	−18.0	142.9	4.6			
Lesbos 21	39.2670	26.2850			10	12.4	53.5	428.6	2.3			

Table 1. (continued)

Locality and Lava Site	Lat	Lon	Type	Na	Nc	D	I	k	α95	Age (Ma)	A95	$A95_{min}$
Lesbos 22	39.2990	26.3130			9	356.1	67.8	347.8	2.7			
Lesbos 23	39.3230	26.3020			8	321.9	54.4	269.2	3.4			
Lesbos 24	39.3490	26.3220			8	154.9	−46.0	875.0	1.9			
Lesbos 26	39.1560	25.9570			10	25.8	45.1	187.5	3.5			
Lesbos 27	39.1050	26.0150			7	320.7	41.6	272.7	3.6			
Lesbos 28[b]	39.3630	26.1990			7	150.9	−62.3	18.6	14.4			
Lesbos 29[b]	39.3480	26.2240			5	204.1	−15.9	46.5	11.3			
Lesbos 30	39.2360	26.0170			8	334.6	78.4	106.1	5.4			
Lesbos 31	39.2340	26.0200			7	39.5	73.2	333.3	3.3			
Lesbos 32	39.2430	26.0110			6	31.2	68.2	294.1	3.9			
Lesbos 33	39.2830	26.0040			9	10.0	26.5	210.5	3.5			
Lesbos 34	39.2460	25.9870			7	10.0	51.3	111.1	5.8			
Lesbos 35	39.2080	26.0330			8	9.0	44.7	189.2	4.0			
Lesbos 36	39.2150	26.0300			7	353.3	48.9	400.0	3.0			
Lesbos 37	39.2880	26.1200			10	13.0	63.1	204.5	3.4			
Lesbos 38	39.1910	26.1670			8	196.4	−42.4	538.5	2.4			
Lesbos 39	39.1520	26.1360			8	194.1	−56.5	194.4	4.0			
Lesbos 40	39.1360	26.1180			8	193.4	−49.4	777.8	2.0			
Lesbos 41[b]	39.1180	26.0910			7	155.3	−35.0	9.0	21.2			
Lesbos 42	39.1350	26.0830			8	179.7	−49.8	411.8	2.7			
Lesbos 43	39.1500	26.0580			8	178.2	−64.5	636.4	2.2			
Lesbos 45	39.1480	25.9830			7	359.3	54.1	1000.0	1.9			
Lesbos 46	39.1720	25.9380			8	8.5	26.7	241.4	3.6			
Lesbos 47	39.2270	25.9730			10	1.5	17.3	88.2	5.2			
Lesbos 48	39.2500	26.0470			10	344.4	16.4	187.5	3.6			
Lesbos 49a	39.3170	26.2350			6	34.8	70.5	185.2	4.9			
Lesbos 49b	39.3170	26.2530			4	51.6	47.6	300.0	5.2			
Lesbos 50	39.3170	26.2530			8	230.9	−40.6	72.9	6.5			
Afyon [*Gürsoy et al.*, 2003]										21–8 (13)		
Afyon-1	38.2221	30.6846			4	200.9	8.3	92.2	9.6			
Afyon-2	38.2387	30.4035			7	187.9	−48.4	966.2	1.9			
Afyon-3	38.4256	30.6960			8	37.8	−32.8	177.9	4.2			
Afyon-4[b]	38.5778	30.4940			5	93.5	51.2	43.5	11.7			
Afyon-5	38.5793	30.4865			3	94.7	−55.5	57.8	16.4			
Afyon-6	38.5612	30.4910			5	158.5	−50.7	201.5	5.4			
Afyon-7	38.6109	30.3674			5	238.0	−45.6	423.8	3.7			
Afyon-8	38.5959	30.3614			6	207.0	−55.7	76.8	7.7			
Afyon-9	38.6079	30.3448			8	173.3	−47.8	57.6	7.4			
Afyon-10	38.5959	30.3011			6	177.8	−42.6	305.0	3.8			
Afyon-11	38.5989	30.2996			6	184.4	−41.9	209.3	4.6			
Afyon-12	38.8008	30.4579			4	89.2	74.4	243.2	5.9			
Afyon-13[b]	38.6833	30.3569			6	174.9	−40.9	49.3	9.6			
Afyon-14[b]	38.5702	30.2785			5	215.9	−36.3	31.3	13.9			
Afyon-15	38.6622	30.4036			5	193.1	−40.8	452.9	3.6			
Afyon-16	38.7586	30.4533			6	24.7	63.6	267.8	4.1			
Afyon-17	38.7451	30.4051			4	202.3	67.7	275.3	5.5			
Afyon-18	38.7330	30.5600			7	199.3	−45.5	118.5	5.6			
Afyon-19	38.7230	30.5446			5	229.3	−48.0	76.7	8.8			
Afyon-20	38.7423	30.5323			6	81.7	29.4	181.2	5.0			
Afyon-21	38.7591	30.5430			5	89.9	68.2	60.4	9.9			
Afyon-22	38.7607	30.5553			7	61.6	−23.1	172.9	4.6			
Afyon-23	38.7823	30.5584			6	74.5	7.8	58.4	8.8			
Afyon-24[b]	38.7776	31.0783			4	288.6	3.7	15.7	24.0			
Afyon-25	38.7807	31.0998			7	172.5	−59.0	183.5	4.5			
Afyon-26	38.9176	31.2198			7	219.1	−22.2	820.5	2.1			
Afyon-27	38.9084	31.2167			7	204.2	−29.5	56.4	8.1			
Afyon-28	38.8961	31.2121			6	56.6	35.3	117.9	6.2			
Afyon-29	38.8407	31.2198			7	44.5	24.9	116.7	5.6			
Afyon-30	38.8192	31.1059			7	161.5	74.9	128.7	5.3			
Afyon-31	38.8192	31.1290			7	192.6	−36.8	116.6	5.6			
Afyon-32	38.8330	31.1752			7	178.1	−4.5	92.9	6.3			
Afyon-33	38.8223	31.1582			8	185.3	33.7	93.7	5.8			
Afyon-34	38.8915	31.1521			6	191.0	−56.6	199.7	4.8			
Afyon-35	38.8730	31.1659			7	197.0	−60.3	95.3	6.2			
Afyon-36	38.8653	31.1705			5	12.3	67.5	169.4	5.9			
Afyon-37	38.8499	31.2028			5	227.0	−45.7	95.2	7.9			
Afyon-38	38.8899	30.7876			7	207.9	−50.0	357.3	3.2			
Afyon-39	38.9038	30.8183			6	203.6	−51.6	129.9	5.9			

Table 1. (continued)

Locality and Lava Site	Lat	Lon	Type	Na	Nc	D	I	k	α95	Age (Ma)	A95	$A95_{min}$
Afyon-43	38.9776	30.7753			7	57.6	41.4	135.4	5.2			
Afyon-44	38.9822	30.7830			7	62.2	22.5	87.3	6.5			
Afyon-45	38.9191	30.8645			5	14.2	40.2	240.6	4.9			
Afyon-47	38.8961	30.8168			8	209.0	−47.2	596.5	2.3			
Afyon-48	39.0360	30.5430			7	5.9	35.0	1034.2	1.9			
Afyon-49	39.0483	30.5477			5	8.2	36.9	839.6	2.6			
Afyon-50	39.0576	30.5553			7	23.6	41.3	559.1	2.6			
Afyon-51	39.1652	30.5830			7	34.7	47.1	485.5	2.7			
Afyon-52	39.2452	30.5861			7	24.5	7.7	82.8	6.7			
Afyon-53	39.4251	30.4046			6	175.8	−29.8	124.7	6.0			
Afyon-54[b]	39.4375	30.4092			6	152.9	13.5	11.2	20.9			
Afyon-55	39.4113	30.3985			6	143.0	−47.1	314.4	3.8			
Afyon-56	39.3959	30.4062			5	237.1	−54.3	83.6	8.4			
Afyon-57	39.1452	30.4108			7	14.0	40.6	141.9	5.1			
Afyon-58	39.1683	30.4169			7	10.6	40.4	364.2	3.2			
Afyon-59	39.2637	30.3739			7	29.2	40.8	112.1	5.7			
Afyon-60	39.2560	30.3785			5	9.1	41.8	196.9	5.5			
Afyon-61	39.4328	30.5969			7	7.8	52.8	539.6	2.6			
Afyon-62	39.4528	30.5923			7	353.4	57.1	346.9	3.2			
Afyon-63	39.4605	30.5861			6	11.1	63.3	176.8	5.1			
Afyon-64	39.3421	30.5876			5	31.3	38.7	210.6	5.3			
Afyon-65[b]	39.4436	30.6015			7	275.8	3.9	26.4	12.0			
Afyon-66	39.4482	30.6061			6	68.2	−32.7	117.3	6.2			
Afyon-67	39.4836	30.4169			5	244.9	−40.0	53.8	10.5			
Afyon-68	39.4697	30.4154			7	168.0	−48.7	118.0	5.6			
Afyon-69	39.4559	30.4169			5	191.0	−61.7	405.3	3.8			
Afyon-70	39.4467	30.4431			7	20.9	63.3	212.1	4.2			
Afyon-71	39.4390	30.4415			5	250.7	58.7	73.1	9.0			
Afyon-72	39.4328	30.4369			7	19.0	42.5	524.5	2.6			
Afyon-73	38.8730	30.1524			7	211.8	−23.4	86.2	6.5			
Afyon-74	38.8730	30.1170			5	160.2	−30.6	112.7	7.2			
Afyon-75	38.7976	30.1385			7	231.1	−53.7	271.9	3.7			
Afyon-76	38.8007	30.4477			7	40.2	49.8	1278.0	1.7			
Afyon-77	38.7761	30.4800			4	72.6	62.6	221.4	6.2			
Afyon-78	38.7484	30.7568			5	179.8	−63.4	405.1	3.8			
Afyon-79	38.9115	30.6968			7	188.8	−26.6	485.8	2.7			
Afyon-80	38.7822	30.5585			7	359.5	49.8	245.2	3.9			
Afyon-81[b]	38.7608	30.5552			6	39.6	−53.9	36.9	11.2			
Afyon-82	38.7608	30.5554			7	61.7	0.5	75.1	7.0			

[a]Lat, latitude; Lon, longitude; type, gc, great circle; and L, entirely overprinted by lightning; Na, number of demagnetized samples; Nc, number of samples used to calculate average; D, declination; I, inclination; k, *Fisher* [1953] precision parameter; α95, 95% cone of confidence. Dashes indicate no data. References for ages are 1, *Bingöl* [1977], cited by *Aydar* [1998]; 2, *Seyitoglu et al.* [1997]; 3, *Ercan et al.* [1996], cited by *Ersoy and Helvaci* [2007]; 4, *Purvis et al.* [2005]; 5, *Ersoy et al.* [2008]; 6, *Kaya et al.* [2007]; 7, *Aldanmaz et al.* [2000]; 8, *Borsi et al.* [1972]; 9, *Benda et al.* [1974], cited by *Aydar* [1998]; 10, *Akay and Erdogan* [2004]; 11, *Fytikas et al.* [1984]; 12, *Pe-Piper and Piper* [1993]; 13, *Gürsoy et al.* [2003, and references therein].

[b]Sites with k value <50; removed from further analysis.

[c]Sites representing the same spot reading of paleosecular variation; these are binned to 1 direction for further analysis.

[d]Lightning-induced direction: removed from further analysis.

rhyolite plugs (~21–18 Ma old) in the Gördes basin [*Purvis et al.*, 2005].

[23] With the purpose to study synexhumation rotations, 509 paleomagnetic samples were collected from 73 sites in 12 larger or smaller granitoid bodies in the northern, central and southern Menderes Massif, as well as on the Aegean islands of Ikaria and Kos. Although none of these granite bodies yielded sensible paleomagnetic directions, we will briefly provide demagnetization characteristics and rock magnetic properties. Sampling locations are given in auxiliary material.[1] The granites we sampled postdate MMM [*Hetzel et al.*, 1995b; *Bozkurt and Park*, 1999; *Bozkurt*, 2001b; *Bozkurt and Oberhänsli*, 2001; *Bozkurt and Sözbilir*, 2004; *Isik et al.*, 2004; *Catlos and Cemen*, 2005; *Glodny and Hetzel*, 2007; *Catlos et al.*, 2010]. In the northern Menderes Massif, we collected 14 sites from the northern and southern part of the Eğrigöz granite and 8 from the Koyunoba granite, which were dated at 20.0 ± 0.7 to 21.0 ± 0.2 by K-Ar and $^{40}Ar/^{39}Ar$ dating on biotite, as well as SIMS U-Th-Pb analysis [*Bingöl et al.*, 1982; *Isik et al.*, 2004; *Ring and Collins*, 2005]. Furthermore we collected samples from a previously undated, but undeformed granite of Deliçoban and a pegmatite body near Gördes.

[24] In the central Menderes Massif, we collected four sites in the least deformed parts of the Salihli granitoid, which is located immediately below, and is deformed within the Alaşehir detachment, which bounds the CMM in the north.

[1]Auxiliary materials are available in the HTML. doi:10.1029/2009TC002596.

Ionprobe monazite dating of this granite yield an age range from 21.7 ± 4.5 to 9.6 ± 1.6 Ma [*Catlos and Cemen*, 2005; *Catlos et al.*, 2010], U-Pb dating gave 15.0 ± 0.3 Ma [*Glodny and Hetzel*, 2007] and biotite $^{40}Ar/^{39}Ar$ recorded cooling at 12.2 ± 0.4 Ma [*Hetzel et al.*, 1995b].

[25] In the southern Menderes Massif, we collected seven sites from one leucogranite intrusion near Kafaca, described by *Bozkurt* [2004], who concluded that the age of this granite should at least be younger than a 36 ± 2 Ma cooling age reported by *Lips et al.* [2001]. Additionally, we collected four sites from undated leucogranitic dikes near Sakarkaya and Kayabükü.

[26] Finally, in an attempt to correlate foreseen paleomagnetic results from Menderes granites to previously published paleomagnetic data from the Cycladic granitoids [*Morris and Anderson*, 1996; *Avigad et al.*, 1998], we collected a total of 15 sites from two granite bodies on the island of Ikaria (Figure 2), known as the I- and S-type granites [*Altherr et al.*, 1982], with biotite $^{40}Ar/^{39}Ar$ cooling ages of 17.9 ± 0.5 and 10.7 ± 0.3 Ma, respectively [*Kumerics et al.*, 2005]. Seven more sites were collected from an undeformed monzonite body exposed on the island of Kos, which was dated at ~12 Ma [*Altherr et al.*, 1976], intruded at shallow crustal levels deduced from a contact metamorphic aureole [*Gralla*, 1982; *Kalt et al.*, 1998].

[27] Recently, *van Hinsbergen et al.* [2010] concluded that the rotation of Bey Dağları postdated the emplacement of the Lycian Nappes over the Bey Dağları Platform. If that is correct, the Lycian Nappes should have experienced this same rotation phase. Moreover, the Lycian Nappes may have experienced rotations during their early Miocene southward transport, documented by the development of an Aquitanian to Burdigalian foreland basin on top of Bey Dağları [*Hayward and Robertson*, 1982; *Hayward*, 1984a]. Therefore, we collected 344 samples from 27 sites in four sedimentary basins that developed in the Lycian Nappes between the Oligocene and Pleistocene (Table 2). In the northwest, around the transition between the nonmetamorphic and HP-LT metamorphic domains, lies the Kale basin, which was previously interpreted by *Seyitoglu et al.* [2004] to have formed above the southern breakaway fault of late Oligocene to early Miocene part of the Menderes metamorphic core complex. The Kale basin is filled with Chattian to Aquitanian (~28–21 Ma) terrestrial clastic deposits dominated by clays, and many coal-bearing horizons. Near Kale, these are unconformably overlain by shallow marine carbonates of Burdigalian age (~21–16 Ma). Palynological dating of the stratigraphy of the Kale basin was provided by *Akgün and Sözbilir* [2001]. From the upper Oligocene to Aquitanian clastic deposits, we collected a total of 96 samples from seven sites. Additionally, we collected 40 samples at two sites in the Burdigalian limestones.

[28] South of the Kale basin, we collected samples from the Çameli Basin. Covering the Lycian Nappes in the northeast of this basin, near Acıpayam, Burdigalian limestones correlated to those near Kale overlie terrestrial red sandstones, conglomerates and lacustrine limestones [*Hakyemez*, 1989; see also *Alçiçek and ten Veen*, 2008, and references therein]. We collected 68 samples at 7 sites from both the terrestrial and marine lower Miocene deposits here. Additionally, we collected 70 samples from 4 sites in beige marls and blue clays in the Çameli basin. The basin fill was dated at upper Miocene to Pliocene (~11–3 Ma [*Alçiçek et al.*, 2005, 2006, and references therein]).

[29] Finally, 70 samples were collected from 7 sites in upper Plio-Pleistocene blue lacustrine marls near Burdur [*Kazanci and Erol*, 1987; *Kazanci*, 1990; *Sentürk and Yagmurlu*, 2003; *Schulz-Mirbach and Reichenbacher*, 2008]. These deposits form rhythmically bedded, several hundreds of meter thick successions along the southern border of lake Burdur, and we collected these samples to corroborate the finding of *Kissel and Poisson* [1986] and *Tatar et al.* [2002] that rotations in SW Anatolia predate the late Plio-Pleistocene.

4. Paleomagnetic and Supporting Rock Magnetic Methods

[30] Samples were collected with a water-cooled, generator-powered electric drill or a handheld gasoline-powered drill with water-cooled diamond-coated drill bits. The orientation was measured with a magnetic and if needed sun compass, and corrected for local declination (4°). They were cut into standard specimens of 1 inch diameter and 22 mm length.

[31] Demagnetization was mostly performed with alternating fields (AF) with 5–10 mT increments up to 100 mT, with a degausser interfaced with a magnetometer through a laboratory-built automated handling device. A selection of samples was thermally demagnetized with small temperature increments of 20°C–80°C in a magnetically shielded, laboratory-built furnace to check for consistency of directions between AF and thermal demagnetization. The natural remanent magnetization (NRM) and isothermal remanent magnetization (IRM) were measured on a 2G Enterprises horizontal DC-SQUID magnetometer (noise level 3×10^{-12} A m^2).

[32] To support paleomagnetic interpretations, various rock magnetic properties were determined of selected samples. Thermomagnetic data were acquired from seven sedimentary samples and three granite samples, representative for the sampled populations, with a modified horizontal translation type Curie balance that uses a cycling field between 150 and 300 mT rather than a fixed applied field [*Mullender et al.*, 1993], noise level ~4×10^{-9} A m^2). About 40 mg of sample material was weighed in a quartz glass sample holder. To discriminate between magnetic behavior and chemical alteration we applied the so-called segmented run protocol in which heating is applied to a certain temperature followed by cooling of 100°C before heating to the next temperature. Magnetic behavior is documented by reversible heating and cooling branches while chemically induced changes up to the temperature of interest are manifested by irreversible magnetic behavior.

[33] For the lower Miocene lavas, we determined the variation of the low-field magnetic susceptibility from room temperature to 700°C. Therefore, we used a KLY3 Kappabridge susceptibility meter with attached CS-3 furnace (noise level ~5×10^{-8} SI). Crushed powder material (~200 mg) was taken from a total of 18 characteristic specimens, at least one per locality, which were heated and cooled in air in two successive cycles: 40°C–400°C–40°C and 40°C–700°C–40°C.

Table 2. Paleomagnetic Results and Ages for Sites in the Lycian Nappes[a]

					Tilt Corrected									
Locality Site	Lat	Lon	Na	Nc	D	ΔDx	I	Dix	K(vgp)	A95(vgp)	$A95_{min}$	$A95_{max}$	Lithology	Age (Ma)
Kale			136	50	340	3.3	36.2	4.6	42.3	**3.1**	**3.6**	6.6		Oligocene–early Miocene (1)
KL 1[b]	37.4501	28.8368	20	14	21.5	31	34.3	44	2.9	**28.7**	5.4	**15.8**	limestone	early Miocene
KL 2[b]	37.4494	28.8348	20	8	0.3	100	68.5	33.0	2.3	**47.1**	6.5	**23.1**	limestone	early Miocene
KL 3	37.5405	28.7919	20	16	198	11	54.2	9.1	18.0	8.9	5.2	14.4	blue clay	Oligocene
KL 4	37.4731	28.7237	11	6	154	14.9	−35.0	21	23.8	14.0	7.2	28.1	blue clay	Oligocene
KL 5	37.4730	28.6989	10	9	338.3	8.5	53.3	7.3	54.8	7.0	6.3	21.3	sandstone	Oligocene
KL 6	37.5145	28.8238	14	8	170	5.9	−17	11	92.6	**5.8**	**6.5**	23.1	blue clay	Oligocene
KL 7	37.5669	28.8623	16	14	338	3.9	33.0	5.7	119	**3.7**	**5.4**	15.8	blue clay	Oligocene
KL 8	37.5659	28.8617	15	12	155	6.9	−38	9.2	47.2	6.4	5.7	17.5	blue clay	Oligocene
KL 9	37.5932	28.2914	10	9	168	7.8	−37	11	51	7.3	6.3	21.3	blue clay	Oligocene
Acıpayam			68	46	351	3.4	48.4	3.4	51.2	3.0	3.7	7.0		early Miocene (2)
AC 1	37.3988	29.2908	10	8	357	8.9	44.8	10.0	49.7	7.9	6.5	23.1	limestone	
AC 2	37.3986	29.2914	10	7	356	8.3	44.2	9.5	66.8	7.4	6.8	25.3	limestone	
AC 3	37.3972	29.2924	10	9	4.6	100	51.0	100	1.2	**104.4**	6.3	**21.3**	limestone	
AC 4	37.4083	29.3187	9	9	353.0	7.4	48.3	7.5	64.9	6.4	6.3	21.3	blue silt	
AC 5	37.4105	29.3320	9	9	340	5.7	51.8	5.1	118	**4.8**	**6.3**	21.3	red clay	
AC 6	37.4103	29.2897	10	6	350	17.0	50.3	16	22.4	14.5	7.2	28.1	limestone	
AC 7	37.4166	29.3285	10	8	348	9.4	47.7	9.7	46.2	8.2	6.5	23.1	red clay	
Kelekçi			70	48	347	6.7	51.8	6.1	14.3	5.6	3.6	6.8		late Mio–Pliocene (3)
KE 1	37.2316	29.3070	10	8	186	23	−24	39	7.3	22.1	6.5	23.1	blue silt	
KE 2	37.2350	29.3561	20	9	355	15	59.6	10.0	21.8	11.3	6.3	21.3	marl	
KE 3	37.2285	29.3547	20	12	336	12	57	8.8	22.8	9.3	5.7	17.5	marl	
KE 4	37.2233	29.3326	20	20	343	9.9	54.1	8.3	17.1	8.1	4.8	12.4	blue clay	
Burdur			70											Pleistocene (4)
BU 1	37.7187	30.2979	10	9	178	14	−58	10	23.5	10.8	6.3	21.3	blue clay	
BU 2	37.7186	30.2980	10	0	-	-	-	-	-	-			blue clay	
BU 3	37.7176	30.2981	10	0	-	-	-	-	-	-			blue clay	
BU 4	37.7170	30.2983	10	0	-	-	-	-	-	-			blue clay	
BU 5	37.7167	30.2983	10	0	-	-	-	-	-	-			blue clay	
BU 6	37.7167	30.2983	10	0	-	-	-	-	-	-			blue clay	
BU 7	37.7167	30.2983	10	0	-	-	-	-	-	-			blue clay	

[a]Bold values indicate the A95 value falls outside the A95min-max envelope; bold A95min-max values indicate whether A95 is higher than A95max or lower than A95min, respectively. Lat, latitude; Lon, longitude; Na, number of demagnetized samples; Nc, number of samples used to calculate average; D, declination; ΔD_x, error on declination; I, inclination; ΔD_x, error on inclination; $K_{(vgp)}$, *Fisher* [1953] precision parameter (determined on the virtual geomagnetic poles); $A95_{(vgp)}$, 95% cone of confidence around the average virtual geomagnetic pole. $A95_{min}$ and $A95_{max}$ delimit the boundaries of A95 values that can be straightforwardly explained by paleosecular variation alone (Deenen et al., submitted manuscript, 2010). Dashes indicate no data. References for ages are 1, *Akgün and Sözbilir* [2001]; 2, *Hakyemez* [1989], see also *Alçiçek and ten Veen* [2008, and references therein]; 3, *Alçiçek et al.* [2005, 2006, and references therein]; 4, *Kazanci and Erol* [1987], *Kazanci* [1990], *Sentürk and Yagmurlu* [2003], and *Schulz-Mirbach and Reichenbacher* [2008].
[b]A95 ≫ A95 max: removed from further analysis.

[34] IRM acquisition curves were measured up to 700 mT with 57 steps. Nine curves were acquired from representative granite samples, 28 from sediments and eight from the lower Miocene lavas. The lavas, some granites and sediments showed high NRM intensities and small portions of 30–200 mg of these samples were embedded in epoxy cylinders to be measured. The robotized 2G Enterprises SQUID magnetometer with in-line AF demagnetization, ARM and IRM acquisition facilities was utilized to this end. IRM acquisition was done from the so-called AF demagnetized starting state: prior to the IRM acquisition the samples were demagnetized in three orthogonal axes at 300 mT AF with a laboratory-built demagnetization coil. This ensures that the shape of the measured IRM acquisition curves deviates minimally from a cumulative log Gaussian distribution [cf. *Heslop et al.*, 2004].

[35] From 13 samples, one for each granite and for two sampling locations in the I type granite of Ikaria, hysteresis loops (between ±2 T) were determined with a MicroMag 2900 alternating gradient magnetometer (Princeton, New Jersey, noise level ~4×10^{-11} A m^2). Averaging time for each data point was 0.2 s and the field increment between subsequent data points was 10.0 mT. For the back field curves a waiting time of 0.2 s was adopted. Unfortunately, in most cases samples appeared to be very weakly magnetic which precluded determination of meaningful loops.

5. Paleomagnetic Results

5.1. Rock Magnetic Properties

5.1.1. Temperature Dependence of Magnetization and Low-Field Susceptibility

[36] Examples of thermomagnetic runs are shown in Figure 4. Most granites appear to have a very weak magnetization (Figure 4a). The dominant magnetic mineral is magnetite that is oxidized above its Curie temperature to hematite, illustrated by the cooling branch lying below the heating branch. The few strongly magnetic granites (Figure 4b) show that during the segmented heating branches some magnetiza-

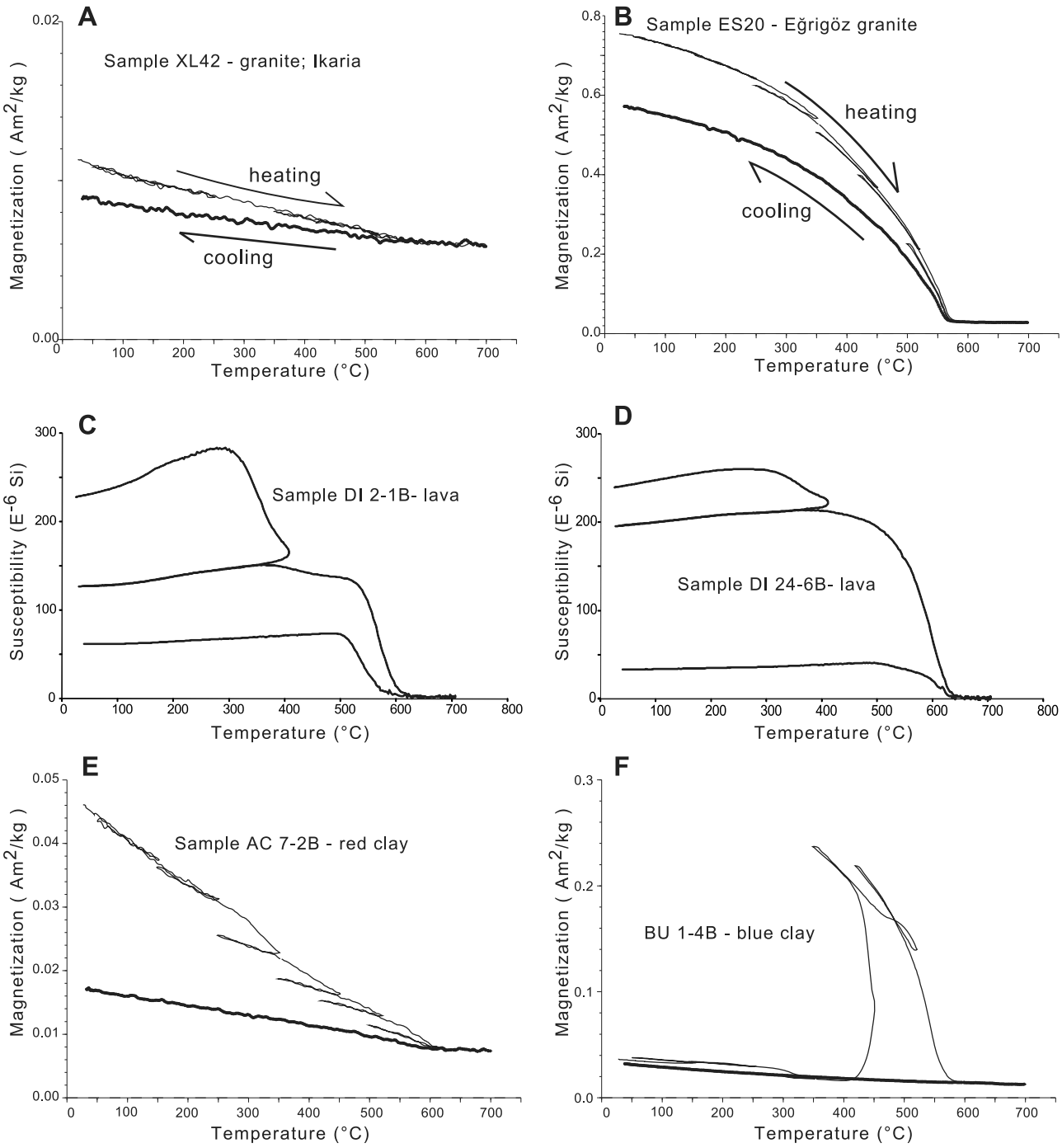

Figure 4. (a, b, e, f) Thermomagnetic curves generated with the segmented heating protocol. The final cooling segment is indicated with the thicker black line. The noisy appearance testifies the weak magnetic signals. See text for explanation of the thermomagnetic behavior; (c, d) Typical weak field thermomagnetic curves of normalized susceptibility for representative samples during cycles of heating and subsequent cooling with two cycles at 40°C–400°C–40°C and then 40°C–700°C–40°C.

tion is already lost presumably related to maghemitized surface layers that are inverted to the considerably less magnetic hematite. The interval between ~300°C and ~450°C shows a larger decrease. The Curie temperature is ~575°C (determined by the two-tangent method). During the final cooling branch again some magnetization is lost. In the volcanic samples, the removal of maghemitized surface layers (or discrete maghemite particles) is also inferred from the irreversible loss in low-field susceptibility between ~300°C and ~400°C (Figures 4c and 4d). The second major decrease is occurring

between ~500°C and ~600°C and testifies the dominance of magnetite that can be variably oxidized: note that sample DI24.5B (Figure 4d) has a tail well beyond 600°C. The final cooling branch is below the heating branch indicating that the magnetite has been partially oxidized to hematite during the experiment.

[37] Most of the sediments are essentially paramagnetic and show reversible thermomagnetic curves. Some of the more magnetic samples are shown in Figures 6e and 6f. Sample AC 7.2B (red clay) shows reversible behavior up to 250°C and continuous removal of magnetization at higher temperatures. The extra decay between ~300°C and ~450°C is likely due to removal of maghemite or maghemitized surface layers. Greigite (Fe_3S_4) alteration is not likely as an explanation because the peak in magnetization related to the oxidation of pyrite (see Figure 4f) that always accompanies greigite is absent. Partially maghemitized magnetite is largely removed upon heating to 700°C because the final cooling branch is well below the heating branches. Sample BU1.4B (blue clay) is shown in Figure 4f. The minor increase in magnetization occurring from 100°C to 150°C could be related to the presence of goethite (α-FeOOH) that shows an increase in magnetization because it is cycled in a non-saturating magnetic field [*de Boer and Dekkers*, 1998]. The decrease in magnetization between 300°C and 350°C is likely related to greigite because associated pyrite is oxidized via magnetite to hematite. The magnetite occurrence generates the large increase in magnetization between 420°C and 580°C. It is a transient phase in the experiment because the final cooling branch does not show a discontinuity at ~580°C indicative of magnetite's Curie temperature. The dominance of (maghemitized) magnetite in the sample collection makes demagnetization of the NRM by alternating fields attractive.

5.1.2. Hysteresis Loops

[38] The granites show erratic directional NRM demagnetization behavior yet individual samples yield technically correct demagnetization diagrams (see section 5.2). In an attempt to shed light on this phenomenon, hysteresis loops were determined. In line with the thermomagnetic analysis most sites show extremely low magnetizations. After correction for the high-field slope in the hysteresis loops, noisy and noninterpretable loops are the result. Three sites that yield sufficient quality loops (EN 12, EN 20, and KM 4), provide M_{rs}/M_s ratios of 0.028, 0.006, and 0.007, while B_{cr}/B_c is 5.3, 19.7, and 20.1, respectively, all indicating large multidomain particles. Therefore, we relate the erratic directional behavior to insufficient averaging because of large grain size.

5.1.3. Component Analysis of IRM Acquisition Curves

[39] IRM acquisition curves were fit with two or three coercivity components using the software package of *Kruiver et al.* [2001]. "Component 1" is a low-coercivity component, "component 2" the high-coercivity component, and "component 3" is a very low coercivity component required for proper fitting in the lowest coercivity component. This latter component is not assigned physical meaning [cf. *Heslop et al.*, 2004] and its amount is added to component 1 since both components reflect the same magnetic mineral. Overall component 1 is magnetite of a certain grain size depending on its $B_{1/2}$ while component 2 is interpreted to be hematite. Examples of fits are shown in Figure 5 while all results are compiled in Table 3 grouped according to lithology. Component 1 in granites has an average of ~60 mT with a DP of 0.30 log units. In almost all cases no component 3 is required for a decent fit. Therefore, we interpret the fairly high DP as indication for the presence of a wide grain size range including multidomain particles. $B_{1/2}$ of component 2 is ~200 mT with one exception (KO 36B, 700 mT). Note that the amount of magnetic minerals as expressed by the total IRM on a mass-specific basis is very low. In the volcanics $B_{1/2}$ of component 1 is ~46 mT with a DP of ~0.28 log units, associated with magnetite. It is remarkable that the granites have a harder magnetite than the volcanics. DP is smaller indicating a more confined grain size distribution. A tentative explanation could be that the multidomain particle fraction has their IRM relaxed on short time scales. In the volcanics component 2 is present in small amounts (a few percent) with $B_{1/2}$ of ~300 mT which indicates a minute amount of hematite or a tail of hard titanomaghemite. It occurs dominantly in some reddish oxidized samples from site AY. The sediments are grouped according to lithology. Component 1 (~95% of the total IRM) of blue clay samples has $B_{1/2}$ of ~47 mT and DP of ~0.28 log units, very similar to those of *van Hinsbergen et al.* [2010]. They are typical of detrital magnetite. The remaining ~5% is component 2, interpreted to be hematite. As in the work by *van Hinsbergen et al.* [2010], component 1 of the limestones has a higher $B_{1/2}$ (~57 mT) than that of the blue clays representing a higher proportion of SD magnetite particles. Marls resemble the blue clays in line with their raised detrital component. The red beds are notably soft with a $B_{1/2}$ of component 1 of ~35 mT. The amount of hematite is low (~7%) although that could be an underestimate because of the maximum available pulse field of 700 mT. One of the two siltstone samples resembles the blue clays while the other is similar to the limestones. All lithologies are dominated by low-coercivity magnetic minerals making the collection amenable to processing with alternating fields.

5.2. NRM Demagnetization Results

[40] Identification of the characteristic remanent magnetization (ChRM) was done upon inspection of decay curves, equal-area projections and vector endpoint diagrams [*Zijderveld*, 1967]. Initial intensities for the sediments of the Lycian Nappes were variable, ranging between 5 μA/m and 100 mA/m. For the volcanic samples, these ranged typically from 0.5 to 2.0 A/m and initial intensities in the granites were in most cases low, between 20 μA/m and 20 mA/m, with the exception of the Kos monzonite and the Eğrigöz granite, which had very high initial intensities between 1 and 7 A/m.

[41] In most samples from the Kale, Ayvalık and Kelekçi, univectorial decay toward the origin of 90% of the NRM occurs between 15 and 70 mT and is thus defined as the ChRM (Figures 6n, 6o, and 6p). The upper Plio-Pleistocene blue clays from Burdur generally give a very poor result (Figure 6q), and only in one site, technically sensible directions were obtained.

[42] The volcanic rocks reveal fairly simple demagnetization behavior (Figures 6e and 6f). Alternating field and thermal demagnetization yielded similar results (Figures 6g and 6h). Univectorial decay toward the origin of 90% of the

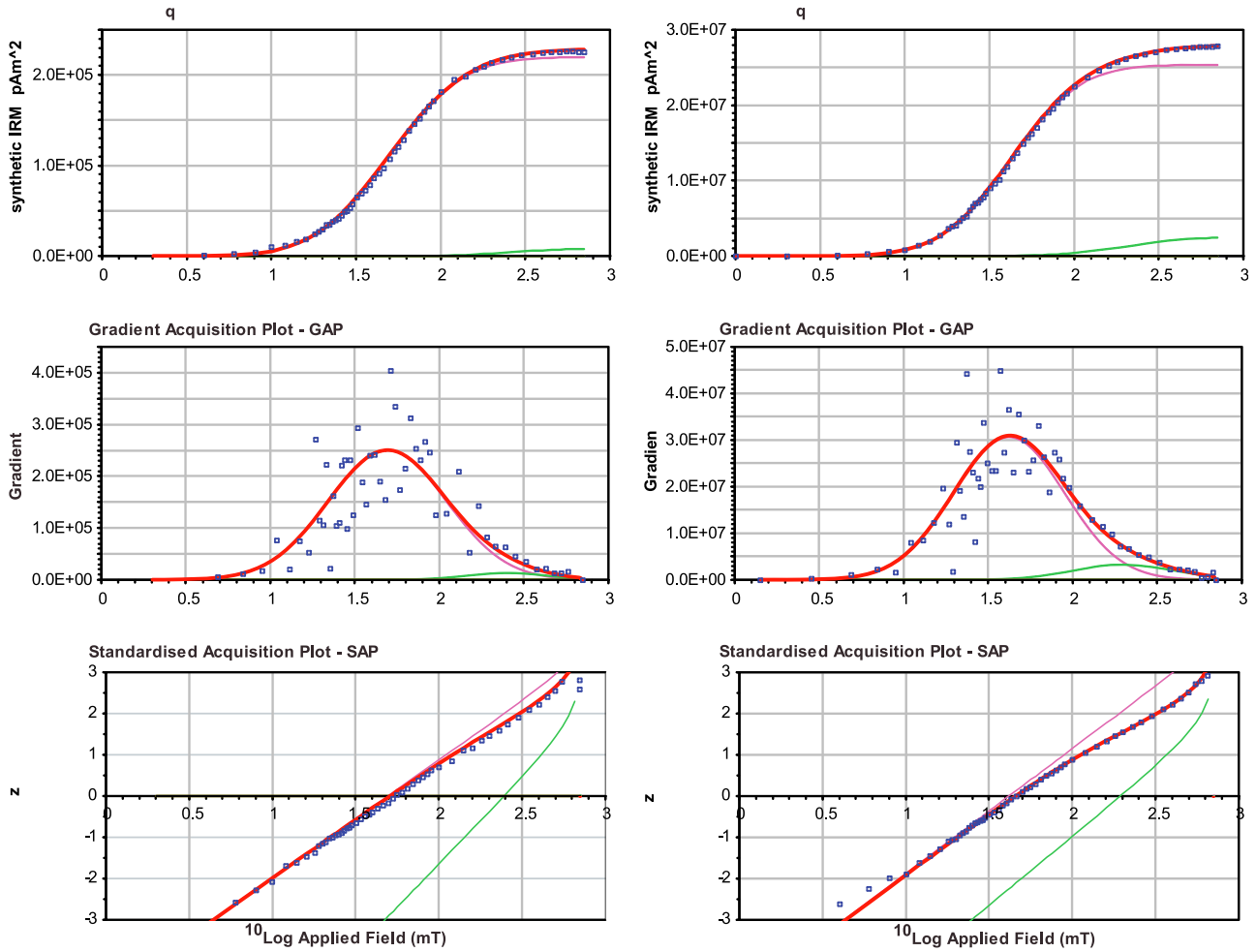

Figure 5. Examples of the interactive fitting of IRM acquisition curves [*Kruiver et al.*, 2001]. In most limestones component 1 (purple), interpreted to be magnetite, is harder than in the blue clays. Component 3 (green) is given no physical meaning; it is a consequence of the fitting procedure that works with symmetric distributions in the log-field space; further explanation is provided in the text. Component 2 (blue) is interpreted as hematite. The sum of the components is given by the red curves; interactively difference between measured data points (open squares) and the red model curve is minimized in the three representations of the data. The complete outcome of the fitting is provided in Table S2 in the auxiliary material.

NRM occurs between 15 and 70 mT and is thus defined as the ChRM. This range of unblocking is typical for titanomagnetite or titanomaghaemite coercivities [*Dunlop and Özdemir*, 1997]. Frequently, however, one or several samples of a site have overprints overlapping the ChRM, typically of abnormally high magnetic intensity with random directions. These are likely related to lightning strikes (Figures 6j and 6k). Because this possibility was already foreseen, we applied a sampling strategy in which samples were collected across several tens of meters in a single flow unit. Therefore, the lightning-induced overprint direction is in most cases strongly variable, and the intersection point of remagnetization great circles [*McFadden and McElhinny*, 1988], which describe the plane defined by the ChRM and the lightning-induced remagnetization direction, allows identification of the ChRM (Figure 6m). In some sites from Yuntdağ, Bergama and Dikili, only an average great circle could be reconstructed in a lava site (Figure 6l).

[43] From all granites we thermally demagnetized one sample per site to test demagnetization behavior, and from locality Eğrigöz south (ES), all samples were thermally demagnetized. The results can be subdivided into two clusters: the vast majority of samples yielded no interpretable paleomagnetic direction, largely owing to very low initial intensities (below 20 μA/m; Figures 6c and 6d). Exceptions were formed by the Eğrigöz granite and the Kos monzonite, of which most samples give very clear, but entirely random directions (Figures 6a and 6b). The results for 41 samples from the seven sites of Eğrigöz south reveal a gunshot pattern (Figure 7). We owe this behavior to the multidomain character of the carrying magnetite. To make sure these results are not caused by some unidentified thermal demagnetization effect, we demagnetized 7 samples from selected granites

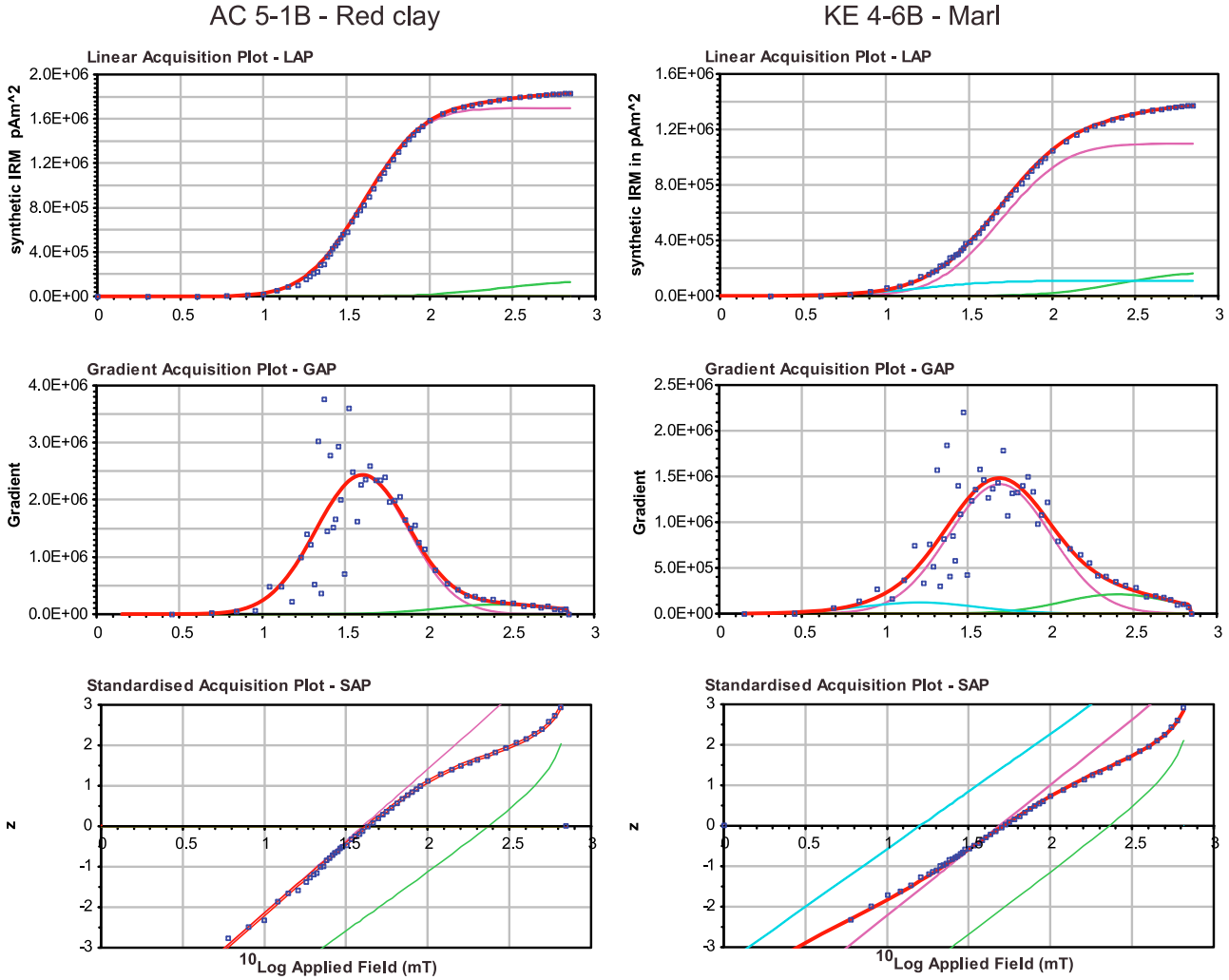

Figure 5. (continued)

through alternating field demagnetization, but these did not provide sensible results either. Unfortunately, the paleomagnetic analysis of the 12 granite bodies of the Menderes, Kos and Ikaria do not provide paleomagnetic information that can be used to constrain their kinematic histories.

5.3. ChRM Direction Analysis

[44] ChRM directions were calculated by principal component analysis [*Kirschvink*, 1980] or remagnetization great circles were determined [*McFadden and McElhinny*, 1988]. ChRM directions or great circles with maximum angular deviation exceeding 15° were rejected from further analysis. Thus, from the sedimentary samples, 153 ChRM directions were determined from 344 analyzed specimens. For the lavas, 911 directions were obtained from 974 analyzed specimens.

5.3.1. Lycian Basins: Sediments

[45] For each site and locality from the basins on the Lycian Nappes, the *Vandamme* [1994] cutoff was applied to discard widely outlying ChRM directions. Averages and cones of confidence were determined using *Fisher* [1953] statistics applied on virtual geomagnetic poles (VGP), because these are more Fisherian (i.e., a Gaussian dispersion on a sphere) than directions, which have a (latitude-dependent) elongated distribution [*Tauxe and Kent*, 2004; *Tauxe et al.*, 2008; M. H. Deenen et al., New reliability criteria for paleomagnetic data sets: An alternative statistical approach in paleomagnetism, submitted to *Geophysics Journal International*, 2010]. Errors in declination and inclination are given separately, as ΔD_x and ΔI_x, following [*Butler*, 1992; Deenen et al., submitted manuscript, 2010] (Table 1). In the total average of the Kale locality, three directions were eliminated by the *Vandamme* [1994] variable cutoff procedure, one in the Acıpayam final average, and three for Kelekçi (Figure 8).

[46] Recently, Deenen et al. (submitted manuscript, 2010) defined reliability criteria for paleomagnetic data, that test whether an observed distribution can be straightforwardly explained by paleosecular variation (PSV) alone. Therefore,

Table 3. Statistical Properties of the Various Localities of NW Anatolian Lavas Defined and Discussed in This Paper[a]

Locality	Reversal Test	Critical Angle	Angle	Na	Tilt Corrected							$A95_{min}$	$A95_{max}$
					vD	D	ΔD	I	ΔI	K(vgp)	$A95_{(vgp)}$		
West Anatolian lower Miocene lavas	negative	6.1	7.9										
All lavas				235	210	12.4	3.6	47.9	3.7	10.5	**3.2**	2.2	**2.8**
Normal				112	99	8.5	5.2	50.7	5	10.9	4.5	2.9	4.7
Reversed				123	104	197.0	5.1	−43.7	5.9	10.2	4.6	2.8	4.6
Afyon[b] (classification C)	positive	13.0	12.5	71	57	21.3	6.0	45.5	6.7	13.2	5.4	3.4	6.9
Normal				35	32	30.7	10.6	43.6	12.2	8.1	9.5	4.1	10.2
Reversed				38	34	196	8.9	−43.5	10.3	10.4	8.0	4.1	9.8
NMM Basins (classification C)	positive	12.8	0.5	40	38	13.4	9.2	52.7	8.0	10.2	7.7	3.9	9.1
Normal				22	20	14.9	14.3	53.8	12.0	8.7	11.7	4.8	14.0
Reversed				18	16	194.6	11.6	−54.3	9.6	15.0	9.5	5.2	16.3
West Mainland	negative	16.2	28.6	64	52	16.0	8.7	42.6	10.3	7.3	**7.9**	3.5	**6.5**
Normal				20	19	358.0	12.0	45.8	13.1	10.9	10.7	4.9	12.8
Reversed				44	38	217.2	13.9	−41.0	17.2	4.3	12.7	3.9	8.0
Ayvalık_Bergama (classification C)	positive	14.2	7.1	25	23	5.5	9.6	49.6	9.4	14.3	8.3	4.6	11.3
Normal				14	13	2.0	14.1	51.8	12.7	13.2	11.9	5.6	16.6
Reversed				11	10	189.6	14.0	−46.7	14.9	16.3	12.3	6.1	19.8
Lesbos_TC[c]	negative	10.4	12.1	60	58	6.3	6.2	47.9	6.3	13.0	5.4	3.4	6.0
Normal				37	37	0.5	7.9	49.0	7.8	12.8	6.8	3.9	8.2
Reversed				23	20	196.8	8.6	−44.3	9.9	18.7	7.8	4.8	12.4
Lesbos_No TC[c] (classification C)	positive	10.8	9.7	60	56	5.2	6.3	49.7	6.1	13.4	5.4	3.4	6.2
Normal				37	37	1.6	8.6	53.1	7.5	11.8	7.2	3.9	8.2
Reversed				23	20	189.9	9.4	−45.0	10.5	16.1	8.4	4.8	12.4
Lesbos_Ayvalık_Bergama	negative	7.9	8.9	85	79	5.3	5.2	49.7	5.0	13.8	4.4	3.1	4.9
Normal				51	50	1.7	7.2	52.8	6.3	12.3	6.0	3.6	6.6
Reversed				34	30	189.8	7.4	−45.6	8.2	16.7	6.6	4.2	9.4
Lesbos_Ayvalık_Bergama_NMM	negative	6.9	6.5	125	113	6.8	4.3	50.7	4.1	14.0	3.7	2.7	3.8
Normal				73	68	3.7	6.2	52.7	5.4	12.1	5.2	3.2	5.4
Reversed				52	45	190.7	5.7	−47.5	5.9	18.9	4.8	3.7	7.1

[a]Bold A95 values indicate values outside the A95 reliability envelope of Deenen et al. (submitted manuscript, 2010). The study area exhibits two paleomagnetically internally coherent rotation domains, one defined by the region around Afyon [*Gürsoy et al.*, 2003], rotating ~20° clockwise since the middle Miocene, and one stretching from the northern Menderes Massif basins to the island of Lesbos, rotating ~7° clockwise, which is insignificant with respect to the Eurasian APWP. Lat, latitude; Lon, longitude; Na, number of demagnetized samples; Nc, number of samples used to calculate average; D, declination; ΔD_x, error on declination; I, inclination; ΔD_x, error on inclination; $K_{(vgp)}$, *Fisher* [1953] precision parameter (determined on the virtual geomagnetic poles); $A95_{(vgp)}$, the 95% cone of confidence around the average virtual geomagnetic pole. $A95_{min}$ and $A95_{max}$ delimit the boundaries of A95 values that can be straightforwardly explained by paleosecular variation alone (Deenen et al., submitted manuscript, 2010). Reversals test is taken from *McFadden and McElhinny* [1990]. See text for further discussion. The Afyon and Lesbos_Ayvalık_Bergama_NMM are used in this study.

[b]Taken from *Gürsoy et al.* [2003].

[c]Taken from *Kissel et al.* [1989] and *Beck et al.* [2001].

Figure 6. Typical demagnetization behavior in Zijderveld diagrams [*Zijderveld*, 1967] of the various populations of samples collected in this study. (a, b) The Eğrigöz granite revealed clear demagnetization behavior but entirely random directions (see also Figure 7). (c, d) Typical examples of all demagnetization behavior of all other granites. Apart from the Eğrigöz granite and the Kos monzonite, these revealed uninterpretable demagnetization diagrams owing to very viscous behavior and low intensity. (e) Example of magnetite-bearing welded tuff. (f) Lower intensity nonwelded tuff sample, still yielding excellent, single component results. (g, h) Thermal and alternating field demagnetization yield similar results; in general, the AF results measured on the robotized measuring device provide less scattered results. (j, k, i) Frequently, mafic lavas have strong overprints, in many cases probably as a result of lightning strikes. These overprint components, together with the ChRM, span great circles [*McFadden and McElhinny*, 1988]. In the case of site Yuntdağ (YD) 1, all samples have a similar overprint direction, and only an average great circle could be determined. (m) Excellent example of lightning-induced random remagnetization great circles which crosscut in the direction of the ChRM. (l, n, o, p) Typical demagnetization behavior of the sediments of localities Kale (KL), Acıpayam (AC), and Kelekçi (KE) yielding counterclockwise rotations. (q) Locality Burdur (BU) yielded mostly viscous behaving samples, from which no ChRM direction could be determined.

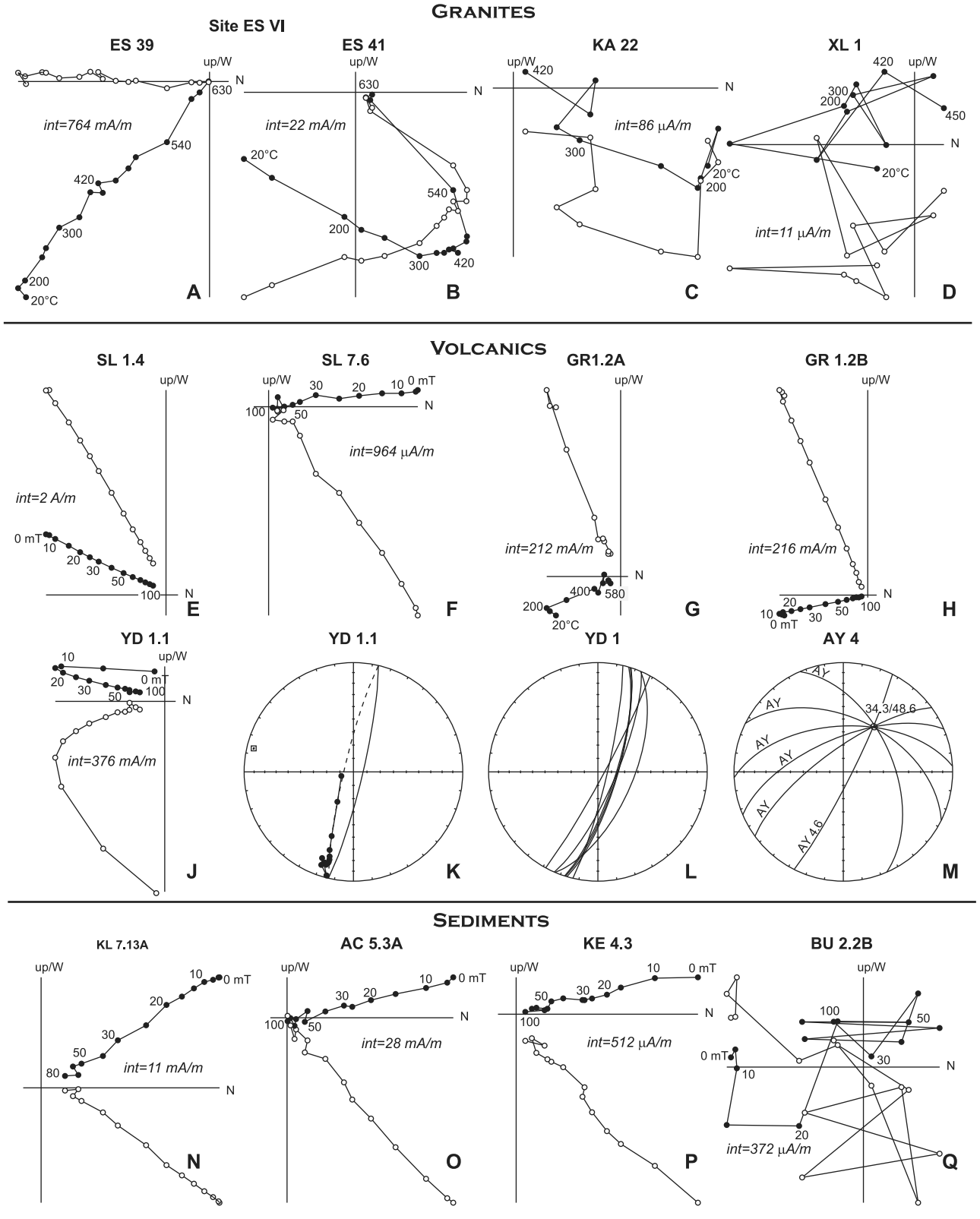
GRANITES
Site ES VI
ES 39
up/W
N
630
540
420
300
200
20°C
int=764 mA/m
A
ES 41
up/W
630
N
20°C
540
200
300
420
int=22 mA/m
B
KA 22
up/W
420
N
300
20°C
200
int=86 μA/m
C
XL 1
420
up/W
300
200
450
N
20°C
int=11 μA/m
D
VOLCANICS
SL 1.4
up/W
int=2 A/m
0 mT
10
20
30
50
100
N
E
SL 7.6
up/W
30
20
10
0 mT
N
100
50
int=964 μA/m
F
GR1.2A
up/W
N
400
580
200
20°C
int=212 mA/m
G
GR 1.2B
up/W
int=216 mA/m
N
20
50
100
10
0 mT
30
H
YD 1.1
10
up/W
20
30
0 mT
50
100
N
int=376 mA/m
J
YD 1.1
K
YD 1
L
AY 4
AY
AY
AY
AY
AY
34.3/48.6
AY 4.6
M
SEDIMENTS
KL 7.13A
up/W
10
0 mT
20
30
50
80
int=11 mA/m
N
N
AC 5.3A
up/W
10
0 mT
30
20
100
50
N
int=28 mA/m
O
KE 4.3
up/W
10
0 mT
50
30
20
N
100
int=512 μA/m
P
BU 2.2B
up/W
100
50
0 mT
30
N
10
20
int=372 μA/m
Q

Figure 6

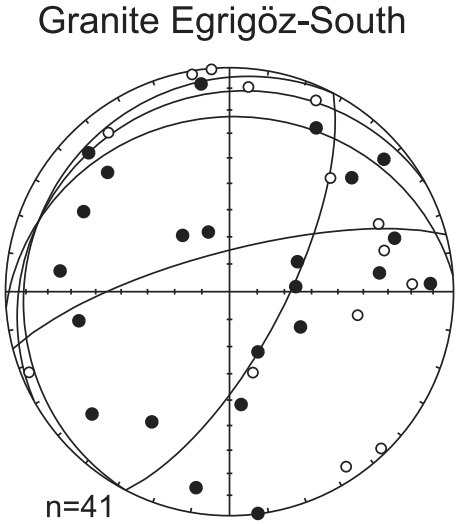

Figure 7. Results for all samples from seven sites in the Eğrigöz south (ES) locality, from which paleomagnetic directions are well determined in most cases (see Figures 6a and 6b) but which provide random directions from which no sensible tectonic information can be derived. Black (open) dots represent normal (reversed) directions.

they introduced the terms $A95_{min}$ and $A95_{max}$, which form an envelope around the possible range of A95 values as a function of n (the amount of averaged spot readings) for the vast majority of PSV scatters that have been reconstructed throughout earth history, from equator to pole [*McFadden et al.*, 1991; *Biggin et al.*, 2008a, 2008b; *Lawrence et al.*, 2009]: a VGP distribution with an A95 lower than $A95_{min}$ underrepresents PSV (e.g., due to remagnetization, sampling too short a time span, or smoothing of PSV within individual sediment cores), whereas an A95 higher than $A95_{max}$ likely contains an additional source of scatter besides PSV (e.g., rotation differences between sites within a locality, unresolved overprints, large orientation or measurement errors or lightning induced remagnetizations). A95 values of three sites in the Kale and Acıpayam localities are much higher than $A95_{max}$ (Table 2). We conclude that these sites contain a very large additional source of uncertainty, in this case probably resulting from poor data quality due to low intensity, and these sites were eliminated from further analysis. Three sites, as well as the averages of the Kale and Acıpayam localities, give dispersions a little lower than $A95_{min}$, which suggests underrepresentation of PSV. This can be straightforwardly explained by the fact that the sediment samples represent a time range and not a spot reading. Therefore, PSV is already smoothed to some extent within individual samples. We consider these averages reliable, and representative for the average paleomagnetic direction of their respective age ranges. The Kale locality provides the opportunity to carry out a reversals test [*McFadden and McElhinny*, 1990], which is negative. This is largely the result of a lower inclination of the reversed directions than the normal ones and may be explained by a not entirely resolved present-day field overprint, suppressing the reversed inclinations, and possibly slightly enhancing the normal inclinations. We note that the declinations, relevant for the rotation study in this paper, show an insignificant difference of 4.3° ± 6.8° (Figure 8). Combining the normal and reversed directions therefore does not significantly change the declination, and hence the assessment of the rotation of the Lycian Nappes since the late Oligocene. The upper Oligocene, lower Miocene and upper Miocene localities of the Lycian Nappes all show consistently westerly deviations of the declination of 10°–20°. The single site from the upper Plio-Pleistocene clays of Burdur is not significantly deviating from south.

5.3.2. West Anatolian Volcanics

[47] Lava sites should represent spot readings of the Earth's magnetic field, and within-site scatter should be randomly dispersed. Therefore, we applied *Fisher* [1953] statistics on the directions within a single lava site (Table 1). Directions from the few cases where only an average great circle were obtained by determining the closest position of the great circle to the mean of the other site means from the same locality, following *McFadden and McElhinny* [1988]. Because dispersion within a single lava site should be minimal, we discarded all lava sites with a k value lower than 50 (which corresponds to an $\alpha 95$ of ~8°–11° for typical *n* in lava sites (i.e., 5–8)), following, e.g., *Biggin et al.* [2008a], *Johnson et al.* [2008], *van Hinsbergen et al.* [2008b], and Deenen et al. (submitted manuscript, 2010).

[48] In localities Ahmetler and Demirci, we sampled a lava stratigraphy. As shown in Table 1, sites AH1–3, DC 1–5 and DC 7–10 show very similar directions, which may indicate underrepresentation of secular variation. Likewise, each of the two rhyolite plugs of Gördes yielded very similar directions. Combined, these sites give A95 values well below $A95_{min}$ (Figure 9 and Table 1), suggesting that these readings are not a random sampling of PSV-induced dispersion but represent more or less the same spot reading. Therefore, we have combined the sites in all five occasions into five single directions, which we will treat as individual spot readings.

[49] A potential source of error in paleomagnetic directions is formed by uncertainty with respect to bedding tilt. In this study, we chose not to correct for bedding tilt for any of the newly sampled or previously published lavas. There are two main reasons for this. First, sediments in the NMM basins generally are subhorizontal or only mildly inclined (generally <10°). Because and lavas and ignimbrites may follow local topography, and their surfaces in outcrop may be highly irregular and the flanks of volcanoes may have initial dips of well over 10°, the potential error introduced by correcting the lavas for their present-day tilt is likely much larger than when geographic coordinates are used. A similar conclusion was reached by *Beck et al.* [2001], based on their large data set from Lesbos (n = 50; Table 1). They noted that the dispersion of VGPs prior to or after bedding tilt correction did not make a significant difference, but that the distribution of VGPs prior to bedding tilt correction was more circular, and therefore likely more reliable. Moreover, applying a reversals test to the tectonically corrected data from Lesbos, we obtain a negative reversals test, whereas a positive reversals test is obtained when using the uncorrected data (Table 3). This strengthens our choice not to correct for bedding tilt.

[50] With the above criteria, we arrived at 235 lava sites, from the island of Lesbos in the west, to the volcanic fields of

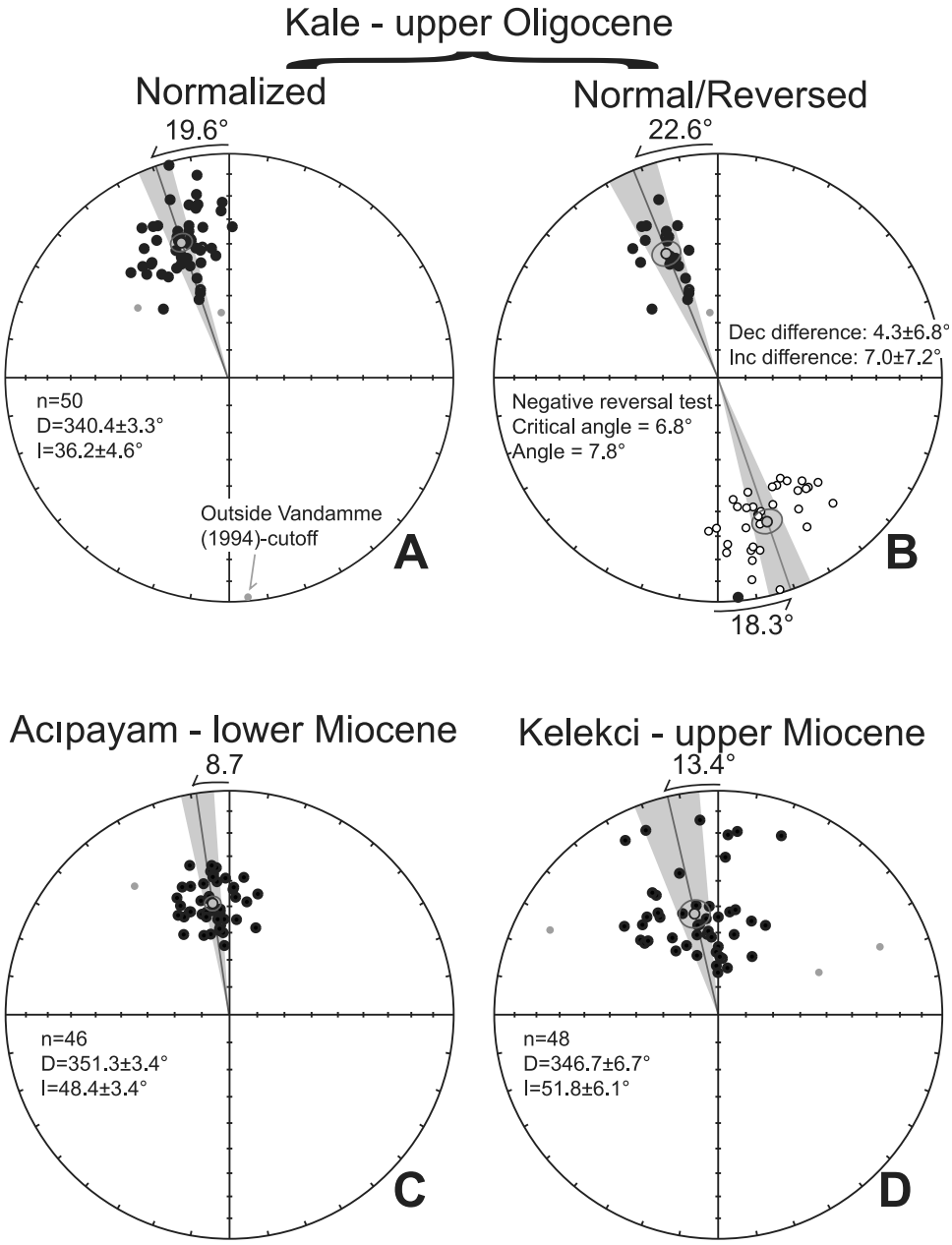

Figure 8. Upper (lower) hemisphere projections for normal (reversed) directions indicated with black (open) circles for the localities in the Lycian Nappes. Reversals test results were calculated by the method of *McFadden and McElhinny* [1990]. Grey data points fell outside the *Vandamme* [1994] cutoff.

Afyon in the east, north of the central Menders Massif. These include 60 previously published lava sites from the island of Lesbos (15 lava sites from *Kissel et al.* [1989], 45 from *Beck et al.* [2001], 104 new sites, and 71 sites near Afyon, published by *Gürsoy et al.* [2003]. *Kissel et al.* [1989] also published some results from sites near Bergama, Dikili, Ayvalık, and Yuntdağ, but because individual site locations were not given, we do not incorporate these in our analyses.

[51] Determining rotation differences in a region with only data from lava sites is not straightforward: although the paleomagnetic direction within a lava site is very well determined, that value may be 25° or more deviating from the geocentric axial dipole (GAD) as a result of PSV. Averaging PSV then inevitably involves averaging results from much larger areas than is the case of sediment sites (where PSV can be averaged with relatively small errors within a single site).

[52] We chose a statistical approach, using the n-dependent reliability criteria for paleomagnetic data from Deenen et al. (submitted manuscript, 2010) to identify paleomagnetically coherent blocks, and to determine their rotation history. For the purpose of this study, it is important to determine whether the region north of the central Menderes Massif experienced regional vertical axis block rotation, and to determine the

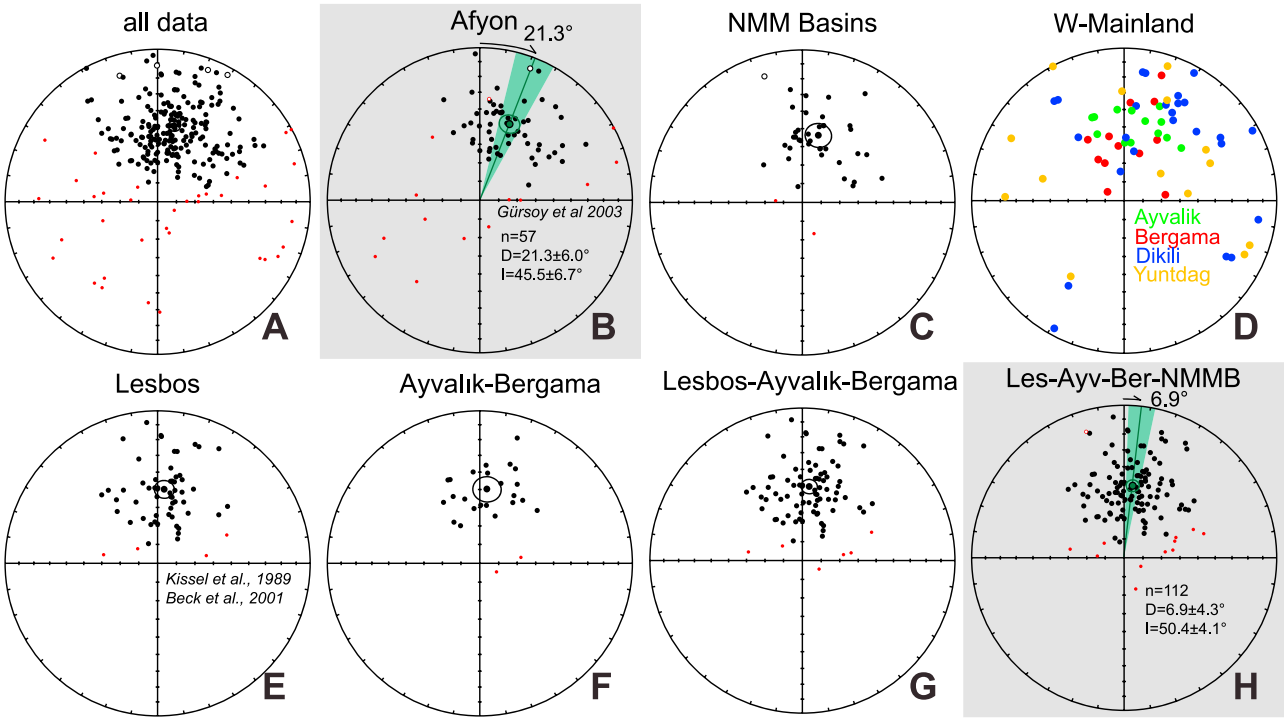

Figure 9. Upper (lower) hemisphere projections for normal (reversed) directions indicated with black (open) circles for the various chosen localities in the lower Miocene lavas in northwestern Turkey. Reversals test results were calculated by the method of *McFadden and McElhinny* [1990]. Red data points fell outside the *Vandamme* [1994] cutoff. The choice of the various localities is discussed in the text. We conclude that the study area exhibits two paleomagnetically internally coherent rotation domains, one defined by the region around Afyon [*Gürsoy et al.*, 2003], rotating ~20° clockwise since the middle Miocene, and one stretching from the northern Menderes Massif basins to the island of Lesbos, rotating ~7° clockwise, which is insignificant with respect to the Eurasian APWP.

size of these blocks. Therefore, we initially combined all new and published lava site data from the wide area north of the CMM, including the published sites from Afyon and Lesbos (Figure 9a), and tested whether the thus obtained dispersion can be straightforwardly explained by PSV alone, i.e., whether the obtained A95 value describing the dispersion of the VGPs lies between $A95_{min}$ and $A95_{max}$, after exclusion of data points outside the *Vandamme* [1994] cutoff. As can be seen in Table 3, this is not the case: with all data combined, A95 lies well above $A95_{max}$, and an additional source of scatter, for instance vertical axis rotation differences within the averaged region, must be present. We can therefore not consider the entire region as a single, internally paleomagnetically coherent block. Moreover, we obtain a clearly negative reversals test.

[53] Consequently, we have to subdivide the region into smaller regions to find the largest region that can be considered as a paleomagnetically stable region (i.e., a region within which the entire paleomagnetic variation can be explained by secular variation alone). We subdivided the region into four regions, the size of which is largely driven by the data density (Figures 9b–9e). The NMM basins all share a NE–SW structural trend (Figure 2) [*Bozkurt*, 2003; *Purvis and Robertson*, 2005], and this structural similarity may indicate that these are not significantly rotated with respect to each other. Hence, this is a logical region to test the paleomagnetic coherence for. We positively test this prediction with the method outlined above: A95 lies between $A95_{max}$ and $A95_{min}$, and we obtain a positive reversals test. Hence, we can consider the NMM basins as (part of) a paleomagnetically stable block (Figure 9c).

[54] We then averaged the data of *Gürsoy et al.* [2003] from the Afyon volcanic fields (Figure 9b) and Lesbos (Figure 9e) [from *Kissel et al.*, 1989; *Beck et al.*, 2001], and for both regions, we obtain positive reversals tests and A95 values that can be straightforwardly explained by PSV alone. The volcanic sites of Afyon cover a larger age range than the rest of the region (21–8 Ma [*Gürsoy et al.*, 2003]). However, selecting only the lower Miocene lavas here yields a statistically indistinguishable result from combining all data, suggesting that we cannot statistically show rotation differences through time.

[55] The final locality, depicted "west Mainland," combined the Ayvalık, Bergama, Dikili, and Yuntdağ localities. The thus obtained data set cannot be explained by PSV alone, as A95 exceeds $A95_{max}$ (Table 3) and we show the data from all four localities in Figure 9d. It is clear that localities Yuntdağ and Dikili are widely dispersed, whereas Ayvalık and Bergama are clustered. The reason for this dispersion remains open to speculation. Possibly, the lavas in these localities have been influenced by, e.g., local rotations, or

Table 4. Results of Common True Mean Direction Tests Between All Lava Localities Discussed in This Paper[a]

	NMM	L_A_B_N	L_A_B	L	A_B
Afyon	neg	neg	neg	neg	neg
NMM		B	B	B	B
L_A_B_N			B	B	B
L_A_B				B	B
L					B

[a]For the common true mean directions tests, see *McFadden and Lowes* [1981]. Note that we cannot demonstrate any statistical differences between the northwest Aegean localities and that all localities significantly differ from locality Afyon of *Gürsoy et al.* [2003]. N, northern Menderes Massif basins; L, Lesbos; A, Ayvalik; and B, Bergama. Hence, L_A_B_N, paleomagnetic data from Lesbos, Ayvalik, Bergama, and the northern Menderes Massif basins; L_A_B, paleomagnetic data from Lesbos, Ayvalik, and Bergama.

uncorrected tilts. We note that previous authors also concluded strong and poorly understood rotations in this region [*Kissel et al.*, 1989] and speculated upon a transform zone affecting the region [*Ring et al.*, 1999a]. Regardless of the reason for this increased dispersion, we conclude that Yuntdağ and Dikili do not fulfill our criteria to be part of a regionally paleomagnetically coherent block, and the southwestern part of the west Anatolian volcanic province may have undergone local rotations. Combining localities Ayvalık and Bergama, however, does provide a scatter that can result from PSV alone and leads to a positive reversals test (Table 3).

[56] Thus, we have obtained four individual regions, large or small, within which we have no reason to assume significant vertical axis rotations. We now test whether these regions share a common true mean direction (CTMD) in the sense of *McFadden and Lowes* [1981]. If so, their data sets can be considered statistically similar and can be combined. Table 4 shows that the directions of Lesbos and Ayvalık-Bergama share a CTMD, and we combined these. The resultant direction depicted L_A_B in Table 4 shares a CTMD with the direction obtained from the northern Menderes Massif basins, and we also combined these (Figures 9g and 9h). All possible combinations in western Turkey share a CTMD, and none of these are statistically similar to the results from Afyon (Table 4). Interestingly, the data from Lesbos and Ayvalık-Bergama each provide positive reversals tests, and are statistically indistinguishable, but when combined, a negative reversals test is obtained, largely owing to a declination difference between normal and reversed directions. The normal directions are close to north, whereas the reversed show a deviation from south of ~10° (which is also present in the sets from Lesbos). We have no reason to assume that the normal directions have been affected by a present-day field overprint, and we cannot straightforwardly explain this result. If indeed a present-day field overprint is present and unresolved, this will suppress the declination by a few degrees, but it will not affect our conclusions significantly, and the significant difference with Afyon remains.

[57] The above analysis leads us to identify three paleomagnetic domains in western Turkey north of the CMM: the region including Dikili and Yuntdağ likely underwent local rotations; the region from Lesbos to the NMM basins formed an internally coherent paleomagnetic block since the early Miocene, and the region around Afyon did the same. These latter two, however, rotated with respect to each other, with a declination in the Lesbos-NMM block of 6.8° ± 4.3° and in the Afyon block of 21.3° ± 6.0° (Table 3).

6. Discussion

6.1. Timing and Amount of Rotations in Western Turkey

[58] The Bey Dağları region, rotating 20° counterclockwise (CCW) between 16 and 5 Ma, forms part of the eastern limb of the Aegean orocline [*Kissel and Laj*, 1988; *van Hinsbergen et al.*, 2010]. The results presented in section 5.3 now allow further definition of the dimensions of this limb and placement of its development within the regional tectonic context.

[59] The Lycian Nappes have previously been described as a megaklippe that traveled southward during the early Miocene [*Hayward and Robertson*, 1982; *Hayward*, 1984a, 1984b; *Collins and Robertson*, 1998, 2003], contemporaneous with the exhumation of the NMM and SMM. During this period, the Lycian Nappes thrusted southward over the Bey Dağları platform, as evident from Aquitanian to lowermost Langhian foreland basin deposits at the leading southeastern edge of the Nappes, as well as from overthrusted Burdigalian foreland basin deposits in windows below them [*Hayward*, 1984a]. During this time, it may have been possible for the Lycian Nappes to rotate with respect to the Bey Dağları platform. After the earliest Langhian, however, there is no major structure to accommodate regional rotation differences between the Lycian Nappes and the Bey Dağları platform [see also *van Hinsbergen et al.*, 2010].

[60] The upper Oligocene to lower Miocene Kale basin reveals a CCW rotation of 20°, comparable to the Miocene Bey Dağları results, which leads us to infer (1) that the Lycian Nappes share the rotation of the Bey Dağları region (between 16 and 5 Ma) and (2) that the Lycian Nappes did not undergo significant rotation during their thrusting over the Bey Dağları platform during the exhumation of the NMM and SMM. The results from the lower Miocene deposits of locality Acıpayam reveal a somewhat smaller CCW rotation, but the loosely dated upper Miocene of Kelekçi in the Çameli basin, indicating 16° CCW rotation, suggest that this is likely the result of minor local rotations, e.g., due to formation of the Çameli basin and other Neogene basins in the Lycian Nappes [*Price and Scott*, 1994; *Alçiçek et al.*, 2005, 2006; *Alçiçek*, 2007; *Alçiçek and ten Veen*, 2008; *ten Veen et al.*, 2009]. Note that the Bey Dağları platform also reveals minor rotation variations related to local tectonics [*Kissel and Poisson*, 1987; *Morris and Robertson*, 1993; *van Hinsbergen et al.*, 2010]. Hence, we conclude that the Lycian Nappes form part of the eastern counterclockwise rotating limb of the Aegean orocline, which underwent a single phase of rotation between 16 and 5 Ma (Figure 10).

[61] This rotation is regionally consistent and does not suggest that there are major accommodating discontinuities within the Bey Dağları platform. *van Hinsbergen et al.* [2010] recently argued that the eastern limit of the rotating block was formed by two faults in center of the Isparta Angle: the Aksu thrust and the Kırkkavak fault, which partition transpression

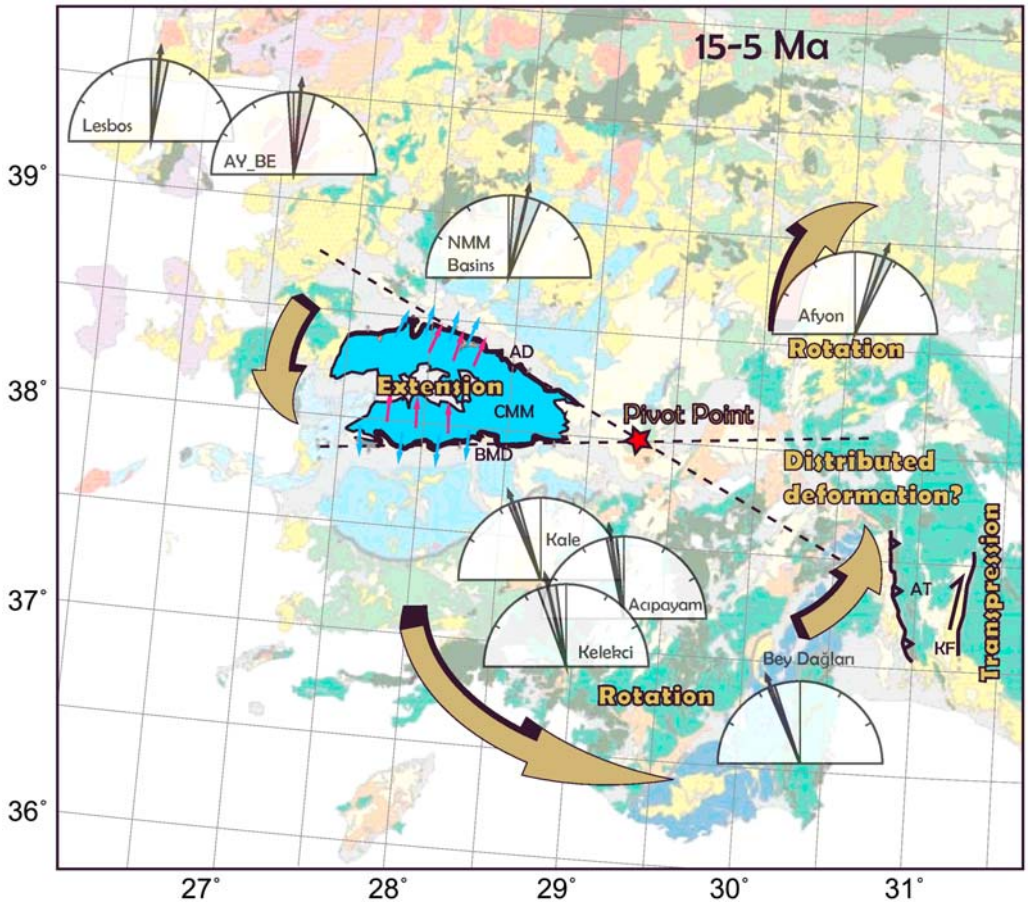

Figure 10. Results and interpretations summarizing the relationships between tectonics and rotations in western Turkey for the period between 15 and 5 Ma. The opening of the triangular central Menderes Massif (CMM) along two bivergent detachments is accommodated by counterclockwise rotation of the southern block, including the Lycian Nappes and Bey Dağları, with respect to the northern block, which includes the island of Lesbos, the region of Ayvalık and Bergama, and the northern Menderes Massif basins. The rotation difference across the CMM is approximately 25°–30°, in line with the angle defined by the two divergent (Alaşehir and Büyük Menderes; AD and BMD, respectively) detachments and with the regional pattern of stretching lineations (see Figure 3). These define a pivot point, west of which rotation is accommodated by extension. To the east, the rotation is likely delimited by the transpressional deformation along the Aksu Thrust (AT) and the Kırkkavak right-lateral strike-slip fault (KF) [see *van Hinsbergen et al.*, 2010]. The regionally consistent counterclockwise rotation of the Bey Dağları region, up to AT and KF, predicts compression east of the pivot point. The structural accommodation of this convergence remains open for further research, but the presence of post–early Miocene tectonic activity is evident from the clockwise rotation of the Afyon volcanic fields [*Gürsoy et al.*, 2003], which may reflect a response to semirigid indentation of the Bey Dağları (and Lycian Nappes) block or a response to distributed right-lateral strike slip induced by the rotation. Base map modified is after modified after *MTA* [2002]; see Figure 2 for legend.

into a thrust and a right-lateral strike-slip fault, respectively [see also *Çiner et al.*, 2008].

[62] Our new data from northwestern Turkey now allow us to identify the northern limit of the rotating domain: the region north of the CMM, including the island of Lesbos and the lower Miocene volcanics covering the region of Ayvalık and Bergama, as well as those in the NMM basins, reveal an internally coherent clockwise rotation of 6.8° ± 4.3°, and we can straightforwardly conclude that this region does not form part of the counterclockwise rotating region of the Lycian Nappes and Bey Dağları (Figure 10).

[63] Previous reviews of paleomagnetic data from Turkey (largely ignoring the possibility of local, e.g., strike-slip-induced rotations) have suggested that the Anatolian microplate as a whole underwent a 20°–30° counterclockwise rotation phase since the middle Miocene [*Platzman et al.*, 1998; *Kissel et al.*, 2003]. This is not in line with our data from northwestern Turkey: if we compare our findings with

the most recent apparent polar wander path for Eurasia [*Torsvik et al.*, 2008], we conclude that there was no significant rotation difference between western Anatolia (and Lesbos) and Eurasia: The 20 Ma pole of *Torsvik et al.* [2008] predicts a declination (for a coordinate in the Selendi basin, site SL1, see Table 1) of 5.9° ± 3.6° and the 10 Ma Eurasian reference pole predicts D ± ΔD_x of 3.5° ± 3.0°. Our result of 6.8° ± 4.3 for this region shows an insignificant difference of 0.9° ± 5.6° and 3.2° ± 5.2°, respectively. Given the absence of major middle Miocene and younger compressional (or extensional) regions between our study area and the Eurasian continent, it is unlikely that this region underwent a 20°–30° clockwise rotation to annihilate the equal but opposite rotation of the Anatolian microplate inferred by *Platzman et al.* [1998] and *Kissel et al.* [2003]. We conclude that the activity of the major North Anatolian Fault Zone that runs in between the study area and the Eurasian continent, did not lead to a paleomagnetically measurable, regional rotation of the entire Anatolian microplate. We note, however, that the region of Afyon, where *Gürsoy et al.* [2003] found a clockwise rotation of 21.3° ± 6.0° (see Table 3) did experience a significant rotation with respect to Eurasia of 15.2° ± 7.0° or 17.8° ± 6.7° with respect to the 20 and 10 Ma reference poles of *Torsvik et al.* [2008], respectively. A possible reason for this rotation will be discussed in section 6.3.

6.2. Identification of the Rotation Pole

[64] We do not have paleomagnetic data from the southern Menderes Massif, but the fact that this region was exhumed by the end of the early Miocene [*Gessner et al.*, 2001b; *Ring et al.*, 2003a; *Seyitoglu et al.*, 2004] makes it very unlikely that there was significant extension here. The only candidate to accommodate the rotation difference between the Lycian Nappes and the northwest Anatolian volcanic fields is formed by the central Menderes Massif, which exhumed contemporaneous with the SW Anatolian rotations [*Gessner et al.*, 2001b; *Lips et al.*, 2001; *Ring et al.*, 2003a; *Catlos and Cemen*, 2005; *Çiftçi and Bozkurt*, 2009a; *Sen and Seyitoğlu*, 2009; *Catlos et al.*, 2010]. Our paleomagnetic data reveal a rotation difference of ~27° (or 25°–30°), which is perfectly in line with (1) the angle between the Alaşehir and Büyük Menderes detachments along which the CMM was exhumed and (2) the angle between the regional stretching lineation pattern on either side of, as well as within the CMM (Figures 3 and 10). The intersection point of the CMM-bounding detachments, as well as the midpoint of the circle that is defined by the stretching lineation trend, define a pivot point around which the counterclockwise rotation of the Bey Dağları platform and the Lycian Nappes occurred. A similar way of determining the rotation pole for the western limb of the Aegean orocline was recently applied by integration of paleomagnetic and structural data in the Rhodope core complex of northern Greece and Bulgaria [*Brun and Sokoutis*, 2007; see also *van Hinsbergen et al.*, 2008a].

[65] A pivot point (or rotation pole) defines the location where only rotation occurs: to the west of this point, the rotation difference was accommodated by extension as pointed out in section 6.1. In most reconstructions thus far, the pivot point was suggested to lie in the Isparta Angle [e.g., *Kissel and Laj*, 1988; *Gautier et al.*, 1999; *Piper et al.*, 2002b] (Figure 1), which forms the hinge point where the counterclockwise rotated Bey Dağları and Lycian Nappes region meets with the clockwise rotated region of the central Taurides (with a pre-Miocene age, Figure 1 [see *Kissel et al.* [1993]). The fact that the pivot point is located near the eastern limit of the CMM has an important tectonic implication: east of the pivot point, up to the longitude defined by the Aksu Thrust and the Kırkkavak strike-slip fault, the coherent rotation of the eastern limb of the Aegean orocline must have been accommodated by N–S shortening (Figure 10). The exact way of accommodating this shortening cannot be resolved at this moment. However, evidence for post-Oligocene compression was documented in the Denizli basin, which was folded and thrusted [*Sözbilir*, 2005]. Additionally, the region of the Isparta Angle contains a large number of thrust faults, but absence of evidence for Miocene sediments involved in thrusting does not allow testing of a synrotational age for these thrust faults. The rotation results obtained by *Gürsoy et al.* [2003] for the Afyon region, indicating a significant clockwise rotation of 20°, however, show that this region has been tectonically active since the middle Miocene (Figure 10).

[66] This clockwise rotation seems to be localized to the Afyon region because (1) clockwise rotations in the central Taurides (Figure 1) are demonstrably pre–early Miocene in age [*Kissel et al.*, 1993], (2) our data show that the region WNW of Afyon experienced no significant rotation with respect to Eurasia and are significantly different from the Afyon rotation, and (3) central and eastern Anatolia only exhibit counterclockwise rotations [*Tatar et al.*, 1996, 2002; *Gürsoy et al.*, 1998; *Platzman et al.*, 1998; *Piper et al.*, 2002a, 2010; *Kissel et al.*, 2003]. Clockwise rotations in Anatolia are mainly limited to strike-slip-related rotations within the North Anatolian Fault Zone [*Tatar et al.*, 1995; *Piper et al.*, 1996, 1997], although even that is debated [*Platzman et al.*, 1994], and the Afyon region lies well outside of the strands of this fault zone. It is possible that the shortening that we postulate to accommodated the rotation of the Bey Dağları region is accommodated by distributed right-lateral shear, leading to clockwise rotations in the Afyon area. Alternatively, the Bey Dağlari region may behave as a semirigid indentor, leading to a coherent clockwise rotation to its north (Figure 10). Either way, the significant clockwise rotations of the Afyon region support our prediction that the region east of the pivot point was affected by deformation during the rotation history. Moreover, if the rotation pole would be located further west, e.g., within the Isparta Angle such as suggested previously, the extensional region now represented by the CMM should have been much larger, and reached up to the Isparta Angle. There is no evidence for widespread extension amounting tens of kilometers here (as required by the 25°–30° rotation difference) and younger compression to obscure such a history leads to the same lack of evidence.

[67] Despite the fact that loci of accommodation of the shortening east of the rotation pole remains enigmatic, the paleomagnetic coherence of the Bey Dağları region in combination with the excellent correspondence of the both the

shape and the stretching lineation pattern of the CMM, and the evidence for localized rotational deformation in the Afyon region suggest a middle to late Miocene rotation-deformation history at the eastern end of the Aegean orocline as outlined in Figure 10.

6.3. Kinematic and Geodynamic Implications

[68] We can demonstrate that the evolution of the CMM was associated with rotation and formation of the Aegean orocline, likely in tandem with shortening east of the CMM. Absence of late Oligocene to early Miocene rotation in the Bey Dağları region and the Lyian Nappes shows that the first stage of exhumation of the Menderes Massif, bringing the SMM and NMM to the surface between the late Oligocene (~25 Ma) and the middle Miocene (~16 Ma) was most likely not associated with rotations. There is no paleomagnetic information from upper Oligocene rocks to the north of the northern Menderes Massif. Although such rocks are exposed (Figure 2), it is probably not possible to obtain conclusive regional rotation patterns there as a result of the intense right-lateral strike-slip deformation associated with the North Anatolian Fault Zone. However, a regional rotation history that may have been accommodated by opening of the southern and northern Menderes Massif in a comparable way to the central Menderes Massif is unlikely, given the absence of major late Oligocene shortening: the only notion of significant Oligocene motion led to the exhumation of the rather local Uludağ massif [*Okay et al.*, 2008], which was interpreted to occur in a strike-slip setting.

[69] The late Oligocene–early Miocene extension in the Menderes Massif was therefore most likely accommodated along distributed or discrete transforms. The southeastern boundary of the NMM appears to be a discrete NE–SW trending lineament, subparallel to the main stretching lineation in the NMM (Figure 3), which may have served as this bounding structure. No late Oligocene to early Miocene core complexes are known east of this boundary. The western limit of the NMM is also a discrete lineament, but to the west of this lineament evidence for early Miocene extension is widely present, e.g., in the Kazdağ massif [*Okay and Satir*, 2000; *Bonev et al.*, 2009; *Cavazza et al.*, 2009] (Figure 3) and in the Cyclades [*Gautier et al.*, 1999; *Ring et al.*, 1999b; *Jolivet et al.*, 2004; *Tirel et al.*, 2009; *Jolivet and Brun*, 2010].

[70] The relationship between deformation and rotation in western Turkey outlined in section 6.2 shows that Aegean back-arc extension, suggested to have started around 25 Ma [*Gautier et al.*, 1999; *Jolivet*, 2001; *Jolivet and Brun*, 2010] or even earlier [*Jolivet and Faccenna*, 2000; *Forster and Lister*, 2009], did not a priori lead to rotations in the west Anatolian region. It was likely accommodated during the first 10 Ma of back-arc extension by the transform fault formed by the southeastern boundary of the Menderes Massif (Figure 3). Back-arc extension in western Turkey was oriented N(N)E–S(S)W, and the N–S stretching lineations in the SMM passively rotated into that position in the early Miocene, after its exhumation.

[71] If the Aegean back arc was bounded by a discrete fault rather than a distributed region of rotation, this may reflect that the Aegean slab, the roll-back of which is generally assumed to cause back-arc extension, also has a discrete eastern boundary, which already existed in the late Oligocene. Recent papers have shown that the eastern Aegean slab edge (STEP [*Govers and Wortel*, 2005] bypassed southeastern Greece in the Pliocene [*van Hinsbergen et al.*, 2007; *Zachariasse et al.*, 2008] and may have left a volcanic trace in western Turkey [*Dilek and Altunkaynak*, 2009], but our new result may imply that it already existed, or came into existence, since the late Oligocene to early Miocene.

[72] The rotation of the eastern limb of the Aegean orocline is comparable in age to the western limb (middle to late Miocene [*van Hinsbergen et al.*, 2005b, 2008a, 2010; this paper] and because these rotations seem to be accommodated by extension, a large part of the roll-back-related extension seems to be middle Miocene and younger. The previously postulated relation to Anatolian extrusion (which is largely younger than early Pliocene [*Hubert-Ferrari et al.*, 2009]) by, e.g., *Taymaz et al.* [1991] and *Kissel et al.* [2003] is shown in section 6.1 to be an unlikely candidate as well. The shortening we infer east of the west Anatolian pivot point (Figure 10) rather suggests that around 16 Ma the central segment of the Isparta Angle underwent shortening together with Africa. The African-Eurasian shortening rate in the Miocene of ~1 cm/yr [*Müller et al.*, 1993; *Torsvik et al.*, 2008] would be sufficient to accommodate the southwest Anatolian rotations. A comparable conclusion was reached for the western Aegean limb [*van Hinsbergen et al.*, 2008a].

7. Conclusions

[73] In this paper we provide a large set of new paleomagnetic data from western Turkey, and integrate these with the regional structural evolution to test the causes and consequences of oroclinal bending in the Aegean region. Our main findings can be summarized as follows:

[74] 1. The Lycian Nappes and Bey Dağları region share a counterclockwise rotation phase of ~20°, which occurs between 16 and 5 Ma and define the eastern limb of the Aegean orocline. This rotation phase is contemporaneous with the exhumation of the Central Menderes Core Complex, which formed in the center of the late Oligocene to early Miocene northern and southern Menderes core complex(es).

[75] 2. There is no evidence for rotation of the Lycian Nappes during their early Miocene thrusting history over the Bey Dağları platform, and the exhumation of the northern and southern Menderes massifs.

[76] 3. The volcanic region from Lesbos to Uşak underwent no significant rotation (with respect to Eurasia) since the middle Miocene. There is a significant rotation difference between this region and the region of Afyon, where a clockwise rotation of ~20° was reported.

[77] 4. We have no reason to infer a Mio-Pliocene 20°–30° counterclockwise rotation phase of the entire Anatolian microplate, as previously suggested by *Platzman et al.* [1998] and *Kissel et al.* [2003].

[78] 5. Our paleomagnetic data show that exhumation of the central Menderes core complex along the Alaşehir and Büyük Menderes detachments was associated with a rotation difference between the northern and southern Menderes massifs of ~25°–30°.

[79] 6. This result is in excellent agreement with (1) the angle between the Büyük Menderes and Alaşehir detachments and (2) the angle defined by the regional stretching lineation pattern in the southern Menderes Massif (N–S) and the northern Menderes Massif (NE–SW).

[80] 7. The rotation pole of the west Anatolian rotations is defined by the intersection point of the Büyük Menderes and Alaşehir detachments.

[81] 8. The rotation of the southern domain, including the southern Menderes Massif, the Lycian Nappes and Bey Dağları, must have led to N–S contraction east of this pole.

[82] 9. Transpression along the Aksu thrust and Kırkkavak Fault in the central eastern part of the Isparta angle accommodates the rotation in the east. The clockwise rotation of the volcanic fields near Afyon may be the result of distributed N–S shortening. The precise accommodation of this shortening history remains open for investigation. The absence of significant middle Miocene extension east of our inferred rotation pole and the rotational deformation near Afyon is in line with our inferences.

[83] 10. Exhumation of the northern and southern Menderes massifs in the late Oligocene and early Miocene was not accompanied by vertical axis rotations. Late Oligocene to early Miocene extension in the eastern part of the Aegean back arc was NE–SW oriented and likely bounded by a discrete transform fault, presently seen as a lineament at the eastern boundary of the northern Menderes Massif.

[84] 11. The transform bounding the Menderes core complex may be associated with an early evolution of the eastern Aegean slab edge (STEP), which could thus already have existed since at least the early Miocene.

[85] 12. Aegean roll-back commenced well before the rotation of the eastern limb of the Aegean orocline. Oroclinal bending in the eastern Aegean region is likely related to a reconnection of its eastern limit with the African northward moving plate, comparable to a recently postulated scenario for western Greece.

[86] **Acknowledgments.** We thank Inge Loes ten Kate, Flora Boekhout, Annemiek Asschert, and Erhan Gülyüz for their invaluable help in the field. Nuretdin Kaymakcı is thanked for discussions in and outside the field and logistical support. Laurent Jolivet and Fabio Speranza are thanked for their reviews. Ercan Aldanmaz provided useful information on sampling targets in the lower Miocene volcanic. The Netherlands Science Foundation (NWO) is acknowledged for funding the robotized magnetometer we used in this study. D.J.J.v.H. was supported by an NWO VENI grant and acknowledges financial support from Statoil (SPlates project).

References

Akay, E., and B. Erdogan (2004), Evolution of Neogene calc-alkaline to alkaline volcanism in the Aliaga-Foca region (western Anatolia, Turkey), *J. Asian Earth Sci.*, *24*, 367–387, doi:10.1016/j.jseaes.2004.01.015.

Akgün, F., and H. Sözbilir (2001), A palynostratigraphic approach to the SW Anatolian molasse basin: Kale-Tavas molasse and Denizli molasse, *Geodin. Acta*, *14*, 71–93, doi:10.1016/S0985-3111(00)01054-8.

Akkök, R. (1983), Structural and metamorphic evolution of the northern part of the Menderes massif: New data from the Derbent area and their implication for the tectonics of the massif, *J. Geol.*, *91*, 342–350, doi:10.1086/628777.

Alçiçek, M. C. (2007), Tectonic development of an orogen-top rift recorded by its terrestrial sedimentation pattern: The Neogene Esen Basin of southwestern Anatolia, *Sediment. Geol.*, *200*, 117–140, doi:10.1016/j.sedgeo.2007.04.003.

Alçiçek, M. C., and J. H. ten Veen (2008), The late early Miocene Acipayam piggy-back basin: Refining the last stages of Lycian nappe emplacement in SW Turkey, *Sediment. Geol.*, *208*, 101–113, doi:10.1016/j.sedgeo.2008.05.003.

Alçiçek, M. C., N. Kazanci, and M. Özkul (2005), Multiple rifting pulses and sedimentation pattern in the Çameli Basin, southwestern Anatolia, Turkey, *Sediment. Geol.*, *173*, 409–431, doi:10.1016/j.sedgeo.2003.12.012.

Alçiçek, M. C., J. H. ten Veen, and M. Özkul (2006), Neotectonic development of the Çameli Basin, southwestern Anatolia, Turkey, in *Tectonic Development of the Eastern Mediterranean Region*, edited by A. H. F. Robertson and D. Mountrakis, *Geol. Soc. Spec. Publ.*, *260*, 591–611, doi:10.1144/GSL.SP.2006.260.01.25.

Aldanmaz, E., J. A. Pearce, M. F. Thirlwall, and J. G. Mitchell (2000), Petrogenetic evolution of late Cenozoic, post-collision volcanism in western Anatolia, Turkey, *J. Volcanol. Geotherm. Res.*, *102*, 67–95, doi:10.1016/S0377-0273(00)00182-7.

Altherr, R., J. Keller, and K. Kott (1976), Der jungtertiäre Monzonit von Kos und sein Kontakthof (Ägäis, Griechenland), *Bull. Soc. Geol. Fr.*, *18*(7), 403–412.

Altherr, R., H. Kreuzer, I. Wendt, H. Lenz, G. A. Wagner, J. Keller, W. Harre, and A. Hohndorf (1982), A late Oligocene/early Miocene high temperature belt in the Attica Cycladic crystalline complex (SE Pelagonian, Greece), *Geol. Jahrb., Reihe E*, *23*, 97–164.

Altunkaynak, S., and Y. Yilmaz (1998), The Mount Kozak magmatic complex, western Anatolia, *J. Volcanol. Geotherm. Res.*, *85*, 211–231, doi:10.1016/S0377-0273(98)00056-0.

Andriessen, P. A. M., N. A. I. M. Boelrijk, E. H. Hebeda, H. N. A. Priem, E. A. T. Verdurmen, and R. H. Verschure (1979), Dating the events of metamorphism and granitic magmatism in the Alpine Orogen of Naxos (Cyclades, Greece), *Contrib. Mineral. Petrol.*, *69*, 215–225, doi:10.1007/BF00372323.

Ashworth, J. R., and M. M. Evirgen (1984), Garnet and associated minerals in the southern margin of the Menderes massif, south-west Turkey, *Geol. Mag.*, *121*, 323–337, doi:10.1017/S0016756800029228.

Aubouin, J. (1957), Essai de corrélation stratigraphique de la Grèce occidentale, *Bull. Soc. Geol. Fr.*, *7*, 281–304.

Avigad, D., Z. Garfunkel, L. Jolivet, and J. M. Azañon (1997), Back-arc extension and denudation of Mediterranean eclogites, *Tectonics*, *16*, 924–941, doi:10.1029/97TC02003.

Avigad, D., G. Baer, and A. Heimann (1998), Block rotations and continental extension in the central Aegean Sea: Palaeomagnetic and structural evidence from Tinos and Mykonos (Cyclades, Greece), *Earth Planet. Sci. Lett.*, *157*, 23–40, doi:10.1016/S0012-821X(98)00024-7.

Aydar, E. (1998), Early Miocene to Quaternary evolution of volcanism and the basin formation in western Anatolia: A review, *J. Volcanol. Geotherm. Res.*, *85*, 69–82, doi:10.1016/S0377-0273(98)00050-X.

Beck, M. E., R. F. Burmester, D. P. Kondopoulou, and A. Atzemoglou (2001), The palaeomagnetism of Lesbos, NE Aegean, and the eastern Mediterranean inclination anomaly, *Geophys. J. Int.*, *145*, 233–245, doi:10.1111/j.1365-246X.2001.00376.x.

Benda, L., F. Innocenti, R. Mazzuoli, F. Radicati, and P. Steffens (1974), Stratigraphic and radiometric data of the Neogene in northwest Turkey, *Z. Dtsch. Geol. Ges.*, *125*, 183–193.

Berckhemer, H. (1977), Some aspects of the evolution of marginal seas deduced from observations in the Aegean region, in *International Symposium on the Structural History of the Mediterranean Basins*, edited by B. Biju-Duval and L. Montadert, pp. 303–313, Technip, Paris.

Bernoulli, D., P. C. DeGraciansky, and O. Monod (1974), The extension of the Lycian Nappes (SW Turkey) into the SE Aegean islands, *Eclogae Geol. Helv.*, *67*, 39–90.

Biggin, A., D. J. J. van Hinsbergen, C. G. Langereis, G. B. Straathof, and M. H. Deenen (2008a), Geomagnetic secular variation in the Cretaceous Normal Superchron and in the Jurassic, *Phys. Earth Planet. Inter.*, *169*, 3–19, doi:10.1016/j.pepi.2008.07.004.

Biggin, A. J., G. H. M. A. Strik, and C. G. Langereis (2008b), Evidence for a very-long-term trend in geomagnetic secular variation, *Nat. Geosci.*, *1*, 395–398, doi:10.1038/ngeo181.

Bingöl, E. (1977), The geology of Muratdagi on the petrology of the main rock units, *Bull. Geol. Soc. Turk.*, *20*, 13–66.

Bingöl, E., M. Delaloyle, and G. Araman (1982), Granitic intrusions in western Anatolia: A contribution to the geodynamic study of this area, *Eclogae Geol. Helv.*, *75*, 437–446.

Bonev, N., L. Beccaletto, M. Robyr, and P. Monie (2009), Metamorphic and age constraints on the Alakeci shear zone: Implications for the extensional exhumation history of the northern Kazdag Massif, NW Turkey, *Lithos*, *113*, 331–345, doi:10.1016/j.lithos.2009.02.010.

Bonneau, M., and J. R. Kienast (1982), Subduction, collision et schistes bleus: L'exemple de l'Egée (Grèce), *Bull. Soc. Geol. Fr.*, *24*, 781–791.

Borsi, S., G. Ferrara, F. Innocenti, and R. Mazzuoli (1972), Geochronology and petrology of recent volcanics in the eastern Aegean Sea (west Anatolia and Lesvos Island), *Bull. Volcanol.*, *36*, 473–496, doi:10.1007/BF02597122.

Bozkurt, E. (2000), Timing of extension on the Büyük Menderes Graben, western Turkey, and its tectonic implications, in *Tectonics and Magmatism in Turkey and the Surrounding Area*, edited by E. Bozkurt

et al., *Geol. Soc. Spec. Publ.*, *173*, 385–403, doi:10.1144/GSL.SP.2000.173.01.18.

Bozkurt, E. (2001a), Neotectonics of Turkey—A synthesis, *Geodin. Acta*, *14*, 3–30, doi:10.1016/S0985-3111(01)01066-X.

Bozkurt, E. (2001b), Late Alpine evolution of the central Menderes Massif, western Turkey, *Int. J. Earth Sci.*, *89*, 728–744, doi:10.1007/s005310000141.

Bozkurt, E. (2003), Origin of NE-trending basins in western Turkey, *Geodin. Acta*, *16*, 61–81, doi:10.1016/S0985-3111(03)00002-0.

Bozkurt, E. (2004), Granitoid rocks of the southern Menderes Massif (southwestern Turkey): Field evidence for Tertiary magmatism in an extensional shear zone, *Int. J. Earth Sci.*, *93*, 52–71, doi:10.1007/s00531-003-0369-0.

Bozkurt, E. (2007), Extensional v. contractional origin for the southern Menderes shear zone, SW Turkey: Tectonic and metamorphic implications, *Geol. Mag.*, *144*(1), 191–210, doi:10.1017/S0016756806002664.

Bozkurt, E., and S. K. Mittwede (2005), Introduction: Evolution of continental extensional tectonics of western Turkey, *Geodin. Acta*, *18*, 153–165, doi:10.3166/ga.18.153-165.

Bozkurt, E., and R. Oberhänsli (2001), Menderes Massif (western Turkey): Structural, metamorphic and magmatic evolution—A synthesis, *Int. J. Earth Sci.*, *89*, 679–708, doi:10.1007/s005310000173.

Bozkurt, E., and R. G. Park (1994), Southern Menderes Massif: An incipient metamorphic core complex in western Anatolia, Turkey, *J. Geol. Soc.*, *151*, 213–216, doi:10.1144/gsjgs.151.2.0213.

Bozkurt, E., and G. Park (1997a), Evolution of a mid-Tertiary extensional shear zone in the southern Menderes Massif, western Turkey, *Bull. Soc. Geol. Fr.*, *168*, 3–14.

Bozkurt, E., and R. G. Park (1997b), Microstructures of deformed grains in the augen gneisses of southern Menderes Massif (western Turkey) and their tectonic significance, *Geol. Rundsch.*, *86*, 103–119, doi:10.1007/s005310050125.

Bozkurt, E., and R. G. Park (1999), The structure of the Palaeozoic schists in the southern Menderes Massif, western Turkey: A new approach to the origin of the Main Menderes Metamorphism and its relation to the Lycian Nappes, *Geodin. Acta*, *12*(1), 25–42, doi:10.1016/S0985-3111(99)80021-7.

Bozkurt, E., and M. Satir (2000), The southern Menderes Massif (western Turkey): Geochronology and exhumation history, *Geol. J.*, *35*, 285–296, doi:10.1002/gj.849.

Bozkurt, E., and H. Sözbilir (2004), Tectonic evolution of the Gediz Graben: Field evidence for an episodic, two-stage extension in western Turkey, *Geol. Mag.*, *141*(1), 63–79, doi:10.1017/S0016756803008379.

Bozkurt, E., J. A. Winchester, G. Ruffet, and B. Rojay (2008), Age and chemistry of Miocene volcanic rocks from the Kiraz basin of the Küçük Menderes graben: Its significance for extensional tectonics of southwestern Anatolia, Turkey, *Geodin. Acta*, *21*, 239–257, doi:10.3166/ga.21.239-257.

Boztuğ, D., Y. Harlavan, R. C. Jonckheere, İ. Can, and R. Sari (2009), Geochemistry and K-Ar cooling ages of the Ilica, Çataldag (Balikesir) and Kozak (Izmir) granitoids, west Anatolia, Turkey, *Geol. J.*, *44*, 79–103, doi:10.1002/gj.1132.

B.P. Co. Ltd. (1971), The geological results of petroleum exploration in western Greece, *IGME Spec. Rep. 10*, Inst. of Geol. and Min. Explor., Athens.

Brun, J.-P., and D. Sokoutis (2007), Kinematics of the southern Rhodope Core Complex (northern Greece), *Int. J. Earth Sci.*, *96*, 1079–1099, doi:10.1007/s00531-007-0174-2.

Butler, R. F. (1992), *Paleomagnetism: Magnetic Domains to Geologic Terranes*, 195 pp., Blackwell Sci., Boston, Mass.

Caglayan, A. M., E. M. Öztürk, Z. Öztürk, H. Sav, and U. Akat (1980), Structural observations on the southern Menderes Massif, *Publ. Chamb. Geol. Eng. Turk*, *10*, 9–17.

Candan, O., O. Ö. Dora, R. Oberhänsli, F. Oelsner, and S. Dürr (1997), Blueschist relics in the Mesozoic cover series of the Menderes Massif and correlations with Samos Island, Cyclades, *Schweiz. Mineral. Petrogr. Mitt.*, *77*, 95–99.

Candan, O., Ö. O. Dora, R. Oberhänsli, M. Çetinkaplan, J. H. Partzsch, F. C. Warkus, and S. Dürr (2001), Pan-African high-pressure metamorphism in the Precambrian basement of the Menderes Massif, western Anatolia, Turkey, *Int. J. Earth Sci.*, *89*, 793–811, doi:10.1007/s005310000097.

Candan, O., M. Cetinkaplan, R. Oberhänsli, G. Rimmelé, and C. Akal (2005), Alpine high-P/low-T metamorphism of the Afyon Zone and implications for the metamorphic evolution of western Anatolia, Turkey, *Lithos*, *84*, 102–124, doi:10.1016/j.lithos.2005.02.005.

Catlos, E. J., and I. Cemen (2005), Monazite ages and the evolution of the Menderes Massif, western Turkey, *Int. J. Earth Sci.*, *94*, 204–217, doi:10.1007/s00531-005-0470-7.

Catlos, E. J., C. Baker, S. S. Sorensen, I. Cemen, and M. Hancer (2010), Geochemistry, geochronology, and cathodoluminescence imagery of the Salihli and Turgutlu granites (central Menderes Massif, western Turkey): Implications for Aegean tectonics, *Tectonophysics*, doi:10.1016/j.tecto.2009.06.001, in press.

Cavazza, W., A. I. Okay, and M. Zattin (2009), Rapid early middle Miocene exhumation of the Kazdag Massif (western Anatolia), *Int. J. Earth Sci.*, *98*, 1935–1947, doi:10.1007/s00531-008-0353-9.

Çelik, Ö. F., and M. F. Delaloyle (2003), Origin of metamorphic soles and their post-kinematic mafic dyke swarms in the Antalya and Lycian ophiolites, SW Turkey, *Geol. J.*, *38*, 235–256, doi:10.1002/gj.954.

Çelik, Ö. F., M. F. Delaloyle, and G. Feraud (2006), Precise ^{40}Ar-^{39}Ar ages from the metamorphic sole rocks of the Tauride Belt Ophiolites, southern Turkey: Implications for the rapid cooling history, *Geol. Mag.*, *143*, 213–227, doi:10.1017/S0016756805001524.

Çetinkaplan, M., O. Candan, R. Oberhänsli, and R. Bousquet (2008), Pressure–temperature evolution of lawsonite eclogite in Sivrihisar; Tavsanli Zone–Turkey, *Lithos*, *104*, 12–32, doi:10.1016/j.lithos.2007.11.007.

Çiftçi, N. B., and E. Bozkurt (2009a), Pattern of normal faulting in the Gediz Graben, SW Turkey, *Tectonophysics*, *473*, 234–260, doi:10.1016/j.tecto.2008.05.036.

Çiftçi, N. B., and E. Bozkurt (2009b), Evolution of the Miocene sedimentary fill of the Gediz Graben, SW Turkey, *Sediment. Geol.*, *216*, 49–79, doi:10.1016/j.sedgeo.2009.01.004.

Çiner, A., M. Karabiyikoğlu, O. Monod, M. Deynoux, and S. Tuzcu (2008), Late Cenozoic sedimentary evolution of the Antalya Basin, southern Turkey, *Turk. J. Earth Sci.*, *17*, 1–41.

Collins, A. S., and A. H. F. Robertson (1997), Lycian melange, southwestern Turkey: An emplaced Late Cretaceous accretionary complex, *Geology*, *25*, 255–258, doi:10.1130/0091-7613(1997)025<0255:LMSTAE>2.3.CO;2.

Collins, A. S., and A. H. F. Robertson (1998), Processes of Late Cretaceous to late Miocene episodic thrust-sheet translation in the Lycian Taurides, SW Turkey, *J. Geol. Soc.*, *155*, 759–772, doi:10.1144/gsjgs.155.5.0759.

Collins, A. S., and A. H. F. Robertson (1999), Evolution of the Lycian Allochthon, western Turkey, as a north-facing Late Palaeozoic to Mesozoic rift and passive continental margin, *Geol. J.*, *34*, 107–138, doi:10.1002/(SICI)1099-1034(199901/06)34:1/2<107::AID-GJ817>3.0.CO;2-L.

Collins, A. S., and A. H. F. Robertson (2003), Kinematic evidence for Late Mesozoic–Miocene emplacement of the Lycian Allochthon over the western Anatolide Belt, SW Turkey, *Geol. J.*, *38*, 295–310, doi:10.1002/gj.957.

Davis, P. B., and D. L. Whitney (2006), Petrogenesis of lawsonite and epidote eclogite and blueschist, Sivrihisar Massif, Turkey, *J. Metamorph. Geol.*, *24*, 823–849, doi:10.1111/j.1525-1314.2006.00671.x.

Davis, P. B., and D. L. Whitney (2008), Petrogenesis and structural petrology of high-pressure metabasalt pods, Sivrihisar, Turkey, *Contrib. Mineral. Petrol.*, *156*, 217–241, doi:10.1007/s00410-008-0282-4.

de Boer, C. B., and M. J. Dekkers (1998), Thermomagnetic behaviour of haematite and goethite as a function of grain size in various non-saturating magnetic fields, *Geophys. J. Int.*, *133*, 541–552, doi:10.1046/j.1365-246X.1998.00522.x.

Dilek, Y., and S. Altunkaynak (2009), Geochemical and temporal evolution of Cenozoic magmatism in western Turkey: Mantle response to collision, slab break-off, and lithospheric tearing in an orogenic belt, in *Geodynamics of Collision and Collapse at the Africa-Arabia-Eurasia Subduction Zone*, edited by D. J. J. van Hinsbergen et al., *Geol. Soc. Spec. Publ.*, *311*, 213–234, doi:10.1144/SP311.8.

Duermeijer, C. E., W. Krijgsman, C. G. Langereis, and J. H. ten Veen (1998), Post early Messinian counter-clockwise rotations on Crete: Implications for the late Miocene to Recent kinematics of the southern Hellenic Arc, *Tectonophysics*, *298*(1–3), 77–89.

Dumont, J. F., M. Gutnic, J. Marcoux, O. Monod, and A. Poisson (1972), Le Trias des Taurides occidentales (Turquie). Definition du bassin pamphylien: Un nouveau domain à ophiolites à la marge externe de la chaine taurique, *Z. Dtsch. Geol. Ges.*, *123*, 385–409.

Dunlop, D., and Ö. Özdemir (1997), *Rock Magnetism: Fundamentals and Frontiers*, 573 pp., Cambridge Univ. Press, Cambridge, U. K.

Emre, T., and H. Sözbilir (2007), Tectonic evolution of the Kiraz Basin, Küçük Menderes graben: Evidence for compression/uplift-related basin formation overprinted by extensional tectonics in west Anatolia, *Turk. J. Earth Sci.*, *16*, 441–470.

Ercan, T., M. Satir, G. Steinitz, A. Dora, E. Sarifakioglu, C. Adis, H.-J. Walter, and T. Yildirim (1996), Biga Yarimadasi ile Gökceada Bozcaada ve Tavsan adalarindaki (KB Anadolu) Tersiyer volkanismasinin özellikleri, *Bull. 117*, 55–86, Miner. Res. and Explor. Inst. of Turk., Ankara.

Erduran, M., B. Endrun, and T. Meier (2008), Continental vs. oceanic lithosphere beneath the eastern Mediterranean Sea—Implications from Rayleigh wave dispersion measurements, *Tectonophysics*, *457*, 42–52, doi:10.1016/j.tecto.2008.05.015.

Ersoy, Y., and C. Helvaci (2007), Stratigraphic and geochemical features of the Early Miocene bimodal (ultrapotassic and calc-alkaline) volcanic activity within the NE-trending Selendi basin, western Anatolia, Turkey, *Turk. J. Earth Sci.*, *16*, 117–139.

Ersoy, Y., C. Helvaci, H. Sözbilir, F. Erkül, and E. Bozkurt (2008), A geochemical approach to Neogene–Quaternary volcanic activity of western Anatolia: An example of episodic bimodal volcanism within the Selendi Basin, Turkey, *Chem. Geol.*, *255*, 265–282, doi:10.1016/j.chemgeo.2008.06.044.

Faccenna, C., L. Jolivet, C. Piromallo, and A. Morelli (2003), Subduction and the depth of convection of the Mediterranean mantle, *J. Geophys. Res.*, *108* (B2), 2099, doi:10.1029/2001JB001690.

Fassoulas, C., A. Kilias, and D. Mountrakis (1994), Postnappe stacking extension and exhumation of high-pressure/low-temperature rocks in the island of Crete, Greece, *Tectonics*, *13*, 127–138, doi:10.1029/93TC01955.

Fisher, R. A. (1953), Dispersion on a sphere, *Proc. R. Soc. London, Ser. A*, *217*, 295–305, doi:10.1098/rspa.1953.0064.

Flecker, R. M., A. H. F. Robertson, A. Poisson, and C. Müller (1995), Facies and tectonic significance of two contrasting Miocene basins in south coastal Turkey, *Terra Nova*, *7*, 221–232, doi:10.1111/j.1365-3121.1995.tb00691.x.

Forster, M. A., and G. S. Lister (2009), Core-complex-related extension of the Aegean lithosphere initiated at the Eocene-Oligocene transition, *J. Geophys. Res.*, *114*, B02401, doi:10.1029/2007JB005382.

Fytikas, M., F. Innocenti, P. Manetti, R. Mazzuoli, A. Peccerillo, and L. Villari (1984), Tertiary to Quaternary evolution of volcanism in the Aegean region,

in *The Geological Evolution of the Eastern Mediterranean*, edited by J. E. Dixon and A. H. F. Robertson, *Geol. Soc. Spec. Publ.*, *17*, 687–699, doi:10.1144/GSL.SP.1984.017.01.55.

Gautier, P., and J.-P. Brun (1994), Crustal-scale geometry and kinematics of late-orogenic extension in the central Aegean (Cyclades and Evvia island), *Tectonophysics*, *238*, 399–424, doi:10.1016/0040-1951(94)90066-3.

Gautier, P., J.-P. Brun, and L. Jolivet (1993), Structure and kinematics of upper Cenozoic extensional detachment on Naxos and Paros, *Tectonics*, *12*, 1180–1194, doi:10.1029/93TC01131.

Gautier, P., J.-P. Brun, R. Moriceau, D. Sokoutis, J. Martinod, and L. Jolivet (1999), Timing, kinematics and cause of Aegean extension: A scenario based on a comparison with simple analogue experiments, *Tectonophysics*, *315*, 31–72, doi:10.1016/S0040-1951(99)00281-4.

Gessner, K., S. Piazolo, T. Güngör, U. Ring, A. Kröner, and C. W. Passchier (2001a), Tectonic significance of deformation patterns in granitoid rocks of the Menderes Nappes, Anatolide belt, southwest Turkey, *Int. J. Earth Sci.*, *89*, 766–780, doi:10.1007/s005310000106.

Gessner, K., U. Ring, C. Johnson, R. Hetzel, C. W. Passchier, and T. Güngör (2001b), An active bivergent rolling-hinge detachment system: Central Menderes metamorphic core complex in western Turkey, *Geology*, *29*(7), 611–614, doi:10.1130/0091-7613(2001)029<0611:AABRHD>2.0.CO;2.

Gessner, K., U. Ring, C. W. Passchier, and T. Güngör (2001c), How to resist subduction: Evidence for large-scale out-of-sequence thrusting during Eocene collision in western Turkey, *J. Geol. Soc.*, *158*, 769–784.

Gessner, K., A. S. Collins, U. Ring, and T. Güngör (2004), Structural and thermal history of poly orogenic basement: U-Pb geochronology of granitoid rocks in the southern Menderes Massif, western Turkey, *J. Geol. Soc.*, *161*, 93–101, doi:10.1144/0016-764902-166.

Glodny, J., and R. Hetzel (2007), Precise U-Pb ages of syn-extensional Miocene intrusions in the central Menderes Massif, western Turkey, *Geol. Mag.*, *144*(2), 235–246, doi:10.1017/S0016756806003025.

Gökten, E., T. Havzoglu, and Ö. San (2001), Tertiary evolution of the central Menderes Massif based on structural investigations of metamorphics and sedimentary cover rocks between Salihli and Kiraz (western Turkey), *Int. J. Earth Sci.*, *89*, 745–756, doi:10.1007/s005310000099.

Göncüoglu, C. M., A. Özcan, N. Turhan, and A. Isik (1992), *Stratigraphy of Kütahya Region*, pp. 3–11, Miner. Res. and Explor. Inst. of Turk., Ankara.

Govers, R., and M. J. R. Wortel (2005), Lithosphere tearing at STEP faults: Response to edges of subduction zones, *Earth Planet. Sci. Lett.*, *236*, 505–523, doi:10.1016/j.epsl.2005.03.022.

Gralla, P. (1982), Das Präneogen der Insel Kos (Dodekanes, Griechenland), Ph.D. thesis, 182 pp., Univ. of Braunschweig, Brunswick, Germany.

Gürsoy, H., J. D. A. Piper, O. Tatar, and L. Mesci (1998), Palaeomagnetic study of the Karaman and Karapinar volcanic complexes, central Turkey: Neotectonic rotation in the south-central sector of the Anatolian Block, *Tectonophysics*, *299*, 191–211, doi:10.1016/S0040-1951(98)00205-4.

Gürsoy, H., J. D. A. Piper, and O. Tatar (2003), Neotectonic deformation in the western sector of tectonic escape in Anatolia: Palaeomagnetic study of the Afyon region, central Turkey, *Tectonophysics*, *374*, 57–79, doi:10.1016/S0040-1951(03)00346-9.

Gutnic, M., O. Monod, A. Poisson, and J. F. Dumont (1979), Géologie des Taurides occidentales (Türquie), *Mem. Soc. Geol. Fr.*, *137*, 1–112.

Hakyemez, H. Y. (1989), Geology and stratigraphy of the Cenozoic sedimentary rocks in the Kale-Kurbalik area, Denizli, southwestern Turkey, *Bull. Miner. Res. Explor. Turk.*, *109*, 1–14.

Harris, N. B. W., S. P. Kelley, and A. I. Okay (1994), Post-collision magmatism and tectonics in northwest Anatolia, *Contrib. Mineral. Petrol.*, *117*, 241–252, doi:10.1007/BF00310866.

Hayward, A. B. (1984a), Sedimentation and basin formation related to ophiolite nappe emplacement, Miocene, SW Turkey, *Sediment. Geol.*, *40*, 105–129, doi:10.1016/0037-0738(84)90042-3.

Hayward, A. B. (1984b), Miocene clastic sedimentation related to the emplacement of the Lycian Nappes and the Antalya Complex, S.W. Turkey, in *The Geological Evolution of the Eastern Mediterranean*, edited by J. E. Dixon and A. H. F. Robertson, *Geol. Soc. Spec. Publ.*, *17*, 287–300, doi:10.1144/GSL.SP.1984.017.01.21.

Hayward, A. B., and A. H. F. Robertson (1982), Direction of ophiolite emplacement inferred from Cretaceous and Tertiary sediments of an adjacent autochton, the Bey Daglari, southwest Turkey, *Geol. Soc. Am. Bull.*, *93*, 68–75.

Heslop, D., G. McIntosh, and M. J. Dekkers (2004), Using time- and temperature-dependent Preisach models to investigate the limitations of modelling isothermal remanent magnetization acquisition curves with cumulative log Gaussian functions, *Geophys. J. Int.*, *157*, 55–63, doi:10.1111/j.1365-246X.2004.02155.x.

Hetzel, R., and T. Reischmann (1996), Intrusion age of Pan-African augen gneisses in the southern Menderes Massif and the age of cooling after Alpine ductile extensional deformation, *Geol. Mag.*, *133*, 565–572, doi:10.1017/S0016756800007846.

Hetzel, R., C. W. Passchier, U. Ring, and Ö. O. Dora (1995a), Bivergent extension in orogenic belts: The Menderes massif (southwestern Turkey), *Geology*, *23*(5), 455–458, doi:10.1130/0091-7613(1995)023<0455:BEIOBT>2.3.CO;2.

Hetzel, R., U. Ring, C. Akal, and M. Troesch (1995b), Miocene NNE-directed extensional unroofing in the Menderes Massif, southwestern Turkey, *J. Geol. Soc.*, *152*, 639–654, doi:10.1144/gsjgs.152.4.0639.

Hetzel, R., R. L. Romer, O. Candan, and C. W. Passchier (1998), Geology of the Bozdag area, central Menderes massif, SW Turkey: Pan-African basement and Alpine deformation, *Geol. Rundsch.*, *87*, 394–406, doi:10.1007/s005310050218.

Horner, F., and R. Freeman (1982), Preliminary palaeomagnetic results from the Ionian Zone, western Greece, *Eos Trans. AGU*, *63*(51), 1273.

Horner, F., and R. Freeman (1983), Palaeomagnetic evidence from Pelagic Limestones for clockwise rotation of the Ionian zone, western Greece, *Tectonophysics*, *98*, 11–27, doi:10.1016/0040-1951(83)90208-1.

Hubert-Ferrari, A., G. King, J. van der Woerd, I. Villa, E. Altunel, and R. Armijo (2009), Long-term evolution of the North Anatolian Fault: New constraints from its eastern termination, in *Collision and Collapse at the Africa-Arabia-Eurasia Subduction Zone*, edited by D. J. J. van Hinsbergen et al., *Geol. Soc. Spec. Publ.*, *311*, 133–154, doi:10.1144/SP311.5.

Institute for Geology and Subsurface Research and Institut Français du Pétrole (1966), *Étude Géologique de l'Épire (Grèce nord-occidentale)*, 306 pp., Inst. Fr. du Pétrole, Paris.

Isik, V., and O. Tekeli (2001), Late orogenic crustal extension in the northern Menderes massif (western Turkey): Evidence for metamorphic core complex formation, *Int. J. Earth Sci.*, *89*, 757–765, doi:10.1007/s005310000105.

Isik, V., G. Seyitoglu, and I. Cemen (2003), Ductile-brittle transition along the Alasehir detachment fault and its structural relationship with the Simav detachment fault, Menderes massif, western Turkey, *Tectonophysics*, *374*, 1–18, doi:10.1016/S0040-1951(03)00275-0.

Isik, V., O. Tekeli, and G. Seyitoglu (2004), The $^{40}Ar/^{39}Ar$ age of extensional ductile deformation and granitoid intrusion in the northern Menderes core complex: Implications for the initiation of extensional tectonics in western Turkey, *J. Asian Earth Sci.*, *23*, 555–566, doi:10.1016/j.jseaes.2003.09.001.

Jenkins, D. A. L. (1972), Structural development of western Greece, *AAPG Bull.*, *56*, 128–149.

Johnson, C. L., et al. (2008), Recent investigations of the 0–5 Ma geomagnetic field recorded by lava flows, *Geochem. Geophys. Geosyst.*, *9*, Q04032, doi:10.1029/2007GC001696.

Jolivet, L. (2001), A comparison of geodetic and finite strain pattern in the Aegean, geodynamic implications, *Earth Planet. Sci. Lett.*, *187*, 95–104, doi:10.1016/S0012-821X(01)00277-1.

Jolivet, L., and J.-P. Brun (2010), Cenozoic geodynamic evolution of the Aegean, *Int. J. Earth Sci.*, *99*, 109–138, doi:10.1007/s00531-008-0366-4.

Jolivet, L., and C. Faccenna (2000), Mediterranean extension and the Africa-Eurasia collision, *Tectonics*, *19*, 1095–1106, doi:10.1029/2000TC900018.

Jolivet, L., J.-P. Brun, P. Gautier, S. Lallemant, and M. Patriat (1994a), 3D-kinematics of extension in the Aegean region from the early Miocene to the present, insights from the ductile crust, *Bull. Soc. Geol. Fr.*, *165*(3), 195–209.

Jolivet, L., J.-M. Daniel, C. Truffert, and B. Goffé (1994b), Exhumation of deep crustal metamorphic rocks and crustal extension in arc and back-arc regions, *Lithos*, *33*, 3–30, doi:10.1016/0024-4937(94)90051-5.

Jolivet, L., B. Goffé, P. Monié, C. Truffert-Luxey, M. Patriat, and M. Bonneau (1996), Miocene detachment on Crete and exhumation P-T-t paths of high-pressure metamorphic rocks, *Tectonics*, *15*, 1129–1153, doi:10.1029/96TC01417.

Jolivet, L., C. Facenna, B. Goffé, E. Burov, and P. Agard (2003), Subduction tectonics and exhumation of high-pressure metamorphic rocks in the Mediterranean orogen, *Am. J. Sci.*, *303*, 353–409, doi:10.2475/ajs.303.5.353.

Jolivet, L., G. Rimmelé, R. Oberhänsli, B. Goffé, and O. Candan (2004), Correlation of syn-orogenic tectonic and metamorphic events in the Cyclades, the Lycian Nappes and the Menderes Massif. Geodynamic implications, *Bull. Soc. Geol. Fr.*, *175*, 217–238, doi:10.2113/175.3.217.

Kalt, A., R. Altherr, and T. Ludwig (1998), Contact metamorphism in pelitic rocks on the island of Kos (Greece, eastern Aegean Sea): A test for the Na-in-cordierite thermometer, *J. Petrol.*, *39*(4), 663–688, doi:10.1093/petrology/39.4.663.

Karabiyikoğlu, M., S. Tuzcu, A. Çiner, M. Deynoux, S. Örçen, and A. Hakyemez (2005), Facies and environmental setting of the Miocene coral reefs in the late-orogenic fill of the Antalya Basin, western Taurides, Turkey: Implications for tectonic control and sea-level changes, *Sediment. Geol.*, *173*, 345–371, doi:10.1016/j.sedgeo.2003.08.006.

Karacik, Z., Y. Yilmaz, and J. A. Pearce (2007), The Dikili-Çandarli volcanics, western Turkey: Magmatic interactions as recorded by petrographic and geochemical features, *Turk. J. Earth Sci.*, *16*, 493–522.

Kaya, O., E. Ünay, F. Göktas, and G. Saraç (2007), Early Miocene stratigraphy of central west Anatolia, Turkey: Implications for the tectonic evolution of the eastern Aegean area, *Geol. J.*, *42*, 85–109, doi:10.1002/gj.1071.

Kazanci, N. (1990), Fan-delta sequences in the Pleistocene and Holocene Burdur Basin, Turkey: The role of basin-margin configuration in sediment entrapment and differential facies development, *Spec. Publ. Int. Assoc. Sedimentol.*, *10*, 185–198.

Kazanci, N., and O. Erol (1987), Sedimentary characteristics of a Pleistocene fan-delta complex from Burdur basin, Turkey, *Z. Geomorphol.*, *31*, 261–275.

Kirschvink, J. L. (1980), The least-squares line and plane and the analysis of palaeomagnetic data, *Geophys. J. R. Astron. Soc.*, *62*, 699–718.

Kissel, C., and C. Laj (1988), The tertiary geodynamical evolution of the Aegean arc: A paleomagnetic reconstruction, *Tectonophysics*, *146*, 183–201, doi:10.1016/0040-1951(88)90090-X.

Kissel, C., and A. Poisson (1986), Étude paléomagnetique des formations néogènes du bassin d'Antalya

(Taurides occidentales-Turquie), *C. R. Acad. Sci., Ser. II*, *302*(10), 711–716.

Kissel, C., and A. Poisson (1987), Étude paléomagnetique préliminaire des formations cénozoïques des Bey Daglari (Taurides occidentales, Turquie), *C. R. Acad. Sci., Ser. II*, *304*(8), 343–348.

Kissel, C., M. Jamet, and C. Laj (1984), Paleomagnetic evidence of Miocene and Pliocene rotational deformations of the Aegean area, in *The Geological Evolution of the Eastern Mediterranean*, edited by J. E. Dixon and A. H. F. Robertson, *Geol. Soc. Spec. Publ.*, *17*, 669–679, doi:10.1144/GSL.SP.1984.017.01.53.

Kissel, C., C. Laj, and C. Müller (1985), Tertiary geodynamical evolution of northwestern Greece: Paleomagnetic results, *Earth Planet. Sci. Lett.*, *72*, 190–204, doi:10.1016/0012-821X(85)90005-6.

Kissel, C., C. Laj, A. Poisson, and K. Simeakis (1989), A pattern of block rotations in central Aegean, in *Paleomagnetic Rotations and Continental Deformation*, *NATO ASI Ser., Ser. C*, vol. 254, edited by C. Kissel and C. Laj, pp. 115–129, Kluwer Acad., Dordrecht, Netherlands.

Kissel, C., O. Averbuch, D. Frizon de Lamotte, O. Monod, and S. Allerton (1993), First paleomagnetic evidence for a post-Eocene clockwise rotation of the western Taurides thrust belt east of the Isparta reentrant (southwestern Turkey), *Earth Planet. Sci. Lett.*, *117*(1–2), 1–14, doi:10.1016/0012-821X(93)90113-N.

Kissel, C., F. Speranza, and V. Milicevic (1995), Paleomagnetism of external southern Dinarides and northern Albanides: Implications for the Cenozoic activity of the Scutari-Pec shear zone, *J. Geophys. Res.*, *100*, 14,999–15,007, doi:10.1029/95JB01243.

Kissel, C., C. Laj, A. Poisson, and N. Görür (2003), Paleomagnetic reconstruction of the Cenozoic evolution of the eastern Mediterranean, *Tectonophysics*, *362*, 199–217, doi:10.1016/S0040-1951(02)00638-8.

Koçyiğit, A., H. Yusufoglu, and E. Bozkurt (1999), Evidence from the Gediz graben for episodic two-stage extension in western Turkey, *J. Geol. Soc.*, *156*, 605–616, doi:10.1144/gsjgs.156.3.0605.

Konak, N., N. Akdeniz, and E. M. Öztürk (1987), Geology of the south of Menderes Massif: Correlation of Variscan and pre-Variscan events of the Alpine Mediterranean Mountain Belt, field meeting, IGCP Project 5, *Min. Res. Explor. Inst. Turk. Publ.*, *5*, 42–53.

Koralay, O. E., O. Ö. Dora, F. Chen, M. Satir, and O. Candan (2004), Geochemistry and geochronology of orthogneisses in the Derbent (Alasehir) area, eastern part of the Ödemis-Kiraz submassif, Menderes Massif: Pan-African magmatic activity, *Turk. J. Earth Sci.*, *13*, 37–61.

Kruiver, P. P., M. J. Dekkers, and D. Heslop (2001), Quantification of magnetic coercivity components by the analysis of acquisition curves of isothermal remanent magnetisation, *Earth Planet. Sci. Lett.*, *189*, 269–276, doi:10.1016/S0012-821X(01)00367-3.

Kumerics, C., U. Ring, S. Bricheau, J. Glodny, and P. Monié (2005), The extensional Messaria shear zone and associated brittle detachment faults, Aegean Sea, Greece, *J. Geol. Soc.*, *162*(4), 701–721, doi:10.1144/0016-764904-041.

Laj, C., M. Jamet, D. Sorel, and J. P. Valente (1982), First paleomagnetic results from Mio-Pliocene series of the Hellenic Sedimentary arc, *Tectonophysics*, *86*, 45–67, doi:10.1016/0040-1951(82)90061-0.

Lawrence, K. P., L. Tauxe, H. Staudigel, C. G. Constable, A. A. P. Koppers, W. McIntosh, and C. L. Johnson (2009), Paleomagnetic field properties at high southern latitude, *Geochem. Geophys. Geosyst.*, *10*, Q01005, doi:10.1029/2008GC002072.

Le Pichon, X., and J. Angelier (1979), The Hellenic arc and trench system: A key to the neotectonic evolution of the eastern Mediterranean area, *Tectonophysics*, *60*, 1–42, doi:10.1016/0040-1951(79)90131-8.

Lips, A. L. W., S. H. White, and J. R. Wijbrans (1998), $^{40}Ar/^{39}Ar$ laserprobe direct dating of discrete deformational events: A continuous record of early Alpine tectonics in the Pelagonian zone, NW Aegean area, Greece, *Tectonophysics*, *298*(1–3), 133–153, doi:10.1016/S0040-1951(98)00181-4.

Lips, A. L. W., D. Cassard, H. Sözbilir, and H. Yilmaz (2001), Multistage exhumation of the Menderes Massif, western Anatolia (Turkey), *Int. J. Earth Sci.*, *89*, 781–792, doi:10.1007/s005310000101.

Lister, G., G. Banga, and A. Feenstra (1984), Metamorphic core complexes of Cordilleran type in the Cyclades. Aegean Sea, Greece, *Geology*, *12*, 221–225, doi:10.1130/0091-7613(1984)12<221:MCCOCT>2.0.CO;2.

Loos, S., and T. Reischmann (1999), The evolution of the southern Menderes Massif in SW Turkey as revealed by zircon dating, *J. Geol. Soc.*, *156*, 1021–1030, doi:10.1144/gsjgs.156.5.1021.

Márton, E., D. J. Papanikolaou, and E. Lekkas (1990), Paleomagnetic results from the Pindos, Paxos and Ionian zones of Greece, *Phys. Earth Planet. Inter.*, *62*, 60–69, doi:10.1016/0031-9201(90)90192-Z.

Mauritsch, H. J., R. Scholger, S. L. Bushati, and H. Ramiz (1995), Palaeomagnetic results from southern Albania and their significance for the geodynamic evolution of the Dinarides, Albanides and Hellenides, *Tectonophysics*, *242*, 5–18, doi:10.1016/0040-1951(94)00150-8.

Mauritsch, H. J., R. Scholger, S. L. Bushati, and A. Xhomo (1996), Palaeomagnetic investigations in northern Albania and their significance for the geodynamic evolution of the Adriatic-Aegean realm, in *Palaeomagnetism and Tectonics of the Mediterranean Region*, edited by A. Morris and D. H. Tarling, *Geol. Soc. Spec. Publ.*, *105*, 265–275, doi:10.1144/GSL.SP.1996.105.01.23.

McFadden, P. L., and F. J. Lowes (1981), The discrimination of mean directions drawn from Fisher distributions, *Geophys. J. R. Astron. Soc.*, *67*, 19–33.

McFadden, P. L., and M. W. McElhinny (1988), The combined analysis of remagnetisation circles and direct observations in paleomagnetism, *Earth Planet. Sci. Lett.*, *87*, 161–172, doi:10.1016/0012-821X(88)90072-6.

McFadden, P. C., and M. W. McElhinny (1990), Classification of the reversal test in palaeomagnetism, *Geophys. J. Int.*, *103*, 725–729, doi:10.1111/j.1365-246X.1990.tb05683.x.

McFadden, P. L., R. T. Merril, M. W. McElhinny, and S. Lee (1991), Reversals of the Earth's magnetic field and temporal variations of the dynamo families, *J. Geophys. Res.*, *96*, 3923–3933, doi:10.1029/90JB02275.

Meulenkamp, J. E., M. J. R. Wortel, W. A. Van Wamel, W. Spakman, and E. Hoogerduyn Strating (1988), On the Hellenic subduction zone and the geodynamical evolution of Crete since the late middle Miocene, *Tectonophysics*, *146*, 203–215, doi:10.1016/0040-1951(88)90091-1.

Mineral Research and Exploration Institute of Turkey (MTA) (2002), Geological map of Turkey, sheets Izmir, Ankara, Denizli and Konya, scale 1:500,000, Ankara.

Morris, A. (1995), Rotational deformation during Palaeogene thrusting and basin closure in eastern central Greece: Palaeomagnetic evidence from Mesozoic carbonates, *Geophys. J. Int.*, *121*, 827–847, doi:10.1111/j.1365-246X.1995.tb06442.x.

Morris, A., and M. Anderson (1996), First palaeomagnetic results from the Cycladic Massif, Greece, and their implications for Miocene extension directions and tectonic models in the Aegean, *Earth Planet. Sci. Lett.*, *142*, 397–408, doi:10.1016/0012-821X(96)00114-8.

Morris, A., and A. H. F. Robertson (1993), Miocene remagnetisation of carbonate platform and Antalya Complex units within the Isparta Angle, SW Turkey, *Tectonophysics*, *220*, 243–266, doi:10.1016/0040-1951(93)90234-B.

Mposkos, W. D., and D. K. Kostopoulos (2001), Diamond, former coesite and supersilicic garnet in metasedimentary rocks from the Greek Rhodope: A new ultrahigh-pressure metamorphic province established, *Earth Planet. Sci. Lett.*, *192*, 497–506, doi:10.1016/S0012-821X(01)00478-2.

Mullender, T. A. T., A. J. Van Velzen, and M. J. Dekkers (1993), Continuous drift correction and separate identification of ferrimagnetic and paramagnetic contribution in thermomagnetic runs, *Geophys. J. Int.*, *114*, 663–672, doi:10.1111/j.1365-246X.1993.tb06995.x.

Müller, R. D., J.-Y. Royden, and L. A. Lawver (1993), Revised plate motions relative to the hotspots from combined Atlantic and Indian Ocean hotspot tracks, *Geology*, *21*, 275–278, doi:10.1130/0091-7613(1993)021<0275:RPMRTT>2.3.CO;2.

Oberhänsli, R., O. Candan, Ö. O. Dora, and S. H. Dürr (1997), Eclogites within the Menderes Massif/western Turkey, *Lithos*, *41*, 135–150, doi:10.1016/S0024-4937(97)82009-9.

Oberhänsli, R., P. Monié, O. Candan, F. C. Warkus, J. H. Partzsch, and O. Ö. Dora (1998), The age of blueschist metamorphism in the Mesozoic cover series of the Menderes Massif, *Schweiz. Mineral. Petrogr. Mitt.*, *78*, 309–316.

Oberhänsli, R., J. H. Partzsch, O. Candan, and M. Cetinkaplan (2001), First occurrence of Fe-Mg-carpholite documenting a high-pressure metamorphism in metasediments of the Lycian Nappes, SW Turkey, *Int. J. Earth Sci.*, *89*, 867–873, doi:10.1007/s005310000103.

Okay, A. I. (1981), Lawsonite zone blueschists and a sodic amphibole producing reaction in the Tavsanli region, northwest Turkey, *Contrib. Mineral. Petrol.*, *75*, 179–186, doi:10.1007/BF01166758.

Okay, A. I. (1984), Distribution and characteristics of the northwest Turkish blueschists, in *The Geological Evolution of the Eastern Mediterranean*, edited by J. E. Dixon and A. H. F. Robertson, *Geol. Soc. Spec. Publ.*, *17*, 455–466, doi:10.1144/GSL.SP.1984.017.01.33.

Okay, A. I. (1986), High pressure/low temperature metamorphic rocks of Turkey, in *Blueschists and Eclogites*, edited by B. Evans and E. H. Brown, *Mem. Geol. Soc. Am.*, *164*, 333–348.

Okay, A. I. (1989), Geology of the Menderes Massif and the Lycian Nappes south of Denizli, western Taurides, *Miner. Resour. Explor. Bull.*, *109*, 37–51.

Okay, A. I. (2001), Stratigraphic and metamorphic inversions in the central Menderes Massif: A new structural model, *Int. J. Earth Sci.*, *89*, 709–727, doi:10.1007/s005310000098.

Okay, A. I., and D. Altiner (2007), A condensed Mesozoic succession north of Izmir: A fragment of the Anatolide-Tauride Platform in the Bornova Flysch Zone, *Turk. J. Earth Sci.*, *16*, 257–279.

Okay, A. I., and S. P. Kelley (1994), Tectonic setting, petrology and geochronology of jadeite + glaucophane and chloritoid + glaucophane schists from north-west Turkey, *J. Metamorph. Geol.*, *12*, 455–466, doi:10.1111/j.1525-1314.1994.tb00035.x.

Okay, A. I., and M. Satir (2000), Coeval plutonism and metamorphism in a latest Oligocene metamorphic core complex in northwest Turkey, *Geol. Mag.*, *137*(5), 495–516, doi:10.1017/S0016756800004532.

Okay, A. I., and M. Siyako (1993), The new position of the Izmir-Ankara Neo-Tethyan suture between Izmir and Balikesir, in *Tectonics and Hydrocarbon Potential of Anatolia and Surrounding Regions: Proceedings of the Ozan Sungurlu Symposium*, edited by S. Turgut, pp. 333–355, Ozan Sungurlu Found. for Sci., Educ. and Aid, Ankara.

Okay, A. I., M. Satir, H. Maluski, M. Siyako, P. Monié, R. Metzger, and S. Akyüz (1996), Paleo- and Neo-Tethyan events in northwestern Turkey: Geologic and geochronologic constraints, in *The Tectonic Evolution of Asia*, edited by A. Yin and T. M. Harrison, pp. 420–441, Cambridge Univ. Press, Cambridge, U. K.

Okay, A. I., I. Tansel, and O. Tüysüz (2001), Obduction, subduction and collision as reflected in the Upper Cretaceous–lower Eocene sedimentary record of western Turkey, *Geol. Mag.*, *138*, 117–142, doi:10.1017/S0016756801005088.

Okay, A. I., M. Satir, M. Zattin, W. Cavazza, and G. Topuz (2008), An Oligocene ductile strike-slip shear zone: The Uludag Massif, northwest Turkey—Implications for the westward translation of Anatolia, *Geol. Soc. Am. Bull.*, *120*, 893–911, doi:10.1130/B26229.1.

Önen, A. P. (2003), Neotethyan ophiolitic rocks of the Anatolides of NW Turkey and comparison with Tauride ophiolites, *J. Geol. Soc.*, *160*, 947–962, doi:10.1144/0016-764902-125.

Önen, A. P., and R. Hall (2000), Sub-ophiolite metamorphic rocks from NW Anatolia, Turkey, *J. Metamorph. Geol.*, *18*, 483–495, doi:10.1046/j.1525-1314.2000.00276.x.

Özcan, A., C. M. Göncüoglu, N. Turhan, S. Uysal, and M. Sentürk (1988), Late Paleozoic evolution of the Kütahya–Bolkardag Belt, *Middle East Tech. Univ. J. Pure Appl. Sci.*, *21*, 211–220.

Özer, S. (1998), Rudist bearing Upper Cretaceous metamorphic sequences of the Menderes Massif (western Turkey), *Geobios*, *31*, Suppl. 1, 235–249, doi:10.1016/S0016-6995(98)80080-6.

Özer, S., and H. Sözbilir (2003), Presence and tectonic significance of Cretaceous rudist species in the so-called Permo-Carboniferous Göktepe Formation, central Menderes metamorphic massif, western Turkey, *Int. J. Earth Sci.*, *92*, 397–404, doi:10.1007/s00531-003-0333-z.

Özer, S., H. Sözbilir, I. Özkar, V. Toker, and B. Sari (2001), Stratigraphy of Upper Cretaceous-Palaeogene sequences in the southern and eastern Menderes Massif (western Turkey), *Int. J. Earth Sci.*, *89*, 852–866, doi:10.1007/s005310000142.

Özkaymak, Ç., and H. Sözbilir (2008), Stratigraphic and structural evidence for fault reactivation: The active Manisa fault zone, western Anatolia, *Turk. J. Earth Sci.*, *17*, 615–635.

Paréjas, E. (1940), La tectonique transversale de la Turquie, *Rev. Fac. Sci. Univ. Istanbul, Ser. B*, *5*, 133–244.

Pe-Piper, G., and D. J. W. Piper (1993), Revised stratigraphy of the Miocene rocks of Lesbos, Greece, *Neues Jahrb. Geol. Palaeontol. Monatsh.*, *1993*, 97–110.

Pe-Piper, G., and D. J. W. Piper (2002), *The Igneous Rocks of Greece: The Anatomy of an Orogen*, 573 pp., Gebrüder Borntraeger, Berlin.

Piper, J. D. A., J. M. Moore, O. Tatar, H. Gürsoy, and R. G. Park (1996), Palaeomagnetic study of crustal deformation across an intracontinental transform: The North Anatolian Fault Zone in northern Turkey, in *Palaeomagnetism and Tectonics of the Mediterranean Region*, edited by A. Morris and D. H. Tarling, *Geol. Soc. Spec. Publ.*, *105*, 299–310, doi:10.1144/GSL.SP.1996.105.01.26.

Piper, J. D. A., O. Tatar, and H. Gursoy (1997), Deformational behaviour of continental lithosphere deduced from block rotations across the North Anatolian Fault Zone in Turkey, *Earth Planet. Sci. Lett.*, *150*, 191–203, doi:10.1016/S0012-821X(97)00103-9.

Piper, J. D. A., H. Gürsoy, and O. Tatar (2002a), Palaeomagnetism and magnetic properties of the Cappadocian ignimbrite succession, central Turkey and Neogene tectonics of the Anatolian collage, *J. Volcanol. Geotherm. Res.*, *117*, 237–262, doi:10.1016/S0377-0273(02)00221-4.

Piper, J. D. A., H. Gürsoy, O. Tatar, T. Isseven, and A. Koçigyt (2002b), Palaeomagnetic evidence for the Gondwanian origin of the Taurides and rotation of the Isparta Angle, southern Turkey, *Geol. J.*, *37*, 317–336, doi:10.1002/gj.920.

Piper, D. J. W., H. Gürsoy, M. Tatar, M. E. Beck, A. Rao, F. Kocbulut, and B. L. Mesci (2010), Distributed neotectonic deformation in the Anatolides of Turkey: A palaeomagnetic study, *Tectonophysics*, doi:10.1016/j.tecto.2010.03.008, in press.

Platzman, E. S., J. P. Platt, C. Tapirdamaz, M. Sanver, and C. C. Rundle (1994), Why are there no clockwise rotations along the North Anatolian Fault Zone?, *J. Geophys. Res.*, *99*, 21,705–21,715, doi:10.1029/94JB01665.

Platzman, E. S., C. Tapirdamaz, and M. Sanver (1998), Neogene anticlockwise rotation of Anatolia (Turkey): Preliminary palaeomagnetic and geochronological results, *Tectonophysics*, *299*, 175–189, doi:10.1016/S0040-1951(98)00204-2.

Poisson, A. (1977), Récherches géologiques dans les Taurides occidentales (Turquie), thesis, Univ. de Paris-Sud, Paris.

Price, S. P., and B. C. Scott (1994), Fault-block rotations at the edge of a zone of continental extension, southwest Turkey, *J. Struct. Geol.*, *16*, 381–392, doi:10.1016/0191-8141(94)90042-6.

Purvis, M., and A. Robertson (2005), Miocene sedimentary evolution of the NE–SW-trending Selendi and Gördes basins, W Turkey: Implications for extensional processes, *Sediment. Geol.*, *174*, 31–62, doi:10.1016/j.sedgeo.2004.11.002.

Purvis, M., A. H. F. Robertson, and M. S. Pringle (2005), Ar^{40}-Ar^{39} dating of biotite and sanidine in tuffaceous sediments and related intrusive rocks: Implications for the Early Miocene evolution of the Gördes and Selendi basins, W Turkey, *Geodin. Acta*, *18*, 239–253, doi:10.3166/ga.18.239-253.

Régnier, J. L., U. Ring, C. W. Passchier, K. Gessner, and T. Güngör (2003), Contrasting metamorphic evolution of metasedimentary rocks from the Cine and Selimiye nappes in the Anatolide belt, western Turkey, *J. Metamorph. Geol.*, *21*, 699–721, doi:10.1046/j.1525-1314.2003.00473.x.

Régnier, J.-L., J. E. Mezger, and C. W. Passchier (2007), Metamorphism of Precambrian–Palaeozoic schists of the Menderes core series and contact relationships with Proterozoic orthogneisses of the western Çine Massif, Anatolide belt, western Turkey, *Geol. Mag.*, *144*, 67–104, doi:10.1017/S0016756806002640.

Rimmelé, G., L. Jolivet, R. Oberhänsli, and B. Goffé (2003a), Deformation history of the high-pressure Lycian Nappes and implications for the tectonic evolution of SW Turkey, *Tectonics*, *22*(2), 1007, doi:10.1029/2001TC901041.

Rimmelé, G., R. Oberhänsli, B. Goffé, L. Jolivet, O. Candan, and M. Cetinkaplan (2003b), First evidence of high-pressure metamorphism in the "cover series" of the southern Menderes massif. Tectonic and metamorphic implications for the evolution of SW Turkey, *Lithos*, *71*, 19–46, doi:10.1016/S0024-4937(03)00089-6.

Rimmelé, G., T. Parra, B. Goffé, R. Oberhänsli, L. Jolivet, and O. Candan (2005), Exhumation paths of high-pressure–low-temperature metamorphic rocks from the Lycian Nappes and the Menderes Massif (SW Turkey): A multi-equilibrium approach, *J. Petrol.*, *46*(3), 641–669, doi:10.1093/petrology/egh092.

Rimmelé, G., R. Oberhänsli, O. Candan, B. Goffé, and L. Jolivet (2006), The wide distribution of HP-LT rocks in the Lycian Belt (western Turkey): Implications for accretionary wedge geometry, in *Tectonic Development of the Eastern Mediterranean Region*, edited by A. H. F. Robertson and D. Mountrakis, *Geol. Soc. Spec. Publ.*, *260*, 447–466, doi:10.1144/GSL.SP.2006.260.01.18.

Ring, U., and A. S. Collins (2005), U-Pb SIMS dating of synkinematic granites: Timing of core-complex formation in the northern Anatolide belt of western Turkey, *J. Geol. Soc.*, *162*, 289–298, doi:10.1144/0016-764904-016.

Ring, U., and P. W. Layer (2003), High-pressure metamorphism in the Aegean, eastern Mediterranean: Underplating and exhumation from the Late Cretaceous until the Miocene to Recent above the retreating Hellenic subduction zone, *Tectonics*, *22*(3), 1022, doi:10.1029/2001TC001350.

Ring, U., K. Gessner, T. Güngör, and C. W. Passchier (1999a), The Menderes Massif of western Turkey and the Cycladic Massif in the Aegean—Do they really correlate?, *J. Geol. Soc.*, *156*, 3–6, doi:10.1144/gsjgs.156.1.0003.

Ring, U., S. Laws, and M. Bernet (1999b), Structural analysis of a complex nappe sequence and late-orogenic basins from the Aegean Island of Samos, *J. Struct. Geol.*, *21*, 1575–1601, doi:10.1016/S0191-8141(99)00108-X.

Ring, U., C. Johnson, R. Hetzel, and K. Gessner (2003a), Tectonic denudation of a Late Cretaceous-Tertiary collisional belt: Regionally symmetric cooling patterns and their relation to extensional faults in the Anatolide belt of western Turkey, *Geol. Mag.*, *140*(4), 421–441, doi:10.1017/S0016756803007878.

Ring, U., S. N. Thomson, and M. Bröcker (2003b), Fast extension but little exhumation: The Vari detachment in the Cyclades, Greece, *Geol. Mag.*, *140*(3), 245–252, doi:10.1017/S0016756803007799.

Ring, U., J. Glodny, T. Will, and S. N. Thomson (2007), An Oligocene extrusion wedge of blueschist-facies nappes on Evia, Aegean Sea, Greece: Implications for the early exhumation of high-pressure rocks, *J. Geol. Soc.*, *164*, 637–652, doi:10.1144/0016-76492006-041.

Ring, U., J. Glodny, T. Will, and S. N. Thomson (2010), The Hellenic subduction system: High-pressure metamorphism, exhumation, normal faulting, and large-scale extension, *Annu. Rev. Earth Planet. Sci.*, *38*, 45–76.

Robertson, A. H. F., and J. E. Dixon (1984), Introduction: Aspects of the geological evolution of the eastern Mediterranean, in *The Geological Evolution of the Eastern Mediterranean*, edited by A. H. F. Robertson and J. E. Dixon, *Geol. Soc. Spec. Publ.*, *17*, 1–74, doi:10.1144/GSL.SP.1984.017.01.02.

Satir, M., and H. Friedrichsen (1986), The origin and evolution of the Menderes Massif, W-Turkey: A rubidium/strontium and oxygen isotope study, *Geol. Rundsch.*, *75*, 703–714, doi:10.1007/BF01820642.

Scheepers, P. (1992), No tectonic rotation for the Apulia-Gargano foreland in the Pleistocene, *Geophys. Res. Lett.*, *19*(22), 2275–2278, doi:10.1029/92GL02440.

Schermer, E. R. (1990), Mechanisms of blueschist creation and preservation in an A-type subduction zone, Mount Olympos region, Greece, *Geology*, *18*, 1130–1133, doi:10.1130/0091-7613(1990)018<1130:MOBCAP>2.3.CO;2.

Schuiling, R. D. (1962), On petrology, age and evolution of the Menderes Massif, W-Turkey: A rubidium/strontium and oxygen isotope study, *Bull. Inst. Miner. Res. Explor. Turk.*, *58*, 703–714.

Schulz-Mirbach, T., and B. Reichenbacher (2008), Fossil Aphanius (Teleostei, Cyprinodontiformes) from southwestern Anatolia (Turkey): A contribution to the evolutionary history of a hotspot of freshwater biodiversity, *Geodiversitas*, *30*, 577–592.

Sen, S., and G. Seyitoğlu (2009), Magnetostratigraphy of early–middle Miocene deposits from east-west trending Alasehir and Büyük Menderes grabens in western Turkey, and its tectonic implications, in *Collision and Collapse at the Africa-Arabia-Eurasia Subduction Zone*, edited by D. J. J. van Hinsbergen et al., *Geol. Soc. Spec. Publ.*, *311*, 321–342, doi:10.1144/SP311.13.

Sengör, A. M. C., and Y. Yilmaz (1981), Tethyan evolution of Turkey: A plate tectonic approach, *Tectonophysics*, *75*, 181–241, doi:10.1016/0040-1951(81)90275-4.

Sengör, A. M. C., M. Satir, and R. Akkök (1984), Timing of tectonic events in the Menderes Massif, western Turkey: Implications for tectonic evolution and evidence for Pan-African basement in Turkey, *Tectonics*, *3*, 693–707, doi:10.1029/TC003i007p00693.

Sengün, F., O. Candan, O. Ö. Dora, and O. E. Koralay (2006), Petrography and geochemistry of paragneisses in the Çine submassif of the Menderes Massif, western Anatolia, *Turk. J. Earth Sci.*, *15*, 321–342.

Sentürk, M., and F. Yagmurlu (2003), Acigöl ve Burdur Gölü arasindaki bölgenin jeologiik ve sismotektonik özellikleri, *Suleyman Demirel Univ. Fen Bilimleri Enst. Derg.*, *7*, 11–24.

Seyitoglu, G., B. C. Scott, and C. C. Rundle (1992), Timing of Cenozoic extensional tectonics in west Turkey, *J. Geol. Soc.*, *149*, 533–538, doi:10.1144/gsjgs.149.4.0533.

Seyitoglu, G., D. Anderson, G. Nowell, and B. Scott (1997), The evolution from Miocene potassic to Quaternary sodic magmatism in western Turkey: Implications for enrichment processes in the lithospheric mantle, *J. Volcanol. Geotherm. Res.*, *76*, 127–147, doi:10.1016/S0377-0273(96)00069-8.

Seyitoglu, G., V. Isik, and I. Cemen (2004), Complete Tertiary exhumation history of the Menderes massif, western Turkey: An alternative working hypothesis, *Terra Nova*, *16*(6), 358–364, doi:10.1111/j.1365-3121.2004.00574.x.

Sherlock, S., S. Kelley, S. Inger, N. Harris, and A. I. Okay (1999), $^{40}Ar/^{39}Ar$ and Rb-Sr geochronology of high-pressure metamorphism and exhumation history of the Tavsanli Zone, NW Turkey, *Contrib. Mineral. Petrol.*, *137*, 46–58, doi:10.1007/PL00013777.

Sözbilir, H. (2005), Oligo-Miocene extension in the Lycian orogen: Evidence from the Lycian molasse basin, SW Turkey, *Geodin. Acta*, *18*, 255–282, doi:10.3166/ga.18.255-282.

Speranza, F., and C. Kissel (1993), First paleomagnetism of Eocene rocks from Gargano: Widespread overprint or non-rotation?, *Geophys. Res. Lett.*, *20*(23), 2627–2630, doi:10.1029/93GL02816.

Speranza, F., C. Kissel, I. Islami, A. Hyseni, and C. Laj (1992), First paleomagnetic evidence for rotation of the Ionian zone of Albania, *Geophys. Res. Lett.*, *19*(7), 697–700, doi:10.1029/92GL00575.

Speranza, F., I. Islami, C. Kissel, and A. Hyseni (1995), Palaeomagnetic evidence for Cenozoic clockwise rotation of the external Albanides, *Earth Planet. Sci. Lett.*, *129*, 121–134, doi:10.1016/0012-821X(94)00231-M.

Tatar, O., J. D. A. Piper, R. G. Park, and H. Gürsoy (1995), Palaeomagnetic study of block rotations in the Niksar overlap region of the North Anatolian Fault Zone, central Turkey, *Tectonophysics*, *244*, 251–266, doi:10.1016/0040-1951(94)00241-Z.

Tatar, O., J. D. A. Piper, H. Gürsoy, and H. Temiz (1996), Regional significance of neotectonic counterclockwise rotation in central Turkey, *Int. Geol. Rev.*, *38*, 692–700, doi:10.1080/00206819709465353.

Tatar, O., H. Gürsoy, and J. D. A. Piper (2002), Differential neotectonic rotations in Anatolia and the Tauride Arc: Palaeomagnetic investigation of the Erenlerdag Volcanic Complex and Isparta volcanic district, south-central Turkey, *J. Geol. Soc.*, *159*, 281–294, doi:10.1144/0016-764901-035.

Tauxe, L., and D. V. Kent (2004), A simplified statistical model for the geomagnetic field and the detection of shallow bias in paleomagnetic inclinations: Was the ancient magnetic field dipolar?, in *Timescales of the Paleomagnetic Field*, *Geophys. Monogr. Ser.*, vol. 145, edited by J. E. T. Channell et al., pp. 101–115, AGU, Washington, D. C.

Tauxe, L., K. P. Kodama, and D. V. Kent (2008), Testing corrections for paleomagnetic inclination error in sedimentary rocks: A comparative approach, *Phys. Earth Planet. Inter.*, *169*, 152–165, doi:10.1016/j.pepi.2008.05.006.

Taymaz, T., J. Jackson, and D. McKenzie (1991), Active tectonics of the north and central Aegean Sea, *Geophys. J. Int.*, *106*, 433–490, doi:10.1111/j.1365-246X.1991.tb03906.x.

ten Veen, J. H., S. J. Boulton, and M. C. Alçiçek (2009), From palaeotectonics to neotectonics in the Neotethys realm: The importance of kinematic decoupling and inherited structural grain in SW Anatolia (Turkey), *Tectonophysics*, *473*, 261–281, doi:10.1016/j.tecto.2008.09.030.

Thomson, S. N., B. Stöckhert, and M. R. Brix (1999), Miocene high-pressure metamorphic rocks of Crete, Greece: Rapid exhumation by buoyant escape, in *Exhumation Processes: Normal Faulting, Ductile Flow and Erosion*, edited by U. Ring et al., *Geol. Soc. Spec. Publ.*, *154*, 87–107, doi:10.1144/GSL.SP.1999.154.01.04.

Tirel, C., P. Gautier, D. J. J. van Hinsbergen, and M. J. R. Wortel (2009), Sequential development of interfering metamorphic core complexes: numerical experiments and comparison with the Cyclades, Greece, in *Collision and Collapse at the Africa-Arabia-Eurasia Subduction Zone*, edited by D. J. J. van Hinsbergen et al., *Geol. Soc. Spec. Publ.*, *311*, 257–292, doi:10.1144/SP311.10.

Torsvik, T. H., R. D. Müller, R. Van der Voo, B. Steinberger, and C. Gaina (2008), Global plate motion frames: Toward a unified model, *Rev. Geophys.*, *46*, RG3004, doi:10.1029/2007RG000227.

Tozzi, M., C. Kissel, R. Funiciello, C. Laj, and M. Parotto (1988), A clockwise rotation of southern Apulia?, *Geophys. Res. Lett.*, *15*(7), 681–684, doi:10.1029/GL015i007p00681.

Uzel, B., and H. Sözbilir (2008), A first record of a strike-slip basin in western Anatolia and its tectonic implication: The Cumaovası Basin, *Turk. J. Earth Sci.*, *17*, 559–591.

Vandamme, D. (1994), A new method to determine paleosecular variation, *Phys. Earth Planet. Inter.*, *85*, 131–142, doi:10.1016/0031-9201(94)90012-4.

van der Maar, P. A., and J. B. A. Jansen (1983), The geology of the polymetamorphic complex of Ios, Cyclades, Greece and its significance for the Cycladic Massif, *Geol. Rundsch.*, *72*(1), 283–299, doi:10.1007/BF01765910.

van Hinsbergen, D. J. J., and F. Boekhout (2009), Neogene brittle detachment faulting on Kos (E Greece): Implications for a southern break-away fault of the Menderes metamorphic core complex (western Turkey), in *Collision and Collapse at the Africa-Arabia-Eurasia Subduction Zone*, edited by D. J. J. van Hinsbergen et al., *Geol. Soc. Spec. Publ.*, *311*, 311–320, doi:10.1144/SP311.12.

van Hinsbergen, D. J. J., E. Hafkenscheid, W. Spakman, J. E. Meulenkamp, and M. J. R. Wortel (2005a), Nappe stacking resulting from subduction of oceanic and continental lithosphere below Greece, *Geology*, *33*(4), 325–328, doi:10.1130/G20878.1.

van Hinsbergen, D. J. J., C. G. Langereis, and J. E. Meulenkamp (2005b), Revision of the timing, magnitude and distribution of Neogene rotations in the western Aegean region, *Tectonophysics*, *396*, 1–34, doi:10.1016/j.tecto.2004.10.001.

van Hinsbergen, D. J. J., W. J. Zachariasse, M. J. R. Wortel, and J. E. Meulenkamp (2005c), Underthrusting and exhumation: A comparison between the External Hellenides and the "hot" Cycladic and "cold" south Aegean core complexes (Greece), *Tectonics*, *24*, TC2011, doi:10.1029/2004TC001692.

van Hinsbergen, D. J. J., D. G. van der Meer, W. J. Zachariasse, and J. E. Meulenkamp (2006), Deformation of western Greece during Neogene clockwise rotation and collision with Apulia, *Int. J. Earth Sci.*, *95*(3), 463–490, doi:10.1007/s00531-005-0047-5.

van Hinsbergen, D. J. J., W. Krijgsman, C. G. Langereis, J. J. Cornée, C. E. Duermeijer, and N. van Vugt (2007), Discrete Plio-Pleistocene phases of tilting and counterclockwise rotation in the southeastern Aegean arc (Rhodos, Greece): Early Pliocene formation of the south Aegean left-lateral strike-slip system, *J. Geol. Soc.*, *164*, 1133–1144, doi:10.1144/0016-76492006-061.

van Hinsbergen, D. J. J., G. Dupont-Nivet, R. Nakov, K. Oud, and C. Panaiotu (2008a), No significant post-Eocene rotation of the Moesian Platform and Rhodope (Bulgaria): Implications for the kinematic evolution of the Carpathian and Aegean arcs, *Earth Planet. Sci. Lett.*, *273*, 345–358, doi:10.1016/j.epsl.2008.06.051.

van Hinsbergen, D. J. J., G. B. Straathof, K. F. Kuiper, W. D. Cunningham, and J. R. Wijbrans (2008b), No rotations during transpressional orogeny in the Gobi Altai: Coinciding Mongolian and Eurasian apparent polar wander paths, *Geophys. J. Int.*, *173*, 105–126, doi:10.1111/j.1365-246X.2007.03712.x.

van Hinsbergen, D. J. J., M. J. Dekkers, and A. Koç (2010), Testing Miocene remagnetization of Bey Daglari: Timing and amount of Neogene rotations in SW Turkey, *Turk. J. Earth Sci.*, *19*, 123–156, doi:10.3906/yer-0904-3901.

Verge, N. (1993), The exhumation of the Menderes massif metamorphic core complex in western Anatolia, *Terra Abstr.*, *5*, 249.

Walcott, C. R., and S. H. White (1998), Constraints on the kinematics of post-orogenic extension imposed by stretching lineations in the Aegean area, *Tectonophysics*, *298*(1–3), 155–175, doi:10.1016/S0040-1951(98)00182-6.

Whitney, D. L., and E. Bozkurt (2002), Metamorphic history of the southern Menderes Massif, western Turkey, *Geol. Soc. Am. Bull.*, *114*(7), 829–838, doi:10.1130/0016-7606(2002)114<0829:MHOTSM>2.0.CO;2.

Whitney, D. L., and P. B. Davis (2006), Why is lawsonite eclogite so rare? Metamorphism and preservation of lawsonite eclogite, Sivrihisar, Turkey, *Geology*, *34*, 473–476, doi:10.1130/G22259.1.

Whitney, D. L., C. Teyssier, S. C. Kruckenberg, V. L. Morgan, and L. J. Iredale (2008), High-pressure–low-temperature metamorphism of metasedimentary rocks, southern Menderes Massif, western Turkey, *Lithos*, *101*, 218–232, doi:10.1016/j.lithos.2007.07.001.

Yilmaz, Y., S. C. Genç, F. Gürer, M. Bozcu, K. Yilmaz, Z. Karacik, S. Altunkaynak, and A. Elmas (2000), When did the western Anatolian grabens begin to develop?, in *Tectonics and Magmatism in Turkey and the Surrounding Area*, edited by E. Bozkurt et al., *Geol. Soc. Spec. Publ.*, *173*, 353–384, doi:10.1144/GSL.SP.2000.173.01.17.

Zachariasse, W. J., D. J. J. van Hinsbergen, and A. R. Fortuin (2008), Mass wasting and uplift on Crete and Karpathos (Greece) during the early Pliocene related to beginning of south Aegean left-lateral, strike slip tectonics, *Geol. Soc. Am. Bull.*, *120*, 976–993, doi:10.1130/B26175.1.

Zijderveld, J. D. A. (1967), A.C. demagnetisation of rocks: Analysis of results, in *Methods in Palaeomagnetism*, edited by D. W. Collinson et al., pp. 254–286, Elsevier, Amsterdam.

E. Bozkurt, Department of Geological Engineering, Middle East Technical University, 06531 Ankara, Turkey.

M. J. Dekkers and M. Koopman, Paleomagnetic Laboratory Fort Hoofddijk, Faculty of Geosciences, Utrecht University, Budapestlaan 17, NL-3584 CD Utrecht, Netherlands.

D. J. J. van Hinsbergen, Physics of Geological Processes, University of Oslo, Sem Sælands vei 24, NO-0316 Oslo, Norway. (d.v.hinsbergen@fys.uio.no)